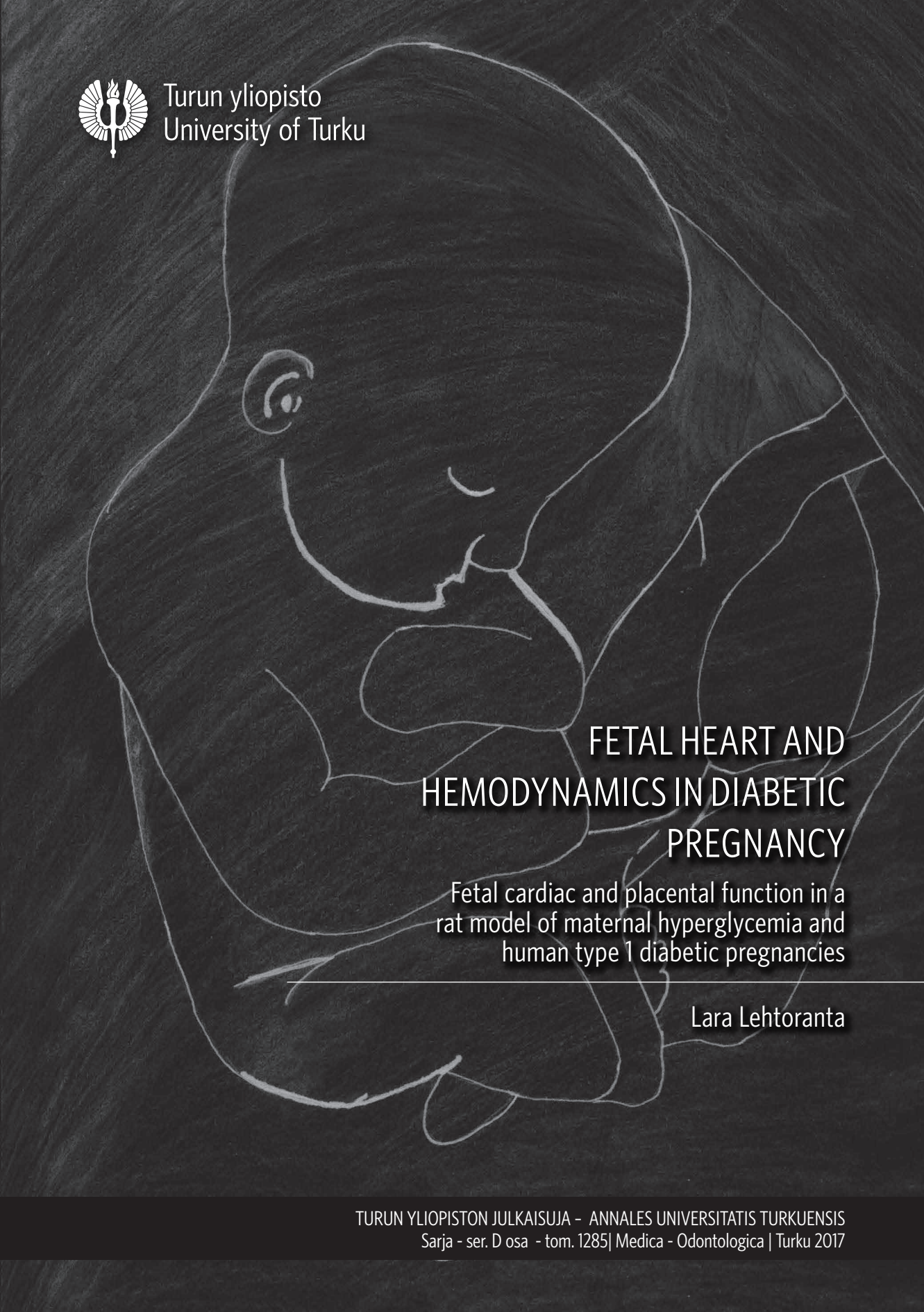




Turun yliopisto
University of Turku



FETAL HEART AND HEMODYNAMICS IN DIABETIC PREGNANCY

Fetal cardiac and placental function in a
rat model of maternal hyperglycemia and
human type 1 diabetic pregnancies

Lara Lehtoranta



Turun yliopisto
University of Turku

FETAL HEART AND HEMODYNAMICS IN DIABETIC PREGNANCY

Fetal cardiac and placental function in a rat model of maternal hyperglycemia and human type 1 diabetic pregnancies

Lara Lehtoranta

University of Turku

Faculty of Medicine

Department of Obstetrics and Gynaecology

University of Turku Doctoral Programme of Clinical Investigation

University of Oulu, Faculty of Medicine

Biomedicine Unit, Physiology, and NordLab Oulu

Supervised by

Professor Juha Räsänen

Department of Obstetrics and Gynaecology

University of Helsinki

Docent Eeva Ekholm

Department of Obstetrics and Gynaecology

University of Turku

Professor Olli Vuolteenaho

Biomedicine Unit, Physiology, and NordLab

University of Oulu

Reviewed by

Professor Helena Gardiner

Department of Obstetrics, Gynecology and
Reproductive Sciences

Department of Pediatric Cardiology

McGovern Medical School at UTHealth

Professor Saemundur Gudmundsson

Department of Urogynaecology and
Reproductive Pharmacology

Lund University

Opponent

Professor Fionnuala McAuliffe

Department of Obstetrics and Gynaecology

University College Dublin

Cover images by Louna Lehtoranta

The originality of this thesis has been checked in accordance with the University of Turku quality assurance system using the Turnitin OriginalityCheck service.

ISBN 978-951-29-6828-2 (PRINT)

ISBN 978-951-29-6829-9 (PDF)

ISSN 0355-9483 (Print)

ISSN 2343-3213 (Online)

Painosalama Oy - Turku, Finland 2016

To Tuomas, Louna, Reino, and Salme

"Of course it is happening inside your head, Harry, but why on earth should that mean that it is not real?" –Dumbledore to Harry Potter, in *Harry Potter and the Deathly Hallows* by J.K. Rowling

ABSTRACT

Lara Lehtoranta

Fetal heart and hemodynamics in diabetic pregnancy - Fetal cardiac and placental function in a rat model of maternal hyperglycemia and human type 1 diabetic pregnancies

University of Turku, Faculty of Medicine, Department of Obstetrics and Gynecology
University of Oulu, Faculty of Medicine, Institute of Biomedicine, Physiology
Turku University Hospital, Department of Obstetrics and Gynecology
University of Turku Doctoral Program of Clinical Investigation

Annales Universitatis Turkuensis, Medica-Odontologica, 2017

Maternal type 1 diabetes mellitus affects fetal and offspring health. We aimed to investigate fetal cardiac and placental function in a rat model of maternal pregestational hyperglycemia, and the effect of gestational hyperglycemia on the offspring heart. In human fetuses of diabetic mothers the aim was to investigate, whether maternal insulin therapy will ameliorate fetal cardiac, hemodynamic, and placental abnormalities.

Fetal cardiac and placental ultrasonography, histology, and gene expressions were examined in streptozotocin-induced maternal hyperglycemia and control rats. Rat offspring cardiac genes and histology were analyzed up to two weeks after birth. In diabetic and healthy human pregnancies, fetal ultrasonography and biochemical markers of cardiac function and fetal hypoxemia, and placental morphology and gene expression were collected.

In rat fetuses of maternal hyperglycemia, signs of diastolic dysfunction persisted throughout the second half of pregnancy, and transient mid-pregnancy cardiac dysfunction was observed. Increased myocardial cell turnover with cardiac hyperplasia and abnormal myocardial gene expression patterns were found. Increased placental vascular impedance and placental morphologic abnormalities were observed in the rat fetuses of maternal hyperglycemia. In the newborn rats of maternal hyperglycemia, cardiac genes controlling contractility, growth, structure, and metabolism were differently expressed when compared to healthy newborn rats. In human diabetic pregnancies, fetal cardiac output was decreased, pulsatility of the aortic isthmus blood flow velocity waveform, and fetal serum concentrations of natriuretic peptides and troponin T were increased at near term.

The rat model shows that maternal hyperglycemia leads to diastolic dysfunction and placental insufficiency. Abnormal expression of genes involved in cardiac contractility, structure, growth, and metabolism were seen in late term fetal and offspring hearts. In human maternal diabetes, fetal cardiac output is decreased with biochemical evidence of myocardial dysfunction.

Keywords: type 1 diabetes mellitus, maternal hyperglycemia, pregnancy, fetal, heart, ultrasonography, streptozotocin, histology, cardiac output, impedance, hyperplasia, cardiac contractility, excess cardiac growth, cardiac output, erythropoietin, diastolic dysfunction, placental insufficiency

TIIVISTELMÄ

Lara Lehtoranta

Diabeetikon sikiön verenkierto – Sikiön sydämen ja istukan toiminta äidin hyperglykemian kokeellisessa eläinmallissa ja tyypin 1 diabeetikoiden raskauksissa

Turun yliopisto, Lääketieteellinen tiedekunta, Synnytys- ja naistentautioppi
Oulun yliopisto, Lääketieteellinen tiedekunta, Biolääketieteen laitos, Fysiologia
Turun yliopistollinen keskussairaala, Naistentaudit ja synnytykset
Turun yliopiston kliininen tohtorihjelma

Annales Universitatis Turkuensis, Medica-Odontologica, 2017

Tyypin 1 sokeritauti (T1DM) vaikuttaa sikiön ja jälkikasvun hyvinvointiin. Tämän tutkimuksen tarkoituksena oli tutkia kokeellisen eläinmallin avulla emon raskaudenaikaisen hyperglykemian vaikutusta sikiön sydämen ja istukan toimintaan sekä jälkeläisten sydämen kehitykseen. T1DM naisten raskauksissa tavoitteena oli tutkia insuliinihoidon vaikutusta sikiön sydämen, verenkierron ja istukan poikkeavuuksiin.

Streptozotosiinilla (STZ) aikaansaatii emon hyperglykemia. STZ- ja verrokkirottien sikiöiltä tutkittiin sydämen ja istukan verenkiertoa ultraäänitutkimuksella, sekä kudosten histologiaa ja geenien ilmentymistä. Rotanpoikasten sydänten histologia ja geenien ilmentyminen tutkittiin 2 viikkoa syntymän jälkeen. Potilasmallissa sikiön verenkiertoa tutkittiin ultraäänellä, jonka lisäksi sydämen toiminnan ja hapenpuutteen sekä istukan rakenteen ja geenien ilmaisu selvitettiin.

Koe-eläinmallissa hyperglykemialle altistuneiden sikiöiden sydämen diastolinen toiminta oli poikkeava ja keskiraskaudessa havaittiin ohimenevä sydämen vajaatoiminta. Sydämen hyperplasia, runsaat mitoottisten ja apoptoottisten solujen määrät ja poikkeava geenien ilmentyminen todettiin hyperglykeemisten emojen sikiöillä. Tämän ryhmän istukan verenkierron impedanssi oli koholla ja rakenteet poikkesivat terveiden verrokien poikasista. Hyperglykeemisten rottien poikasilla sydämen kontraktiiliteettiin, kasvuun, rakenteeseen ja aineenvaihduntaan liittyvien geenien ilmentyminen oli poikkeavaa terveiden emojen poikasiin verrattuna. Potilasmallissa T1DM-äidin sikiön sydämen minuuttitilavuus oli alentunut, ja aortan istmuksen ja alaonttolaskimon verenvirtauksen vastus ja sikiön seerumin natriureettisten peptidien ja troponiini T:n pitoisuudet olivat koholla.

Kokeellisessa eläinmallissa totesimme, että emon hyperglykemia johtaa sikiön sydämen diastolisen toiminnan poikkeavuuteen ja istukan vajaatoimintaan. Sydämen kontraktiiliteettiin, rakenteeseen, kasvuun ja metaboliaan liittyvien geenien ilmentyminen oli poikkeava sikiöillä ja vastasyntyneillä poikasilla. Äidin nuoruustyyppin sokeritauti johtaa sikiön sydämen minuuttitilavuuden laskuun ja biokemiallisiin muutoksiin, jotka liittyvät sydämen toimintahäiriöön.

Avainsanat: tyypin 1 sokeritauti, emon hyperglykemia, raskaus, sikiö, sydän, ultraäänitutkimus, streptozotosiini, histologia, sydämen minuuttitilavuus, impedanssi, hyperplasia, sydämen kontraktiiliteetti, sydämen liikakasvu, sydämen minuuttitilavuus, erytropoietiini, diastolinen vajaatoiminta, istukan vajaatoiminta

TABLE OF CONTENTS

ABSTRACT	4
TIIVISTELMÄ	5
ABBREVIATIONS	9
LIST OF ORIGINAL PUBLICATIONS	12
1 INTRODUCTION	13
2 REVIEW OF LITERATURE	15
2.1 T1DM and pregnancy.....	15
2.1.1 Hyperglycemia and the fetus.....	15
2.1.2 Hyperglycemia and fetal hypoxia	16
2.1.3 Other pregnancy and offspring complications.....	17
2.2 Fetal heart and circulation.....	18
2.2.1 Doppler ultrasonography.....	20
2.2.2 Preload and afterload.....	21
2.2.3 Cardiac output, and systolic and diastolic function	23
2.2.4 Peripheral circulation.....	24
2.2.5 Fetal circulation and hypoxia.....	25
2.2.6 Fetal circulation and maternal hyperglycemia.....	28
2.2.7 Fetal cardiac gene expression in experimental methods of maternal hyperglycemia	32
2.3 The placenta	33
2.3.1 Placental morphology.....	33
2.3.2 Uteroplacental circulation.....	34
2.3.3 Uteroplacental circulation in hypoxia.....	35
2.3.4 Placental morphology in maternal hyperglycemia.....	36
2.3.5 Uteroplacental circulation in maternal hyperglycemia.....	37
2.3.6 Placental gene expression in maternal hyperglycemia	37
2.4 Animal models of maternal hyperglycemia	38
2.4.1 Streptozotocin	38
2.4.2 Animal models of pregestational hyperglycemia	38
2.4.3 Rat pregnancy characteristics.....	39
2.5 Biomarkers of fetal wellbeing	39
2.5.1 Natriuretic peptides	39
2.5.2 Troponin T.....	40
2.5.3 Erythropoietin	41
2.5.4 Activin A	41
2.5.5 Soluble vascular endothelial growth factor receptor-1 (sFlt-1).....	42
3 AIMS OF THE STUDY	43

4	MATERIALS AND METHODS.....	44
4.1	Subject characteristics and study design	44
4.1.1	Rat model of maternal hyperglycemia (I-III).....	44
4.1.2	Rat model of maternal hyperglycemia and pregnancy (I, II)	45
4.1.3	Rat model of maternal hyperglycemia and the rat neonatal heart (III) ..	45
4.1.4	Human T1DM pregnancies (IV)	46
4.2	Gene expression analysis (I-V).....	48
4.2.1	RNA isolation	48
4.2.2	qRT-PCR analysis (I-IV).....	48
4.3	Histological, tomographic, and biochemical analyses.....	50
4.3.1	Morphometric analysis (I-III).....	50
4.3.2	Periodic acid-Schiff (PAS) and PAS diastase stainings (II).....	51
4.3.3	In situ detection of apoptotic cells (I, III).....	51
4.3.4	Immunohistochemistry for Ki-67 staining (I).....	51
4.3.5	Micro-computed tomography analysis (I).....	51
4.3.6	Cytokine bead array analysis (II, IV)	52
4.3.7	Umbilical cord serum immunoassays (IV).....	52
4.4	Ultrasonographic assessment (I, II, IV).....	53
4.4.1	Animal models of maternal hyperglycemia and pregnancy (I, II)	53
4.4.2	Maternal T1DM and pregnancy (IV).....	53
4.5	Statistics.....	54
5	RESULTS.....	56
5.1	Rat model of maternal hyperglycemia (I-III).....	56
5.1.1	Fetal rat cardiac function during the second half of pregnancy.....	56
5.1.2	Intraobserver variability in the experimental rat model.....	56
5.1.3	Fetal rat cardiac morphology at term gestation.....	57
5.1.4	Fetal rat cardiac gene expression	60
5.1.5	Newborn and offspring rat heart.....	60
5.1.6	Newborn and offspring rat cardiac morphology	62
5.1.7	Newborn and offspring rat cardiac gene expression.....	63
5.1.8	Rat placenta.....	63
5.2	Maternal T1DM and the human fetus at near term (IV)	67
5.2.1	Human pregnancy demographics	67
5.2.2	Human fetal heart, and cardiovascular and peripheral hemodynamics	69
5.2.3	Newborn human biochemical markers of cardiac function.....	69
5.2.4	Human placenta	70
6	DISCUSSION	71
6.1	Validation and limitations of methodology.....	71
6.1.1	Rat model of maternal hyperglycemia (I-III).....	71
6.1.2	Human data (IV).....	71
6.1.3	Ultrasonography (I, II, IV).....	72

6.1.4	Histological and biochemical assays (I-IV).....	73
6.2	Fetal and neonatal cardiac development and function in maternal hyperglycemia	73
6.3	Placental function in maternal hyperglycemia	77
6.4	Fetal cardiac metabolism and hypoxia in maternal hyperglycemia	79
6.5	Placental metabolism and hypoxia in maternal hyperglycemia.....	80
6.6	Clinical implications.....	81
7	CONCLUSIONS	82
8	ACKNOWLEDGEMENTS.....	83
9	REFERENCES	86
10	ORIGINAL PUBLICATIONS	101

ABBREVIATIONS

A Spir, placental spiral arteries
Adrb1, β 1-adrenergic receptor
ACA, anterior cerebral artery
ACE, angiotensin-converting enzyme
AGA, appropriate for gestational age
Ao, aorta
AoI, aortic isthmus
ARED, absent or reversed end-diastolic
Atp2a2, sarcoplasmic reticulum Ca^{2+} -ATPase
AUt, uterine artery
AV, aortic valve
AVVR, atrioventricular valve regurgitation
Bmpr1A, bone morphogenetic protein receptor type 1A
BNP, B-type natriuretic peptide
CA/TA, cardiac area to thoracic area ratio
Capza1, Z-line actin-capping protein- α 1
CC/TC, cardiac to thoracic circumference
CCO, combined CO
Cdkn1b, cyclin-dependent kinase inhibitor 1B
CO, cardiac output
CS, cesarean section
CSA, is cross-sectional area
CT, computed tomography
CTG, cardiogram
DA, ductus arteriosus
DAo, descending aorta
dPAS, Periodic acid-Schiff diastase
DV, ductus venosus
E/A-ratio, atrial E-wave to A-wave ratio
ECLIA, electrochemiluminescence immunoassay
Egfr, epidermal growth factor receptor
Egln3, hypoxia-inducible factor prolyl hydroxylase 3
ELISA, enzyme linked immunosorbent assay
Epo, erythropoietin; *Gpx3*, glutathione peroxidase 3
ERBL/ERYT, number of erythroblasts per 100 erythrocytes
ET, ejection time
FHR, fetal heart rate
Flt1, *FMS-related tyrosine kinase 1*
FO, foramen ovale
G-CSF, granulocyte colony-stimulating factor
gHbA1c%, glycosylated hemoglobin content
GD, gestational day
GM-CSF, granulocyte macrophage colony-stimulating factor
GRO-KC, chemokine C-X-C motif ligand 1
H & E, hematoxylin and eosin
Hcn2, hyperpolarization-activated cyclic nucleotide-gated potassium channel 2
HG, hyperglycemia

Hsl, hormone-sensitive lipase
ICT%, proportion of isovolumetric contraction time of total cardiac cycle
IDDM, insulin-dependant diabetes mellitus
IF, inflow
IFN γ , interferon- γ
IGF, insulin-like growth factor
Igf2bp3, insulin-like growth factor 2 mRNA binding protein 3
Igfbp6, insulin-like growth factor binding protein 6
IL, interleukin
IRI, immunoreactive insulin
IRT%, proportion of isovolumetric relaxation time of total cardiac cycle
IUGR, intra-uterine growth restriction
IVC, inferior vena cava
IVS, interventricular septum
Kcnp2, kv-channel interacting protein
Ldha, lactate dehydrogenase A
LGA, large for gestational age
LHV, left hepatic vein
LV, left ventricle
LVW, left ventricular wall
MCA, middle cerebral artery
MCP1, monocyte chemo attractant protein 1
MKI, mitosis-karyorrhexis index
MPI, index of myocardial performance
mRNA, messenger RNA
Myh2, adult skeletal myosin heavy chain 2
Myh3, embryonic skeletal myosin heavy chain 3
Myh6, α -cardiac myosin heavy chain 6
MV, mitral valve
 n^d , number of dams
 n^{fp} , number of fetuses/pups
NA, not applicable
NICU, neonatal intensive care unit
Nppa, atrial natriuretic peptide
Nppb, brain natriuretic peptide
NT-proANP, N-terminal pro-atrial natriuretic peptide
NT-proBNP, N-terminal pro-B-type natriuretic peptide
OF, outflow
 PO_2 , partial arterial pressure of oxygen
P27kip1, see *Cdkn1b*
PAS, Periodic acid-Schiff
Pdgfrb, platelet derived growth factor receptor beta polypeptide
Pdk2, pyruvate dehydrogenase kinase, isozyme 2
PE, pre-eclampsia
Pgdh, hydroxyprostaglandin dehydrogenase 15
PI, pulsatility index
PIV, pulsatility index for veins
PIGF, Placental growth factor
PND, postnatal day
PPA, proximal pulmonary artery

PSV, peak systolic velocity
Ptgs2, cyclo-oxygenase 2 or prostaglandin-endoperoxidase 15
PV, pulmonary valve
Q, volume blood flow
RDS, respiratory distress syndrome
RI, resistance index
RNA, ribonucleic acid
ROS, reactive oxygen species
RV, right ventricle
RVW, right ventricular wall
S/D, systole to diastole ratio
SD, Sprague-Dawley
sFlt1, soluble Fms Related Tyrosine Kinase 1
SGA, small for gestational age
Slc2a3, facilitated glucose transporter 3
Slc2a4, insulin-responsive glucose transporter 4
STZ, streptozotocin
SV, stroke volume
T1DM, type 1 diabetes mellitus
TNF, tumor necrosis factor
Tnfrsf12a, tumor necrosis factor receptor superfamily member 12a
TnT, troponin T
TR, tricuspid regurgitation
TTP, time to peak velocity
TUNEL, terminal deoxynucleotide transferase-mediated dUTP nick-end labeling
TV, tricuspid valve
UA, umbilical artery
ub, umbilical blood
Ucp2, uncoupling protein 2
Ucp3, uncoupling protein 3
UV, umbilical vein
VD, ventricle diameter
VeFo, ventricular ejection force
VEGF, vascular endothelial growth factor
Vegfa, vascular endothelial growth factor A
VFS, ventricular fractional shortening
Vmax, maximal velocity
Vmean, mean velocity
VTI, velocity-time integral

LIST OF ORIGINAL PUBLICATIONS

This thesis is based on the following original publications, which are referred to in the text by the roman numerals I-IV. The original communications have been reproduced with the kind permission of the copyright holders.

- I Lehtoranta L, Vuolteenaho O, Laine J, Koskinen A, Soukka H, Kytö V, Määttä J, Haapsamo M, Ekholm E, Räsänen J. Maternal hyperglycemia leads to fetal cardiac hyperplasia and dysfunction in a rat model. *Am J Physiol Endocrinol Metab* 2013;305(5):E611-9.
- II Lehtoranta L, Vuolteenaho O, Laine VJ, Polari L, Ekholm E, Räsänen J. Placental structural abnormalities have detrimental hemodynamic consequences in a rat model of maternal hyperglycemia. *Placenta* 2016;44:54-60.
- III Lehtoranta L, Koskinen A, Vuolteenaho O, Laine J, Kytö V, Soukka H, Ekholm E, Räsänen J. Gestational hyperglycemia reprograms cardiac gene expression in rat offspring. *Pediatr Res* 2017. doi:10.1038/pr.2017.42. In press.
- IV Lehtoranta L, Haapsamo M, Räsänen J, Palo P, Vuolteenaho O, Ekholm E. Fetal cardiac dysfunction at term gestation in type 1 diabetic pregnancies. Submitted.

1 INTRODUCTION

The incidence of type 1 diabetes mellitus (T1DM) is increasing worldwide (Onkamo et al. 1999). T1DM is a chronic disease defined by the lacking production of insulin in the pancreatic β -cells (American Diabetes Association 2016). Finland is among the countries with the highest prevalence of T1DM in children under 15 years, the incidence reaching 64.9/100000 in 2006 (Harjutsalo et al. 2013). The annual incidence of T1DM among Finnish women with a singleton pregnancy was 0.6% in 2007-2011 (Pallasmaa et al. 2015).

Maternal T1DM affects fetal development. T1DM increases the occurrence of fetal growth disturbances (Persson et al. 2009), oxygen consumption (Milley et al. 1986), erythropoiesis (Stonestreet et al. 1989), hypoxemia (Teramo & Widness 2009; Widness et al. 1981), and ventricular wall thickness (Russell et al. 2008). The prevalence of fetal intrauterine demise is fourfold and of infant deaths twofold in pregestational diabetic pregnancies compared to healthy controls (Tennant et al. 2014).

Ultrasonography is commonly used to assess fetal well-being. However, the findings in diabetic pregnancies are conflicting. Umbilical artery impedance is similar to normal uncomplicated pregnancies in some studies while others have found increased umbilical artery impedance in diabetic pregnancies (Maruotti et al. 2014; Fadda et al. 2001; Johnstone et al. 1992). The largest sample size ($n=102$) investigated a few years back established a decreased umbilical artery PI in macrosomic T1DM fetuses (Maruotti et al. 2014). Also the findings concerning fetal cardiac output (CO) are conflicting (Lisowski et al. 2003; Räsänen & Kirkinen 1987). The most recent study with a small sample ($n=17$) found increased weight-adjusted combined cardiac output (Lisowski et al. 2003), whereas an older study with an equal sample size found decreased left ventricular cardiac output in diabetic pregnancies (Räsänen & Kirkinen 1987). Cardiac diastolic dysfunction is common in T1DM fetuses in older studies with smaller sample sizes ($n=9-31$) (Weiner et al. 1999; Tsyvian et al. 1998; Weber et al. 1994), though more recent studies only found signs of diastolic dysfunction in earlier stages of fetal development (Russell et al. 2008) or found no differences near term (Jaeggi et al. 2001). Several studies report increased cardiac septal wall thickness in these fetuses (Russell et al. 2008; Jaeggi et al. 2001; Macklon et al. 1998; Veille et al. 1993; Rizzo et al. 1992a), some even from second trimester onwards (Macklon et al. 1998; Veille et al. 1993; Rizzo et al. 1992a)

There are several well-established experimental animal models of maternal hyperglycemia (Rees & Alcolado 2005). Administration of streptozotocin (STZ) to rodents creates a T1DM-like state, since it targets pancreatic β -cells (Junod et al. 1969). It is the most common model for studying the effects of maternal hyperglycemia on the developing fetus (Jawerbaum & White 2010). In experimental animal models, maternal hy-

perglycemia during pregnancy alters placental structure and metabolism (Padmanabhan & Shafiullah 2001; Thomas et al. 1990), the immunological responses in the feto-placental unit (Sisino et al. 2013), cardiac growth (Gordon et al. 2015; Dowling et al. 2014), and cardiac function (Corrigan et al. 2013). The offspring are subjected to long-term changes of their pancreatic β -cells (Han et al. 2007), and cardiovascular and renal function (Yan et al. 2014).

In this thesis the effects of maternal hyperglycemia on feto-placental circulation and the hearts of the offspring were studied using a well-established STZ-induced rat model to examine the pathophysiologic changes caused by hyperglycemia on the hemodynamic as well as the cellular level. Further, in human fetuses of diabetic mothers, the aim was to investigate whether maternal insulin therapy will ameliorate fetal cardiac, hemodynamic, and placental abnormalities.

2 REVIEW OF LITERATURE

2.1 T1DM and pregnancy

2.1.1 *Hyperglycemia and the fetus*

Maternal glucose passes the placental barrier. Maternal hyperglycemia leads simultaneously to fetal hyperglycemia in both humans (Schwartz & Teramo 2000) and rats (Han et al. 2007) thus causing excess pancreatic β -cell growth (Han et al. 2007; Schwartz & Teramo 2000). Animal models have shown that maternal hyperglycemia increases basal glucose metabolism by 30–100% in all tissues apart from the brain (Leturque et al. 1987).

The hyperglycemic milieu affects insulin and other growth factor levels. In early pregnancy, maternal nutrient availability is the sole contributor to placental nutrient transport that affects fetal growth in a linear fashion in pregnancies of women with diabetes (Schwartz et al. 1994) and rats of maternal hyperglycemia (Han et al. 2007). Anabolic and mitogenic effects of hyperinsulinemia induce excess cardiac growth, and increased levels of growth factors in the fetus and neonate (Higgins & Mc Auliffe 2010; Cowett & Schwartz 1979). This results in fetal macrosomia, a well-known complication of T1DM pregnancies (Klemetti et al. 2016; Maruotti et al. 2014). Placental growth factor (PIGF), insulin-like growth factor (IGF) -1, IGF-2, and leptin concentrations are increased and serum levels of IGF-axis binding proteins, such as IGFBP1, are decreased in newborns of diabetic mothers (Higgins & Mc Auliffe 2010). Fetal cardiac growth is stimulated by an increase in arterial blood pressure together with elevated circulating IGF-1 and natriuretic peptide concentrations (Thornburg et al. 2011). In human diabetic pregnancies, optimal glucose control does not completely protect the fetal heart, especially the interventricular septum, from abnormal wall growth (Aman et al. 2011; Corrigan et al. 2013). Up to 25–75% of newborns have increased cardiac wall thickness (Oberhoffer et al. 1997; Veille et al. 1992). Inadequate placentation in rat experiments with maternal hyperglycemia may lead to poor placental function and fetal intrauterine growth restriction (IUGR) (Padmanabhan & Shafiullah 2001).

The Pedersen hypothesis states that maternal hyperglycemia results in fetal hyperglycemia (Pedersen 1954). Specifically, before 20 weeks of gestation, the fetal islet cells are incapable of producing insulin and the hyperglycemic insult to fetal tissues is direct. Thus optimal maternal glycemic control is essential. Pregnancy loss, congenital malformations, pre-eclampsia, preterm delivery, perinatal death, and excessive fetal growth, are more common in women with elevated gHbA1c and short-term glucose level variability (Damm et al. 2014). Continuous subcutaneous insulin infusion during pregnancy improves maternal glycemic control, but has no effect on short-term neonatal outcome (Kekäläinen et al. 2016). Precise prandial glucose monitoring reduces the

incidence of excessive fetal growth and pre-eclampsia better than preprandial glucose monitoring in T1DM women (Manderson et al. 2003).

After birth, the neonatal glucose supply decreases rapidly resulting in fetal hypoglycemia (Nold & Georgieff 2004; Schwartz & Teramo 2000) because of hyperinsulinemia (Nessa et al. 2016). A similar phenomenon has been observed in newborn rats (Han et al. 2007). In humans, neonatal hypoglycemia is reversible and lasts for a few hours (Han et al. 2007). Usually, cardiac growth shifts from hyperplastic to hypertrophic 1–2 weeks postnatally in humans (Oparil et al. 1984), whereas in rats this shift occurs earlier, at postnatal days (PND) 3 and 4 (Li et al. 1996). Nevertheless, if there is pregestational maternal hyperglycemia in the rat, the offspring fed a euglycemic diet become insulin resistant by 15 weeks of age (Han et al. 2007). This resembles the pre-metabolic state of human type 2 diabetes. In humans, increased insulin resistance and poor glucose tolerance occurs in 9–17% of pre-to-primary school aged children (Plagemann et al. 1997).

2.1.2 Hyperglycemia and fetal hypoxia

Although increased glycosylated hemoglobin content (gHbA1c%) in red blood cells increases oxygen affinity, the risk of fetal hypoxia is significant in T1DM pregnancies. Low maternal blood pH values in early pregnancy are related to hypoxic events (Madsen & Ditzel 1984). In pregnancies with fetal intrauterine or neonatal death, the placenta shows signs of hypoxic insult (Stanek et al. 2001). Placental histology reveals evidence of decreased diffusing capacity, possibly a mark of fetal hypoxia (Jauniaux & Burton 2006). Hyperglycemia and hyperinsulinemia increase the basal metabolic activity and oxygen consumption of the fetus (Milley et al. 1986; Philipps et al. 1984) resulting in relative hypoxemia in an environment of limited oxygen delivery capacity due to placental insufficiency. In hypoxemia, the oxygen-carrying capacity of the fetus normally increases (Stonestreet et al. 1989; Widness et al. 1981), and this is reflected in increased erythropoietin (EPO) levels in cord blood (Widness et al. 1981), fetal polycythemia, and altered iron distribution. EPO levels are strongly inversely correlated with the oxygen tension and pH of cord blood – signs of acute fetal hypoxia (Rollins et al. 1993). Fetal oxidative stress may induce chronic hypoxia in T1DM (Escobar et al. 2013; Loukovaara et al. 2005). In a lamb model, fetal hyperglycemia increases fetal oxygen consumption and reduces the fetal arterial oxygen content (Philipps et al. 1984). In T1DM pregnancies, amniotic fluid and umbilical cord serum erythropoietin levels are increased (Escobar et al. 2013; Teramo et al. 2004a). Human fetal hyperinsulinemia and hyperglycemia are connected to increased levels of amniotic fluid and cord blood erythropoietin (Schwartz et al. 1994; Widness et al. 1990). In animal studies, simultaneous hypoxia and infusion of glucose induce a 40% decline in fetal oxygenation followed by a rise in EPO (Philipps et al. 1982). In a study on rhesus monkeys, combined maternal hyperglycemia and fetal hypoxemia reduces the fetal pH and increases the lactate level more than fetal hypoxemia alone. These animal studies

have shown that fetal hypoxemia combined with hyperglycemia induces less catecholamine release and insulin than either one alone (Cohn et al. 1992).

2.1.3 Other pregnancy and offspring complications

Hypertension-related complications, preterm birth (Klemetti et al. 2015; Klemetti et al. 2013; Klemetti et al. 2012), and delivery by cesarean section (Pallasmaa et al. 2015) occur more often in T1DM pregnancies than in healthy pregnant women (Persson et al. 2009). Despite intensive surveillance, increased blood pressure (Klemetti et al. 2013), obesity, and poor glycemic control during pregnancy (Klemetti et al. 2012) are still common in diabetic pregnancies.

Poor pregestational glycemic control is associated with an increased risk of congenital anomalies (Persson et al. 2009). White's classification is based on the duration of diabetes, type of treatment used, and organ involvement (White 1949). T1DM women are referred to category B or higher. A recent cohort study from Finland covering the years 1988–2011 found that severe forms of diabetes are associated with poor glycemic control before and during early pregnancy, hypertension, pre-eclampsia, operative mode of delivery, preterm delivery, small-for-gestational age infants, and neonatal intensive care unit admissions (Klemetti et al. 2015). White's classification to some degree can predict maternal and fetal outcome (Klemetti et al. 2015).

Neonates of diabetic mothers are affected by hyperinsulinemic hypoglycemia (Nessa et al. 2016), hypomagnesemia and hypocalcemia (Tsang et al. 1976), polycythemia (Cetin et al. 2011), iron deficiency (Georgieff et al. 1990), RDS and other respiratory disorders (Horowitz et al. 2011; Persson et al. 2009), hyperbilirubinemia (Bollepalli et al. 2010), and impaired CNS development (Kowalczyk et al. 2002). Recent studies suggest that the incidence of stillbirths, neonatal prematurity, and neonatal macrosomia in diabetic pregnancies is declining (Beyerlein et al. 2010).

Maternal diabetes can have long-lasting effects on the offspring (Vlachová et al. 2015). These include abnormal neurobehavioral development (Rizzo et al. 1997), cardiovascular dysfunction (Vessières et al. 2016; Oberhoffer et al. 1997), and abnormalities in insulin- and related growth factor metabolism (Han et al. 2007). The offspring have an increased risk of overall mortality, hospital admissions, and need of medication by the age of 15 years (Knorr et al. 2015). In a Danish study, 300 children aged 17 years whose mothers had T1DM, had higher BMIs and more often reduced glucose tolerance, relative insulin deficiency, and reduced insulin sensitivity than controls (Vlachová et al. 2015).

2.2 Fetal heart and circulation

Fetal heart, still formed as a tube, begins to contract during the third week of life. Complete uteroplacental circulation is formed late during the first trimester. Harvey was the first to describe fetal circulation, though he thought that there is no pulmonary circulation in the fetus (Harvey W. 1628). Fetal circulation has three distinguished shunts. The ductus venosus (DV) directs the oxygenated blood from umbilical vein to vena cava inferior (IVC), where this blood flows to the right atrium and partly through foramen ovale to the left atrium. The third shunt ductus arteriosus (DA) directs the blood flow from the pulmonary artery to the descending aorta. The aortic isthmus (Aol) connects the two cardiac ventricles working in parallel. It is an important arterial watershed area in the arterial circulation between the upper and lower body. A similar watershed area in the venous system is the left portal vein between the main portal stem and the DV.

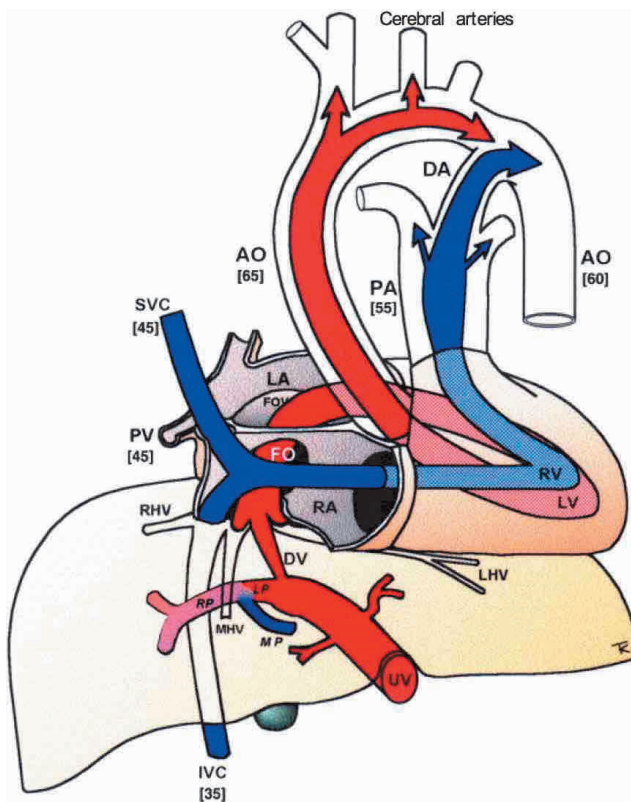


Figure 1. Fetal circulatory system. AO, aorta; Aol, aortic isthmus; DA, ductus arteriosus; DV, ductus venosus; FO, foramen ovale; IVC, inferior vena cava; LA, left atrium; LV, left ventricle; LP, left portal vein; MHV, middle hepatic vein; PV, pulmonary vein; RA, right atrium; RHV, right hepatic vein; RV, right ventricle; RP, right portal vein; SVC, superior vena cava; UV, umbilical vein. Cerebral arteries include (from left to right) the brachiocephalic, left common carotid, and left subclavian arteries. Modified from Kiserud T. *Seminars in Fetal and Neonatal Medicine* 2005;10(6):493–503. Reproduced with permission.

Normally this section directs umbilical blood to the right liver lobe, but under abnormal conditions, such as growth restriction, the blood flow may be reversed and directed from the spleen to the DV (Kiserud et al. 2006). The right ventricle ejects blood through the pulmonary valve to the pulmonary artery and to the ductus arteriosus and descending aorta. In the fetus, a lesser amount of blood flows through the proximal pulmonary arteries (PPA). The left ventricle pumps the blood through the aortic valve to the ascending aorta and the aortic arch. After the branching of the common cerebral artery, left common carotid artery, and left subclavian artery, the left side of the parallel circulation meets the right side in the Aol.

Cardiac muscle fibers contain myosin and actin filaments. The cardiomyocytes are connected by intercalated discs, containing desmosomes that hold the fibers together and gap junctions with receptors for contractile proteins. Cardiac contraction is dependent on the number of cross-bridges between actin and myosin, which are controlled by calcium levels extracted from the sarcoplasmic reticulum during the electric current of action potential or the availability of calcium. Inside the cell, calcium binds to the troponin/tropomyosin complex leading to cardiomyocyte contraction. Active calcium transport into the sarcoplasmic reticulum (by calcium-ATPase pump, SERCA) leads to cardiac relaxation or lusitropy. The positive inotropic or contractile state is increased by sympathetic activation mediated through catecholamines epinephrine and norpephrine, and some drugs, such as digitalis. Through β -adrenergic activation, catecholamines increase the amount of phosphorylated phospholamban, which is a weaker inhibitor of SERCA than the non-phosphorylated form. This in turn leads to enhanced

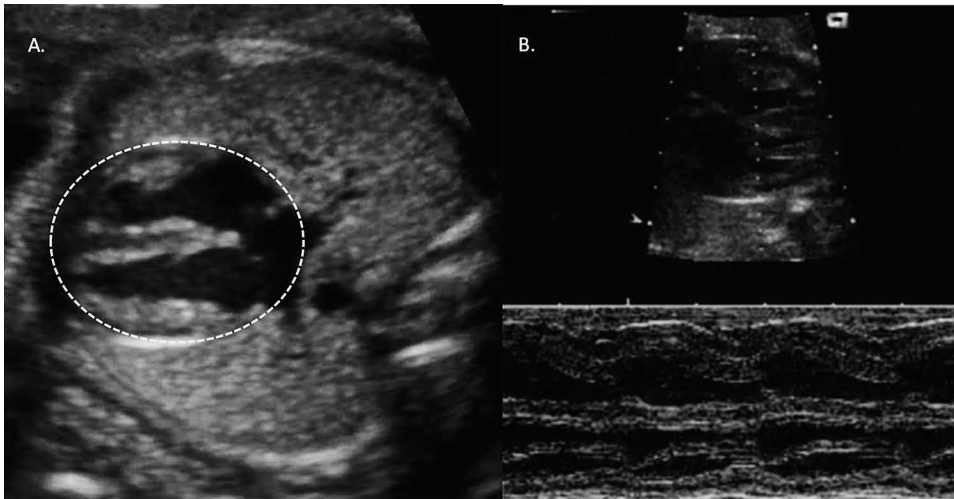


Figure 2. A. A measurement of cardiac circumference (CC) from a four-chamber view of the heart. Usually, the cardiac to thoracic circumference ratio is less 0.60 in the third trimester, but increases with excess fetal cardiac workload (hydrops, cardiac arrhythmias, maternal T1DM) (Leung et al. 2006; Respondek et al. 1992). B. M-mode recording across ventricular walls and interventricular septum. The beam is set just below the atrioventricular valve level.

SERCA function and increased sarcoplasmic reticulum release of calcium during the next contraction (Zhang et al. 2007) and results in increased lusitropy of the heart muscle (Rodriguez & Kranias 2005). Decreasing calcium influx into the cardiomyocyte decreases contractility established through parasympathetic stimuli, anoxia, hypercapnia or acidosis, or cardiomyocyte loss.

2.2.1 Doppler ultrasonography

The Doppler effect is the change in wave frequency for an observer moving relative to the source of the wave. In Doppler ultrasonography, the motion of sound waves and their change is registered and graphically converted to blood flow velocity waveforms as a function of time. The Doppler effect depends on the speed and direction of blood flow, and the operating frequency of the sound emitted from a transducer (Kremkau 1992a; Kremkau 1992b). Pulsed wave Doppler ultrasonography is based on the fact that a transducer emits waves in pulses that can be analyzed from the back-scattered echo from a certain range allowing the analysis of a single blood vessel as a function of time determined by the time the gate remains open (Gill 1987). In high pressure vessels such as arteries, forward flow occurs usually during systole and absence or reverse flow during diastole. The relation between systolic and diastolic flow of a vessel is described by the impedance indices: pulsatility index (PI), resistance index, S/D-ratio, and PI for veins (PIV). These variables depict impedance, i.e. resistance to pulsatile flow but are not a direct estimation of the actual flow (Dickey 1997). The indices are less dependant on the angle of blood flow than volume flow analyses. Blood flow

Table 1. Cardiac and circulatory parameter tools for analysis.

Abbreviation	Variable	Formula
CO	cardiac output	$CO = SV \times FHR = VTI \times CSA \times FHR$
CSA	cross sectional area	$CSA = \pi \times (r)^2$
ICT%	isovolumetric contraction time	$ICT\% = ICT \text{ (ms)} / \text{total cardiac cycle (ms)} \times 100$
IRT%	isovolumetric relaxation time	$IRT\% = IRT \text{ (ms)} / \text{total cardiac cycle (ms)} \times 100$
MPI	index of myocardial performance	$MPI = (ICT+IRT)/ET$
PI	pulsatility index	$PI = (PSV - \text{end-diastolic velocity})/\text{time-averaged maximum velocity over the cardiac cycle}$
PIV	pulsatility index for veins	$PIV = PSV\text{-velocity during atrial contraction}/\text{time-averaged maximum velocity over the cardiac cycle}$
Q	volume flow	$Q = VTI \times FHR \times CSA$ or $Q = V_{\text{mean}} \times CSA$
R	resistance to flow	$R = dP / Q$
RI	resistance index	$RI = (PSV - \text{end-diastolic velocity})/PSV$
S/D	S/D-ratio	$S/D = PSV/\text{end-diastolic velocity}$
Vmean	mean velocity	$V_{\text{mean}} = VTI \times FHR$
VeFo	ventricular ejection force	$VeFo = (1.055 \times CSA \times VTI_{\text{ac}}) \times (PSV/TTP)$
VFS%	ventricular fractional shortening	$VFS\% = [(\text{inner diastolic diameter} - \text{inner systolic diameter})/\text{inner diastolic diameter}] \times 100$

SV, stroke volume; FHR, fetal heart rate; VTI, velocity-time integral; ET, ejection time; PSV, peak systolic velocity (synonymous with Vmax); dP, difference in pressure at the beginning and end of the tube; VTI_{ac}, velocity-time integral during the systolic acceleration period; TTP, time to peak velocity.

analysis can be performed for all vessels, though smaller vessels require high-frequency ultrasound to minimize the risk of error (Kiserud et al. 1999). In volume flow analysis, the diameter, the heart rate, and time-velocity integral need to be known. A time-velocity integral is calculated by planimetry of the area under the Doppler spectrum. Three consecutive waveforms of each cardiac cycle are recommended (Dickey 1997), and the angle of insonation should be kept < 30 degrees (Tessler et al. 1990). However, impedance measures < 60 degrees are still fairly reliable. Different methods for analyzing ultrasonographic presentations are described in Table 1. These mathematical models may incur a magnitude of error unless used in a precise way for each study.

In M-mode imaging (Figure 2B), the transducer is set to collect data from one line of transmission with its own time reference and variations of position as motion displacements. Therefore, M-mode echocardiography shows the current position of one interface in relation to other interfaces. In fetal medicine it is used to calculate cross-sectional diameters for cardiac ventricles, walls, and the fractional shortening of the ventricles. It may also be used in diagnosis of fetal arrhythmias (DeVore et al. 1984). Furthermore, M-mode is used to assess cardiac valve long-axis function, such as when performing modified MPI assessments (Hernandez-Andrade et al. 2005). Mitral and tricuspid annular plane systolic excursion (MAPSE and TAPSE) methods assess longitudinally cardiac function by measuring the annular plane movement towards the apex during systole in fetuses (Matsui et al. 2011).

2.2.2 Preload and afterload

Apart from heart rate and contractility, cardiac function is influenced by action potential conduction velocity, preload, and afterload. Cardiomyocytes, unlike other striated muscle cells, can only increase force generation through changes in fiber length and inotropy. Up to a point, cardiomyocytes respond to the stretching of its fibers by increasing the strength of the following contraction. This phenomenon is called Frank-Starling's law, and it is applicable for the assessment of fetal cardiac function (Lingman et al. 1984).

Preload, the stretching of cardiac fibers, and the capability of ventricular wall to stretch can be estimated from vessels carrying blood to the fetal heart. In humans, the DV carries 18% of the umbilical oxygenated blood to the IVC from gestational week 30 to term (Kiserud et al. 2000b), whereas in experimental animals this proportion at term is closer to 50% (Edelstone et al. 1978). However, both in humans and animal models, DV PIV increases during hypoxemia (Kiserud et al. 2000a; Tchirikov et al. 1998), and the vessel diameter tone is under adrenergic control (Kiserud et al. 2000b). DV shunting directs 70-80% of the umbilical blood into the hepatic circulation. An increase in blood viscosity, not uncommon for fetuses to mothers with T1DM, increases shunting of liver blood flow from the umbilical vein. A lamb model of placental insufficiency showed that

reduced pressure in the umbilical vein reduced the hepatic flow more than the DV flow. After an initial increase, DV PIV is unaffected even until death (Mäkikallio et al. 2010). Pulsatility in DV (Baschat et al. 2001; Gudmundsson et al. 1996) and IVC (Mori et al. 2007; Baschat et al. 2004) reflect atrial contraction and end-diastolic filling pressure.

Tricuspid regurgitation is clinically not a significant finding when it is nonholosystolic, lasts <50% of the total cardiac cycle, and has a maximum velocity of <2 m/s. With normal cardiac anatomy, it occurs in 6.8% of fetuses (Respondek et al. 1994) and can be used to evaluate cardiac contractility if the change in the pressure gradient and time can be calculated. In humans, significant holosystolic tricuspid regurgitation occurs more often when preload and afterload are increased, e.g. in volume overload, increased systemic pressure, and placental insufficiency.

Afterload is the pressure against which the heart works to eject blood during systole. Ejection takes place against the friction generated by the cardiac and vessel walls, central vessel impedance, and peripheral vessel resistance. Laplace's law states that the tension of a wall is the product of the pressure times the radius of a wall. The inverse relationship of wall thickness to tension is used to estimate afterload, as are the resistance and impedance of vessels and mean arterial pressure in fetuses (Mäkikallio et al. 2010; Hawkins et al. 1989). The right ventricle is sensitive to afterload in fetal life (Mäkikallio et al. 2002a).

Afterload is reflected in the cardiac to thoracic circumference ratio (CC/TC) (Figure 2A). Ventricular fractional shortening also reflects fetal cardiac workload. It is measured from M-mode recordings of the fetal heart perpendicular to the interventricular septum below the level of atrioventricular valves from the four-chamber view of the fetal heart (DeVore et al. 1984). Ventricular fractional shortening of both ventricles usually remains constant at 30–40% throughout gestation (DeVore et al. 1984). When abnormal, fractional shortening may reflect myocardial dysfunction or increased cardiac afterload, as seen in fetuses with intrauterine distress where both ventricular end-diastolic diameters are increased but the actual left ventricular size and myocardial function are unaffected (Räsänen et al. 1989). More recent methods to assess fetal afterload are velocity, strain, and strain rate measurements. Tissue Doppler velocity (Watanabe et al. 2009), and strain and strain rate (Dandel et al. 2009) offer more precise methods to acquire data of fetal cardiac function. Two-dimensional (2D) speckle-tracking echocardiography (STE) is a commercially available imaging method that uses longitudinal measurements and differentiates between active and passive movements in the myocardium (Willruth et al. 2011). In the fetus, the right, but not the left, ventricle strain rate decreases with advancing gestation, whereas no differences were found in strain rates between the ventricles in early third trimester (Kapusta et al. 2013).

2.2.3 Cardiac output, and systolic and diastolic function

Cardiac output (CO) depicts the quantity of blood pumped by the heart over a period of time. In the fetus, the stroke volume and heart rate (FHR) define CO. Stroke volume is affected by contractility, preload (cardiac volume filling), afterload (peripheral resistance, blood viscosity), duration of contraction, and heart size. FHR is affected by gestational age, balance between the sympathetic and parasympathetic nervous system, hormonal status, acid-base balance, and humoral factors (Walker et al. 1990). Preload is the major determinant of cardiac output. Weight-adjusted CO is higher in the fetus than that in adults (Severi et al. 2000). As gestation advances, stroke volume and CO, lung volume blood flow, and weight-indexed pulmonary and systemic vascular resistance increase. CO increases >10-fold from 20 weeks to term. From second trimester onwards, fetal cardiac function is dominated by the right ventricle (Rasanen et al. 1996; Kenny et al. 1986). At 38 gestational weeks, the right ventricular CO comprises 60 % of combined CO (Rasanen et al. 1996). Similar findings have been made in fetal sheep (Rudolph 1985). However, the pressures are similar in both ventricles and in both atria since they pump in parallel in fetal life (Thornburg & Morton 1986). This has been found in human fetuses undergoing invasive procedures in the second trimester as well (Johnson et al. 2000). The fetal stroke volume of the right ventricle increases from 0.7 ml at gestational week 20 to 7.6 ml at week 40 and of the left ventricle from 0.7 ml to 5.2 ml (Kenny et al. 1986). Studies on near-term sheep show from combined CO about 2.5% is pumped to the heart, 3.7% to the brain, 8.0% to the lungs, 31% to the carcass, and 45% to the placenta. In human pregnancy, from 20 to 30 weeks of gestation, the pulmonary blood flow proportion of combined CO increased from 13% to 25% after which it remains constant until term. The proportion of blood flow through the ductus arteriosus of the combined CO is approximately 20 % at term gestation (Rasanen et al. 1996).

During gestation the healthy fetal heart adapts to increasing cardiac work load and blood pressure (Johnson et al. 2000). In healthy pregnancies, ventricular systolic and end-diastolic pressures increase in a linear fashion until 28 gestational weeks. The index of myocardial performance (MPI) describes both systolic and diastolic function (Tsutsumi et al. 1999). With advancing gestation, the fetal MPI in both ventricles decreases indicating impaired cardiac function. Cardiac systolic function is estimated by the ventricular ejection force (VeFo), which is usually similar in both ventricles although the right ventricle normally dominates near term (Rasanen et al. 1997; Sutton et al. 1991). It estimates the early systolic flow and the energy transferred from ventricular myocardial shortening to eject the ventricular blood into the circulation (Sutton et al. 1991). During the second trimester, the fetal heart increases its capacity for volume handling. This is seen as an increase in ventricular ejection force in both ventricles (Rasanen et al. 1997; Rizzo et al. 1995; Sutton et al. 1991).

Diastolic function remains stable from early 2nd trimester until term (Tsyvian et al. 1998). Fetal diastolic function is often assessed by cardiac inflow blood flow velocity waveforms. In early first trimester pregnancy cardiac inflow pattern is monophasic, but a biphasic pattern emerges at gestational week 7 (Leiva et al. 1999). E-wave represents early atrial diastolic ventricular filling, whereas the A-wave is formed during subsequent atrial contraction. E- and A-wave velocity ratios (E/A-ratio) are similar in both ventricles, but the maximal velocities are higher in the tricuspid than mitral valve (Tulzer et al. 1994). With advancing gestation, E- and A-wave velocities and E/A-ratios increase (Tulzer et al. 1994).

Isovolumetric relaxation time (IRT%) is the time between the closure of semilunar valve and opening of the atrioventricular valve when the volume of the ventricle remains stable but the pressure decreases by active myocardial relaxation. IRT is used to describe diastolic function of the heart. IRT% has been shown to increase in fetal distress (Mäkikallio et al. 2003).

2.2.4 Peripheral circulation

Blood flow is directly proportional to the radius of the tube (vessel), and inversely proportional to blood viscosity, which in turn is closely related to hematocrit and the number of red blood cells (Poiseuille's law). Laminar flow (Q) has laminae of liquid flowing in separate layers, but flowing at different rates adjacent to each other in the longitudinal direction.

The resistance of each vessel is mainly adjusted by the radius. The pressure is maintained and adjusted individually for each vessel. Therefore, most of the resistance and regulation of the pressure in human and other mammalian systemic circulation is produced by small arterioles, the most abundant vessels with regulatory capabilities. These rest with the smooth muscle lining of the arteriolar walls. Resistance to flow (R) and blood volume distribution are nearly proportional to blood pressure. This has been demonstrated in near-term instrumented sheep where umbilical artery (UA) volume blood flow correlated positively with UA vascular resistance (Acharya et al. 2004).

The middle cerebral artery (MCA) detects fetal circulatory redistribution especially in pregnancies complicated by growth restriction and increased impedance to flow in UA (Mari & Deter 1992; Wladimiroff et al. 1987). During uncomplicated pregnancies, MCA PI increases until 30–32 gestational weeks (Konje et al. 2005). Towards term MCA PI decreases (Locci et al. 1992). In chronic hypoxemia fetal blood flow is distributed to the brain and the heart at the expense of the lower body (Peeters et al. 1979) also seen as a decrease in MCA PI (Locci et al. 1992). The aortic isthmus (Aoi) may be examined from the sagittal view of the aortic arch or from the three-vessel- and trachea-view. Usual measurements include velocities, pulsatility index, antegrade to retrograde VTI – ratio, and presence of retrograde flow during diastole (Mäkikallio et al. 2002b). Aortic

isthmus blood flow velocity profile changes with advancing gestation. At 20 weeks, an end-diastolic notch in the blood flow velocity profile is seen at end-systole that progressively disappears, and by 30 gestational weeks a short-term reverse diastolic flow is present (Fouron et al. 1994). Normally descending aorta has an antegrade flow throughout the cardiac cycle. During gestation the descending aorta blood flow increases with advancing weight until 37 gestational weeks, after which it decreases (Marsál et al. 1987). Aortic wall stiffness can also be measured by an echotracking device that may reflect aortic distensibility (Mori et al. 2011).

Other systemic arteries have also been investigated but are not often used in clinical practice. The coronaries in healthy fetuses are detectable in about 10% of fetuses at 31 gestational weeks and in 50% cases from 37 gestational weeks, but in severe IUGR are easy to locate at 27 gestational weeks already in 20% of cases (Baschat et al. 1997). Abdominal and renal arteries may be technically difficult to detect due to reduced diastolic flow (Tekay & Jouppila 2000; Mari et al. 1995; Mari et al. 1993).

The fetal systemic venous blood flow velocity waveform presents a pulsating pattern reflecting the changes in central venous pressure. The DV, IVC, and hepatic veins have a triphasic pattern with a wave depicting ventricular systole (S-wave), early diastole (D-wave), and atrial contraction (A-wave). The amount of umbilical blood flowing through DV decreases from 28% at 18 gestational weeks to 18% in early third trimester (Kiserud et al. 2000b). In healthy fetuses, the rest of the umbilical venous blood flows through the hepatic veins. Blood containing least oxygen is delivered by the right hepatic vein and IVC to the right atrium. The pulsatility of IVC and hepatic vein blood flow velocity waveform decrease towards term pregnancy (Hecher et al. 1994).

2.2.5 Fetal circulation and hypoxia

Glycolysis is the main energy source for the fetal and neonatal heart (Su & Friedman 1973). Starvation leads to fatty acid oxidation which becomes the predominant energy substrate, similar to the healthy adult heart (Rajabi et al. 2007). Human development depends on high energy supply and aerobic metabolism. Energy is derived from breakdown of glucose (Figure 3), and fatty and amino acid oxidative phosphorylation in the mitochondria (Semenza 2007). Hypoxia affects basal cellular metabolism, which is reflected by the ATP yield per amount of glucose. Fetal organs are well adapted to hypoxic insult (Su & Friedman 1973) but, especially in early pregnancy, poorly adapted to oxidative stress caused by electron leaks in combination with reduced O₂ levels and the subsequent increase in reactive oxygen species (ROS). Some ROS are free radicals that launch chain reactions ultimately causing damage. Free radicals are detected in increased amounts in placentas (Kossenjans et al. 2000) and fetal vascular endothelium (Loukovaara et al. 2005) in T1DM pregnancies.

Fetal development progresses in a relatively hypoxic environment. Despite low partial arterial pressure of oxygen (PO_2) being 25–30 mmHg in contrast to maternal 80–90 mmHg, the delivery of oxygen to tissues is similar. This is due to fetal red blood cells containing fetal hemoglobin which has a higher affinity for oxygen than adult hemoglobin. This facilitates placental O_2 uptake and increases O_2 saturation despite lower PO_2 . Adequate tissue oxygenation is further ensured by high fetal CO.

The healthy human fetus has an extraordinary capacity of adapting to intrauterine stress. The first adaptive response to hypoxemia is a short baroreceptor-mediated decrease in FHR. If intrauterine stress continues, the response switches to increased FHR and redistribution of blood flow in favor of the heart, brain, and adrenals. The heart and adrenals are favored even more than the cerebrum and the cerebellum (Sheldon et al. 1979). High weight-adjusted CO and redistribution of blood flow protect the fetus from hypoxic insult. If hypoxia persists for 30–60 min in a previously healthy individual, circulating catecholamines and vagal stimulation reduce the FHR towards the baseline (LaGamma et al. 1982).

Animal studies have increased the knowledge on how the fetal heart functions and how pressure is regulated in hypoxia. At near term, a sheep fetal heart with an increased afterload caused by placental embolization is able to increase contractility as a response to inotropic stimuli, even during metabolic acidemia (Acharya et al. 2011). This is confirmed by a sheep model, where fetal hypoxemia is rapidly followed by an increase in right ventricular and combined CO (Mäkikallio et al. 2006a). However, if fetal oxygen supply is already compromised, fetal adaptive mechanisms are insufficient.

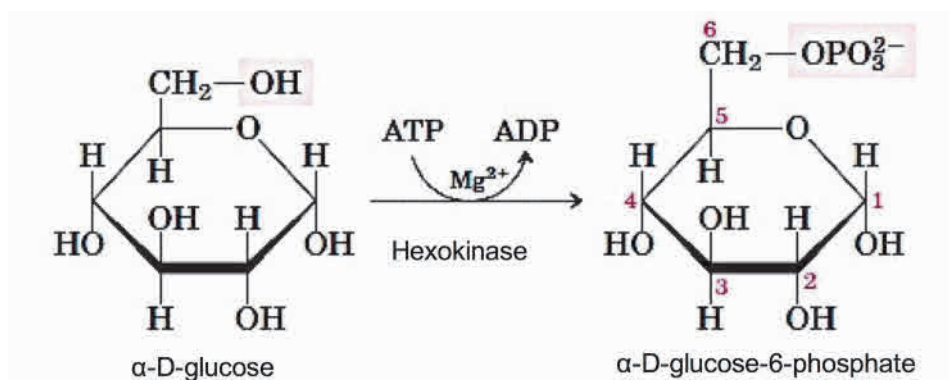


Figure 3. Phosphorylation of glucose precedes the use of glucose as an energy source. It stabilizes glucose molecules inside cells and activates glucose energy production. In mammals, glucose can be used for aerobic or anaerobic respiration, or fermentation. Aerobic metabolism generates 36 molecules of ATP, but some of these molecules are lost through the membranes and the cost of moving pyruvate and ADP into the mitochondrial matrix diminish the net gain to 29–30 ATP molecules per glucose. The equivalent energy yield for anaerobic metabolism for glucose is 2 molecules of ATP. Oxygen-deprived muscles use lactic acid fermentation when the electron transport chain is unattainable.

Another sheep study revealed that administering anti-hypertensive medication for maternal hypertension decreases maternal blood pressure efficiently, but reduces FHR and placental volume blood flow and increases PPA, pulmonary venous, and placental vascular impedances, and enhances retrograde component of AoI blood flow velocity waveform (Erkinaro et al. 2007). As an example, PPA blood flow velocity waveforms are seen in Figure 4. Worsening hypoxemia decreased placental volume blood flow further. Epinephrine reverses these changes, whereas norepinephrine decreases left ventricular CO (Erkinaro et al. 2007). During acute hypoxia, increased fraction of the umbilical venous return is directed to the DV and combined CO, right to left ventricular CO ratio, and the placental blood flow are decreased (Tchirikov et al. 2010). In IUGR, fetal combined CO is significantly diminished (al-Ghazali et al. 1989), and with advancing gestation the left ventricle being more dominant than normally (Rizzo & Arduini 1991).

Brain-sparing phenomenon is seen as a decreased MCA impedance resulting in increased diastolic flow that can occur weeks before antenatal FHR decelerations develop (Arduini et al. 1992). However, fetuses with increased impedance in umbilical artery and decreased MCA impedance still seem to tolerate vaginal birth induced stress despite fetal compromise (Dubiel et al. 1997), as evidenced by normal umbilical cord blood gases (Cheema et al. 2009). In studies with fetal absent or reversed end-diastolic (ARED) UA blood flow velocity waveform patterns, MCA impedance was again normalized and the maximal compensatory dilatation of MCA was lost, simultaneously

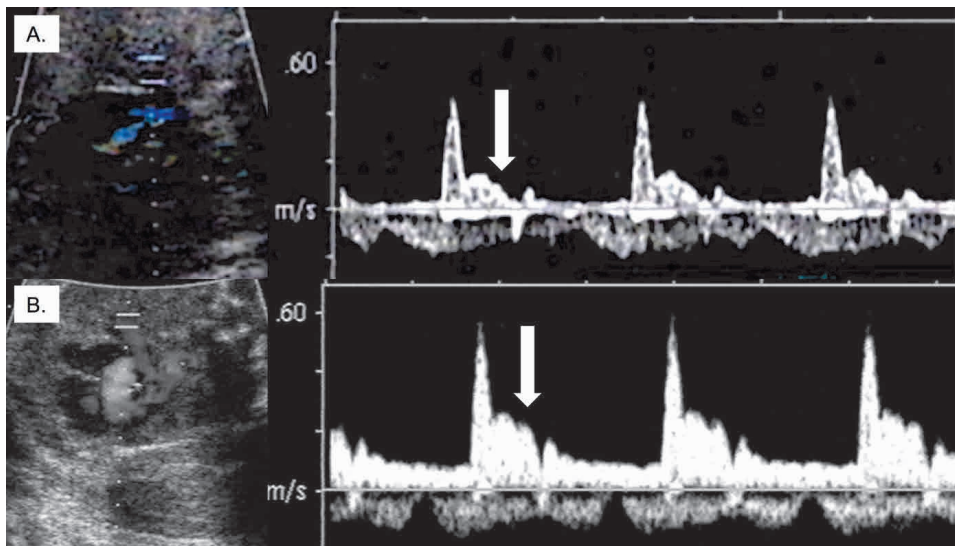


Figure 4. Human fetal proximal pulmonary artery (PPA) blood flow velocity waveforms. **A.** PPA diastolic blood flow (arrow) is decreased indicating increased vascular impedance. **B.** Pulmonary arterial vascular impedance has decreased and blood flow is enhanced as depicted by a higher blood flow velocity during diastole than above (arrow).

with the onset of abnormal fetal CTG-tracings (Weiner et al. 1994). However, in very-low birth infants, decreased MCA and increased UA vascular impedances are associated with reduced brain volumes at term (Maunu et al. 2007). During circulatory redistribution, adrenals and spleen (important for hormone production and erythropoiesis) seem to be favored (Dubiel et al. 2000; Dubiel et al. 1997; Capponi et al. 1997; Mari et al. 1996).

In animals with increased placental vascular resistance, retrograde blood flow in the Aol predicts poor delivery of oxygen to the brain (Fouren et al. 1999). In human growth restricted pregnancies, fetuses with retrograde Aol net blood flow show evidence that right ventricular CO redistributes from pulmonary to systemic circulation, while fetuses with antegrade Aol net blood flow do not show it (Mäkikallio et al. 2003). In human fetuses with placental circulatory insufficiency, decreased aortic isthmus blood flow velocity index, a ratio of systolic and diastolic flow to systolic flow, may indicate poor neurodevelopmental status in childhood (Fouren et al. 2005). Furthermore, high Aol pulsatility index values in IUGR fetuses correlate with adverse perinatal outcome (Del Río et al. 2008).

2.2.6 Fetal circulation and maternal hyperglycemia

Doppler ultrasonographic studies in insulin-dependent diabetic pregnancies are listed in Table 2. The results regarding fetal CO and stroke volume are conflicting due to varying sample sizes, methods, and study design. Some studies do not mention the type of diabetes, but that the mother was treated with insulin. Sample sizes varied between 2 to 155, though majority of the sample sizes were 20–40. Furthermore, ultrasonographic imaging techniques have improved and studies dating back 40 years might easily conflict with modern equipment derived data. A study of 17 women suggested that fetal right ventricular dominance found in normal pregnancies is not present in fetuses of T1DM mothers. On the other hand, increased combined CO is seen (Lisowski et al. 2003). An equally sized study from Finland found decreased contractility and left ventricular CO in fetuses of diabetic mothers (Räsänen & Kirkinen 1987). In newborns of T1DM mothers combined CO was similarly decreased (Van Bel et al. 1991). FHR is increased (Ursem et al. 1999), with increased accelerations during maternal hypoglycemia (Björklund et al. 1996). Furthermore, poor overall cardiac function is reported. Higher values of IMP suggesting cardiac dysfunction are seen at near term in T1DM fetuses (Russell et al. 2008; Tsutsumi et al. 1999). At early and mid-gestation the situation is opposite: MPI is lower in T1DM compared to control fetuses (Bui et al. 2013; Turan et al. 2011). Tissue Doppler measurements of cardiac inflow blood flow velocity waveforms were significantly lower in fetuses of mothers of gestational hyperglycemia, however, this did not associate with maternal glucose control (Ren et al. 2011). MAPSE is found to be decreased in fetuses of gestational diabetics, but similarly this finding does not associate with maternal glucose control (Atiq et al. 2017).

Table 2. Ultrasonographic findings on fetal circulation in insulin-dependent diabetic pregnancies.

Research group	Country	T1DM	IDDM	C	Gestational stage	Study design	Findings in fetuses/offspring of diabetic mothers
Björklund 1996	Sweden		10		3rd trimester	150-min hyperinsulinemic hypoglycemic clamp	UA PI ↑, FHR accelerations ↓, maternal adrenaline and noradrenaline plasma levels ↑
Botto 2003	The Netherlands		32	32	H18-36	liver volume relation to UV volume and Hb1Ac%	liver volume ↑ and positive correlation with maternal HbA1c%, UV flow/kg ↓
Bui 2013	USA	51		69	h17-23	pulsed-wave Doppler-tissue imaging vs spectral Doppler	pulsed-wave Doppler-tissue imaging is more sensitive, less variability, more precise: RV MPI ↓
Dicker 1990	Israel		108		mean 2nd, 3rd trimester		UA S/D ↑ in women who developed PE, IDDM+vasculopathy/hypertensive disorder+UA S/D ↑=IUGR neonate
Fadda 2001	Italy		67		last measurement before delivery	IDDM women without hypertension	UA PI ↑ in 34% of women, with a higher incidence of acute CS, and neonatal RDS, hyperbilirubinemia, hypoglycemia, NICU treatment
Gandhi 1995	USA	2	21	18	H20-h36	I h20-24, II h28-31, III h32-36; M-mode measurements	CATA-ratio, RVW, IVS ↑, RVFS%/LVFS% ↓, h32-36
Grunewald 1996	Sweden		24	25	2x 3rd trimester	well-controlled IDDM women, control women	UA and AUT PI did not decline as seen in control women
Jaeggi 2001	Canada	45		15	h19-h23, h33-h36	well-controlled, uncomplicated T1DM and fetal cardiac development	IVS ↑; no differences h33-36 in AV and PV diameters, TTPV, Vmax; MV and TV E/A-ratio, VFS%, CO, but PV Vmax ↑
Johnstone 1992	Scotland		128	170	h28 -> every 2 weeks	UA RI and HbA 1c%	UA RI similar in both groups; increased RI associates with fetal compromise, but is not excluded by normal UA RI values
Landon 1989	USA		35		h18-h38	repeated UA S/D measurements	UA S/D ↑ in women who developed PE, IDDM+vasculopathy+UA S/D ↑=IUGR neonate
Lisowski 2003	The Netherlands	17			h15 -> every 4 weeks	fetal central circulation in well-controlled T1DM pregnancies	↑ MV & TV outflow Vmean, Vmax, CO, CCO/kg; RVCOLLVCO did not decrease with advancing gestation
Macklon 1998	The Netherlands		10	10	h18-20	inter- and intraobserver variability in M-mode and cardiac flow measurements	IVS ↑ in 2nd trimester in IDDM fetuses; good reproducibility in measurements

Maruotti 2014	Italy	102		1 week before delivery	UA PI and birth weight relation in macrosomia	UA PI ↓ when fetus in macrosomic
Olofsson 1987	Sweden	40	?	early third trimester to term		Q(Dao) ↑, Q(UV) ↑, DAo PI ↓ in early third trimester; UA PI ↑, Q(DAo) ↑ near term; no correlation to White, HbA1c%, hypertension, but poor Doppler -> higher risk of labor distress
Pietryga 2005	Poland	155		h22-h40, last examination	placental Doppler findings and vasculopathy	a correlation between HbA1c and AUt & UA PI, pregestational vasculopathy correlated to AUt PI ↑, AUt & UA PI ↑ in SGA, AUt & UA PI ↓ in LGA
Reece 1994	USA	56	?		14/56 had vascular complications in advance	UA impedance ↑ in DM + vasculopathy pregnancies than in DM and control pregnancies, IUGR and neonatal metabolic complications but not Hb1A% correlated with impedance
Reece 1996	USA	30		h18-38, every 2 weeks	aortic velocity waveforms	labor distress and respiratory abnormalities in neonates had ↑ Ao impedance, but no correlation in neonatal outcome
Rizzo 1991	Italy	42		h20, h38	well-controlled IDDM women; IVS, E/A-ratios, TTPVmax AV/PV	IVS ↑ with no correlation to HbA1c%, E/A-ratios ↓ and related to IVS thickness
Rizzo 1992	Italy	14	10	h20-h36, every 4 weeks	IVS, LVW, RVW, E/A-ratios, TTPVmax AV/PV	normal increase over time for all indices, T1DM: IVS+LVW+RVW ↑, E/A-ratios did not increase over time, Vmax AV/PV ↑, no correlations to HbA1c%
Rizzo 1994	Italy	37		before CS	E/A-ratios, IVS; FHR, UV hematocrit, TTP AV/PV	IVS, hematocrit, FHR independently affected E/A-ratios of MV/TV
Rizzo 1995	Italy	16+11		h12, h16, h20	I control group, II IDDM with HbA1c% <8.5, III IDDM with HbA1c% >8.5	MV/TV E/A-ratio ↓, percentage of IVC retrograde flow ↑, UV pulsations ↑, high HbA1c% more likely to have circulatory changes
Russell 2008	Ireland	26	30	h13, h20, h36	longitudinal follow-up	h13: MV E/A-ratio ↓, IRT ↓, LV MPI ↑, h20: no differences; h36: RV MPI ↓, RVW ↑
Russell 2009	Ireland	45/21	39	h12-14, h20-22, h34-36	fetal serum markers and cardiac function 21/45, other UA, DV, MCA	pro-BNP & TnT ↑, pro-BNP and IVS thickness (not cardiac indices) positive correlation, TnT ↑ with poor perinatal outcome, HbA1c% ↑; TnT and h36 UA PI positive correlation
Räsänen 1987	Finland	18	51	late term pregnancy	I control, II hypertensive, III diabetic pregnancies	Ventricular dimensions, contractility, and LVCO ↓
Räsänen 1988	Finland	18	51	late term pregnancy	I control, II hypertensive (26), III diabetic pregnancies	DAo blood flow volume ↓, DAo impedance/blood flow volume and myocardial FS have an inverse correlation
Stuart 2010	Sweden	86		h24-h40+	DV hemodynamics in T1DM, GDM, reference values of gestational age	DV PIV ↑ (in T1DM and GDM), excluding SGA + UA/UV abnormal patterns -> DV PIV ↑, DV PIV and HbA1c correlate

Tsautumi 1999	Japan	30	50	h18-term, 1-2 postnatal d	I control, II IUGR, III IDDM, IV control neonate/IMP measure	h18-26 no significant differences between the groups, h27-40 MPI significantly higher IMP in IDDM, IUGR
Tsyvian 1998	Russia	15	25	h28-h36	left ventricular diastolic function: I control AGA, II SGA, III IDDM	MV inflow/LV filling rate integral ↓, A-wave ↑/E-wave ↓
Turan 2011	USA	63	63	h11-14	DV, MV/TV E/A-ratio, IMP, UA	IDDM had moderate-poor glycemic control, IRT% ↑, MV E/A-ratio ↓, LV/RV MPI ↓, DV/UA/FHR normal
Ursem 1999	The Netherlands	16	16	h12-21	UA velocities, FHR	increased FHR variability, UA Vmax ↑
Veille 1993	USA	40*	85	h17-24	M-mode: I control 85, II IUGR 27, III diabetes 65 (40 IDDM, 25 GDM)	Free wall & interventricular septum thickness ↑, left ventricular dilatation in the diabetic group (including GDM, IDDM)
Weber 1994	USA	9*	11	h20-26, h27-33, h34-40, 2-3 postnatal d	glycemic control correlation to newborn heart growth and function	TV E/A- and E/E+A-inflow -ratios did not increase during pregnancy as in controls
Weiner 1999	Israel	31	?	h22-h40, every four weeks	fetal central cardiac function	MV/TV E/A-ratio ↓ at h34-38, A-wave Vmax ↑ h34-38
Wong 2003	Australia	21	21	h30-32	M-mode, MV/TV inflow+E/A-ratios, AV/PV Vmax	8/21 good HbA1c 5.4% vs 9/21 poor control 7.4%; TV E/A-ratio lower in poorly controlled IDDM
Zielinsky 2011	Brazil	50?	23	h25-40	fetal aortic isthmus blood flow velocity waveforms in gestational and pregestational-diabetics	decreased aortic isthmus isthmus flow index in all diabetic fetuses
Wong 2010	Australia	82*	82*	h28-h40	DV PIV able to detect poor neonatal outcome	DV PIV abnormal in 25/82, 32 % of abnormal DV PIV IDDM poor neonatal outcome vs. 12% of normal DV PIV, DV PIV sensit. 53% + spes. 75% in predicting poor neonatal outcome
Zimmermann 1992	Finland	53	53	h17-h38, three times during period	UA and glycemic control, predictive value in perinatal morbidity	UA RI did not correlate to HbA1c% nor indicate poor neonatal outcome, UA RI similar in both groups, UV RI slightly ↑ in IDDM, no predictive value
Zimmermann 1994	Finland	43	43		AUT and A. arcuata	AUT supplying the placenta RI ↓, IDDM+vasculopathy AUT RI ↑, notch in IDDM ↑; AUT and a. arcuata no predictive value in IDDM pregnancies

* T2DM/GDM included. IDDM, insulin-dependant diabetes mellitus; UA, umbilical artery; PI, pulsatility index; FHR, fetal heart rate; UV, umbilical vein; RV, right ventricle; MPI, index of myocardial performance; S/D, systole to diastole ratio; PE, pre-eclampsia; IUGR, intra-uterine growth retardation; CS, cesarean section; RDS, respiratory distress syndrome; NICU, neonatal intensive care unit; CAT/A, cardiac area to thoracic area ratio; RWV, right ventricular wall; IVS, interventricular septum; RVFS, right ventricular fractional shortening; LVFS, left VFS; AV, aortic valve; PV, pulmonary valve; MV, mitral valve; TV, tricuspid valve; E/A, atrial E-wave to A-wave ratio; CO, cardiac output; Vmax, maximal velocity; RI, resistance index; Vmean, mean velocity; CCO, combined CO; Q, volume blood flow; DAo, descending aorta; SGA, small for gestational age; LGA, large for gestational age; Ao, aorta; IVC, inferior vena cava; PIV, pulsatility index for veins; BNP, B-type natriuretic peptide; TnT, troponin T; LVCO, left ventricular CO; DV, ductus venosus; SV, stroke volume.

At 11-14 gestational weeks, there are signs of fetal diastolic dysfunction in T1DM women with poor or moderate glycemic control. IRT% is greater and MV E/A-ratio lower in fetuses of T1DM women compared to control pregnancies (Turan et al. 2011). Later in gestation, contradictory results are found. Several studies found decreased TV E/A-ratio and in some studies also MV E/A-ratio was abnormal (Wong et al. 2003; Tsyvian et al. 1998; Rizzo et al. 1995; Rizzo et al. 1992a; Rizzo et al. 1991). It has been shown that in control fetuses TV E/A-ratio increases towards term, while in T1DM fetuses this increase is not observed (Weber et al. 1994). However, it seems that improved accuracy due to enhanced ultrasonographic machinery has enabled more consistent results. More recent studies see no differences between control and T1DM fetuses E/A-ratios in longitudinal studies from 1st trimester until term gestation (Russell et al. 2009; Russell et al. 2008). A commonly reported consequence of maternal T1DM is increased fetal cardiac interventricular septum and/or free wall thicknesses (Jaeggi et al. 2001; Macklon et al. 1998; Rizzo et al., 1994, Rizzo et al. 1991; Russell et al. 2009; Russell et al. 2008; Veille et al. 1993).

Anterior cerebral artery vascular impedance as a sign for brain-sparing (Dubiel et al. 2002) has been investigated, with no differences in insulin-dependent diabetic newborns compared to healthy controls (Van Bel et al. 1991). Normally, the descending aorta blood flow correlates with cardiac size and left ventricular CO, but in fetal growth restriction and maternal hypertensive disorders, and especially in T1DM pregnancies, the descending aorta blood flow vascular impedance decreases (Rasanen et al. 1988). During redistribution of the blood in fetal hypoxia, descending aorta vascular impedance increases (Mäkikallio et al. 2002b; Rasanen et al. 1988), but in diabetic pregnancies no increase in impedance is reported (Reece et al. 1996; Rasanen et al. 1988; Olofsson et al. 1987). Poor maternal glycemic control affects cardiac compliance and blood flow. DV PIV correlates with increased HbA1c% and is increased in fetuses with maternal T1DM (Stuart et al. 2010).

2.2.7 Fetal cardiac gene expression in experimental methods of maternal hyperglycemia

Maternal hyperglycemia in early pregnancy increases the risk for fetal malformations through excess apoptosis and generation of reactive oxygen species (ROS) (Yang et al. 2015). Several genes are associated with diabetic cardiac embryopathy. The cardiac expression levels of cell proliferation regulators *Gata4*, *Gata5* (Moazzen et al. 2014), *Cyclin D1* (Moazzen et al. 2014; Scott-Drechsel et al. 2013), and pro-apoptotic *Casp3*, and *Casp9* (Gutierrez et al. 2009) are decreased, and anti-apoptotic *Bcl2* (Gutierrez et al. 2009), anti-proliferative *p21* (*Cdkn1a*) (Scott-Drechsel et al. 2013), and pro-angiogenic *Vegfa* (Moazzen et al. 2014) increased in hyperglycemic animal models.

Cardiac glucose transporters are effected by maternal hyperglycemia. Cardiac gene expression of glucose transporter *Slc2a1* (*GLUT1*) is increased rapidly after glucose administration, whereas *Slc2a4* (*GLUT4*) responds to insulin administration and is insu-

lin-sensitive (Anderson et al. 2001). Other metabolic disturbances such as activation of reactive oxygen species and lipid abnormalities in diabetes affect cardiac gene expression. Streptozotocin (STZ) administration leads to upregulation of enzyme mRNA involved in the ketone body synthesis pathway (Cook et al. 2017). Abnormal lipid supply in the hyperglycemic fetal hearts leads to decreased levels of *PPARα*-involved genes (Kurtz et al. 2014; Lindegaard & Nielsen 2008). In addition, maternal pregestational mouse model demonstrates downregulated levels of genes associated with lipid metabolism: fatty acid translocase (*FAT/CD36*), fatty acid transport protein 1 (*FATP1*), and lipoprotein lipase (*LPL*) (Lindegaard & Nielsen 2008).

While several genes have abnormal expression levels in hyperglycemic fetal hearts, excess cardiac growth is not related to changes in cardiac gene expression (Cox & Marsh 2014). However, hyperglycemia does affect growth-related cardiac gene expression. Insulin and insulin-like growth factors are expressed at enhanced levels in fetal hearts according to studies on animal models of pregestational maternal hyperglycemia. Increased levels of *insulin-like growth factor (IGF) 1*, *IGF2*, *IGF1 receptor*, *IGF2 receptor*, *insulin receptor*, and *IGF binding proteins (IGFBP) 1, 2, and 3* in fetal hearts near term are reported in maternal hyperglycemia (White et al. 2015). Decreased levels of *Serca2 (Atp2a2)* may contribute to cardiac diastolic dysfunction in an animal model mimicking type 2 diabetes (Abe et al. 2002). Furthermore, the ratio of α -myosin heavy chain (MHC) (*Myh6*) to β -MHC (*Myh7*) increases as a sign of improved cardiac maturation in normal conditions (Hui et al. 2006). *Myh6* is the dominant adult cardiac myosin and has the highest ATPase activity, while *Myh7* has the lowest contractile capacity (Gustafson et al. 1987). In an animal model mimicking type 2 diabetes, adult rat hearts exhibit upregulated levels of *Myh7* and downregulated levels of *Myh6* (Gaber et al. 2014). Other myosins are produced in the fetal heart as well. Skeletal muscle type for adult myosin (*Myh2*) has decreased expression in the adult hearts of mice with type 2 diabetes mimicking disease (Takada et al. 2013). The embryonic skeletal muscle myosin (*Myh3*) is needed for normal fetal cardiac development (Rutland et al. 2011). Interestingly, sinoatrial node mRNA gene expression of natriuretic peptides (*Nppa*, *Nppb*) is increased in adult diabetic rats with decreased heart rate (Ferdous et al. 2016). In neonatal cardiac volume overload, cardiomyocytes exhibit high expression of *Nppa* and *Nppb* (Zhou et al. 2015).

2.3 The placenta

2.3.1 Placental morphology

The decidua basalis on the maternal uterine surface is the site where anchoring villi penetrate maternal endometrium. The junctional zone is the area where trophoblasts and maternal cells interact. The chorionic plate covers the fetal surface of the placenta. Intervillous space lies between the decidual and chorionic plates. Inside the placenta, villi containing capillaries, macrophages known as Hofbauer cells, and fibroblasts are surrounded by

trophoblast and syncytiotrophoblast layers. The villi function as nutrient and gas exchange site. Placental lobules are formed by the tertiary stem villi that penetrate the basal zone. The umbilical cord is formed by the 5th week. Histologically, umbilical arteries are surrounded by smooth muscle cells and inner loose and irregular cells (Meyer et al. 1978).

2.3.2 Uteroplacental circulation

The blood flow through the umbilical cord increases from 35 ml/min at 20 gestational weeks to 240 ml/min by 40 gestational weeks (Kiserud et al. 2000b). UA blood flow velocity waveform patterns reflect the number of functional arteriolar tertiary villi in the human placenta (Trudinger et al. 1985). The uterus receives most of its blood supply through the uterine arteries. Both uterine and arcuate arteries have high vascular impedance in early pregnancy, visible as early diastole notches; these disappear in the

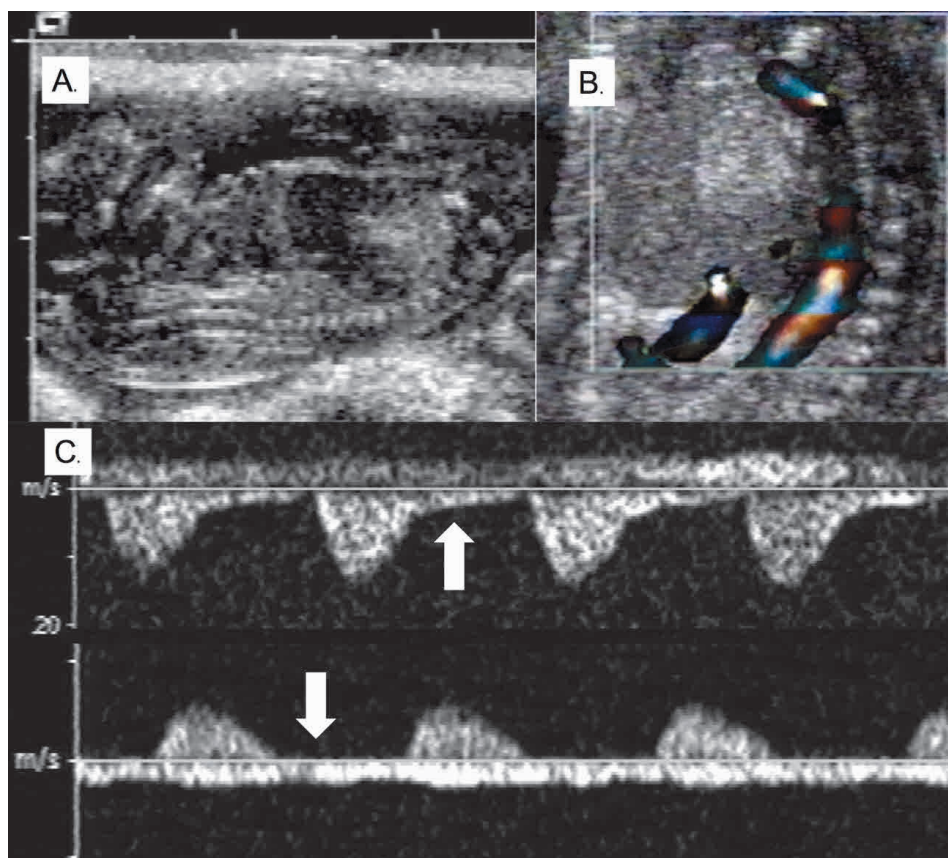


Figure 5. Umbilical artery blood flow velocity waveform in a rat fetus at 20 gestational days (GD) (A). B. Color-Doppler shows the descending aorta. Ductus venosus is identified anteriorly to it with a light, turbulent blood flow velocity pattern. C. Umbilical artery blood flow velocity waveforms. Arrows note the presence (above) or lack (below) of diastolic blood flow in the umbilical artery. The top pattern is from the fetus of a healthy control dam, and the waveform at bottom is recoded from a fetus with maternal hyperglycemia.

beginning of the second trimester. Until 26 gestational weeks early diastolic notch in uterine artery may be physiological (Schulman et al. 1971). The uterine artery impedance is lower on the side of placentation (Bewley et al. 1989). Significant disturbances of the placental circulation are seen as persistent uterine artery notches on both sides, increased impedance, or an abnormally large difference between the uterine artery impedances (Thaler et al. 1992).

Spiral artery remodeling and trophoblast invasion are an essential part of normal placental development. Normal fetal circulation requires low spiral artery vascular impedance that decreases until the beginning of the second trimester. Thereafter, it remains stable until late term (Kurjak et al. 1997). In pregnancies with IUGR and pre-eclampsia, spiral arteries are more sensitive in detecting early signs of emergent fetal distress than uterine arteries (Babic et al. 2015), but altogether spiral artery impedance is abnormal in SGA and pre-eclamptic pregnancies and is associated with poor perinatal outcome (Murakoshi et al. 1996). Reductions in the amount and structural abnormalities of spiral arteries lead to increased impedance in UA (Giles et al. 1985).

Umbilical circulation can be detected by Doppler ultrasonography as of gestational week 7 and a diastolic component is seen as of the 16th gestational week (Wladimiroff et al. 1991). Placental blood flow increases in proportion to fetal growth and weight gain (Sutton et al. 1990). However, the amount of CCO directed to the placenta decreases from 30% at gestational week 20 to approximately 20% at gestational week 32 (Kiserud et al. 2006). UA impedance decreases during gestation, especially during second trimester, due to increasing blood flow velocities (Acharya et al. 2005). Umbilical vein pulsations are physiological up to 13 gestational weeks (Rizzo et al. 1992b). The blood flow in the umbilical vein is nonpulsatile in healthy fetuses as of the second trimester (Rizzo et al. 1992b).

2.3.3 Uteroplacental circulation in hypoxia

Placental oxygenation is low in the 1st trimester and increases after the 12th gestational week. PO₂ remains largely at 45–48 mmHg until early term gestation (Schneider 2011). Experimental studies on rhesus monkeys show that placental ischemic injury and compromised uterine hemodynamics may occur simultaneously (Frias et al. 2011). A fetal sheep model of placental insufficiency showed that worsening hypoxemia increases pulsatility of DV blood flow velocity waveform. However, development of acidemia did not further increase DV pulsatility or decrease CO even before imminent fetal death (Mäkikallio et al. 2010).

A mathematical model showed a steep increase in UA impedance once 60–90% of intraplacental vasculature was obliterated (Thompson & Trudinger 1990). Furthermore, studies on sheep with placental embolization show that UA vascular volume blood flow and UA vascular impedance have a negative correlation (Acharya et al. 2004). ARED

waveform in UA indicates severely increased placental vascular resistance (Thuring et al. 2012; Stewart et al. 1990). Furthermore, UA ARED finding is associated with an enhanced risk for poor neonatal outcome (Rosner et al. 2014). Increased pulsatility in systemic venous blood flow velocity waveforms can be found in IUGR fetuses with UA ARED (Hecher et al. 1995; Reed et al. 1990).

Fetal veins, like umbilical vein, are affected only in later stages of fetal hypoxia. Atrial pulsations in umbilical vein are seen in hydropic fetuses with heart failure and predict increased perinatal mortality (Gudmundsson et al. 1991). These pulsations are suspected to be a late sign of fetal impending death due to hypoxia (Gudmundsson et al. 1996). UV pulsations have been classified as single or double – the latter signifying a higher risk of perinatal mortality (Hofstaetter et al. 2001).

2.3.4 Placental morphology in maternal hyperglycemia

In human T1DM pregnancies, various morphological changes of the placenta as compared to non-diabetic pregnancies have been reported. Nucleated fetal red blood cells are increased and placental structural abnormalities, such as fibrinoid necrosis, villous immaturity, and chorangiosis are observed (Evers et al. 2003). In T1DM pregnancies where fetal growth is considered appropriate for gestational age, placentas are relatively larger than in control pregnancies with appropriately grown fetuses. Intrauterine fetal death in T1DM pregnancies is associated with low placental weight. (Evers et al. 2003). However, in another study placental histology revealed only minor alterations in the T1DM placentas when compared to healthy control placentas, i.e. increased intervillous space and abnormalities in villi development (Nelson et al. 2009). Also increased thickness of muscle layer in the umbilical arteries and altered expression of genes regulating vascular development and function are found in the umbilical cord in diabetic pregnancies (Koskinen et al. 2015).

Experimental mouse (White et al. 2015) and rat (Padmanabhan & Shafiullah 2001) models have shown that placentas are heavier in maternal hyperglycemia, but the weight adjusted to fetal weight is not. Fluctuations in placental weight gain have been reported with advancing gestation (Korgun et al. 2011). In rats, a connection between fetal growth restriction and hyperglycemia was seen (Padmanabhan & Shafiullah 2001). At gestational day 18, the decidua basalis is thin and displays necrotic giant cells, lymphocytic aggregations, perivascular fibrosis, cysts, and degenerated glycogen containing cells when compared to control placentas. Furthermore, signs of inflammation and increased amounts of Hofbauer cells are present in hyperglycemic placentas (Sisino et al. 2013). Also, the levels of placental cytokines and chemokines are increased in a primate model of maternal high fat diet (Frias et al. 2011).

2.3.5 Uteroplacental circulation in maternal hyperglycemia

It seems that uterine artery notching is more frequent and uterine artery vascular impedance is higher in human T1DM pregnancies than in uncomplicated pregnancies (Zimmermann et al. 1994). The physiological decline in the uterine artery impedance is reportedly blunted (Grunewald et al. 1996). Increased uterine artery vascular impedance is associated with maternal vasculopathy and fetal growth restriction (Pietryga et al. 2005).

UA vascular impedance in human T1DM pregnancies has been studied by several investigators. Increased UA impedance is associated with increased maternal circulating catecholamine levels (Björklund et al. 1996), pre-eclampsia or other hypertensive disorders (Dicker et al. 1990; Landon et al. 1989), maternal vasculopathy (Pietryga et al. 2005; Reece et al. 1994; Dicker et al. 1990; Landon et al. 1989), gHbA1c% levels (Russell et al. 2009; Pietryga et al. 2005), and growth restriction (Pietryga et al. 2005) in diabetic pregnancy. However, some studies do not show any differences in UA vascular impedance when compared to control pregnancies (Turan et al. 2011; Zimmermann et al. 1992). It seems that LGA human T1DM fetuses have decreased impedance in UA Doppler velocimetry (Maruotti et al. 2014; Pietryga et al. 2005). The vascular impedance in the descending aorta may be increased or unchanged (Reece et al. 1996; Grunewald et al. 1996; Olofsson et al. 1987).

Some studies have found that the pulsatility of DV is increased and may predict fetal outcome in T1DM pregnancies (Wong et al. 2010; Stuart et al. 2010). Studies concerning umbilical vein blood flow patterns reveal conflicting results (Rizzo et al. 1995; Zimmermann et al. 1992).

2.3.6 Placental gene expression in maternal hyperglycemia

Embryopathy is associated with poor uterine perfusion in hyperglycemic pregnancies (Zabihi et al. 2008). Placental expression of genes involved in protection from oxidative stress are decreased for *catalase (Cat)*, *glutathione peroxidase 1 and 2 (Gpx)*, *paired box protein 3 (Pax3)* and *vascular endothelial growth factor (VEGF) 1* in a rat model (Zabihi et al. 2008). Excess production of reactive oxygen species (ROS) occurs in experimental settings in untreated pregestational maternal hyperglycemia (He et al. 2016). Gestational diabetes mellitus in humans and rats induces pro-inflammatory and ROS-inducing genes (Tang et al. 2015)

Placental growth is affected by maternal hyperglycemia both in humans and animal models. In murine placentas, expression of genes *IGF1*, *IGF2*, *IGF2 receptor*, *IGFBP1* and *3* controlling growth is upregulated near term (White et al. 2015). Placental angiogenesis affects placental growth. Antiangiogenic processed forms of placental prolactin (*bone morphogenetic protein 1*, *cathepsin D*) are upregulated in diabetic and hyperglycemic pregnancies (Perimenis et al. 2014). Indeed some genes of angiogenic factors

are upregulated (*fractalkine 1, fractalkine 1 receptor*) (Szukiewicz et al. 2013) whereas others (*VEGF1, VEGF receptor 1 and 2 and receptor Tie2, angiopoietin 1 and 2, basic fibroblast growth factor (FGF) 2, FGF2 receptor*) remain unchanged in diabetic placentas (Janota et al. 2003). Further, maternal diabetes leads to increased term placental *basic FGF* and receptor gene expression levels (Di Blasio et al. 1997). Some studies have reported increased placental activation of genes involved in cell adhesion, growth factor response, and nutrient transport, more specifically matrix metalloproteinases and genes associated with inflammation (Kappen et al. 2012; Salbaum et al. 2011). Placental growth affects fetal growth, as depicted by the placental *leptin* gene expression, which increases fetal growth in human T1DM pregnancies (Iciek et al. 2013)

Placental metabolism is affected by hyperglycemia during pregnancy. Gene expression levels of glucose transporters *Slc2a1 (GLUT1)* (Gaither et al. 1999), *Slc2a4 (GLUT4)*, *Slc2a9 (GLUT9)* (Stanirowski et al. 2016) are increased in human T1DM pregnancies. Furthermore, STZ-induced untreated hyperglycemia leads to upregulation of *Slc2a3 (GLUT3)* gene, which codes for the nutrient transfer protein located in the labyrinthine zone (Boileau et al. 1995). The expression of genes involved in placental metabolism suggests that lipids are primary nutrients in diabetic placentas (Radaelli et al. 2009). Downregulated LPL (Radaelli et al. 2009), upregulated *endothelial* and *hormone-sensitive lipase* (Lindegard et al. 2006) expression has been reported. Furthermore, in an untreated maternal hyperglycemia rat model, expression of genes involved in placental Ca^{2+} and Mg^{2+} accretion is decreased (Husain et al. 1994). Drug transport by the placenta is similarly downregulated in an untreated maternal hyperglycemia model (Anger et al. 2012).

2.4 Animal models of maternal hyperglycemia

2.4.1 Streptozotocin

Streptozotocin (STZ) increases serum glucose concentration, urine volume, glucosuria, ketonuria, serum immunoreactive insulin (IRI), and pancreatic IRI content (Junod et al. 1969). It has an established role in creating animal models of different types of diabetes and hyperglycemia. It destroys pancreatic β -cells, and is clinically used for treatment of cancer of the islet of Langerhans. Although there are several other models of hyperglycemia and diabetes, STZ-derived models are considered the model-of-choice of experimental hyperglycemia (Arison et al. 1967).

2.4.2 Animal models of pregestational hyperglycemia

Maternal hyperglycemia during rat pregnancy disturbs normal capillary and vessel formation in the embryo and increases fetal malformations in a dose related fashion (Pinter et al. 1986). STZ-induced hyperglycemia in murine dams decreases vascular

endothelial growth factor (VEGF) levels and causes vasculopathy in the embryo, proving that hyperglycemia modulates the VEGF-pathway (Pinter et al. 2001). In hyperglycemia-exposed chicken embryos, it has been shown that angiogenesis does not occur normally, even though the VEGF-pathway is intact (Larger et al. 2004). In a rat model, the embryo hearts have malformations and decreased expression of VEGF indicating that increased oxidative stress process is activated at these sites (Roest et al. 2009). Additionally, cyclo-oxygenase 2 (COX2) activity is reduced in malformed rat fetuses of STZ-induced hyperglycemic pregnancies (Al-Matubsi et al. 2010).

Later in pregnancy, fetal septal and left ventricular wall thicknesses are increased at gestation near term in a mouse model of maternal STZ-induced pregestational hyperglycemia. Transient diastolic dysfunction, prolonged isovolumetric relaxation time, and abnormal cardiac growth are found. However, these findings are normalized at term to 7 days of postnatal life (Corrigan et al. 2013). It seems that hyperglycemia directly causes cardiac wall excess growth (Gordon et al. 2015). Studies concerning placental and fetal growth abnormalities in rats have suggested glucocorticoid involvement (Korgun et al. 2011), poor local immunological responses (Groen et al. 2015), and poor uterine hemodynamics (Chartrel et al. 1990).

Rat neonates from pregnancies with STZ-induced pregestational maternal hyperglycemia have decreased expression of pulmonary gene pathways of cell proliferation and oxidative stress (Koskinen et al. 2010). The long-term effects of maternally STZ-induced hyperglycemia on rat offspring include increased blood pressure, vascular dysfunction, poor adrenergic responses, and increased angiotensin-converting enzyme (ACE) activity in the heart, kidney, and lung (Wichi et al. 2005).

2.4.3 Rat pregnancy characteristics

Human and rodent circulatory anatomy is almost identical (Mestas & Hughes 2004). Laboratory rats have bicornuate uteri, gestation lasts 21-22 days, and the placenta is discoid. After implantation, a peripheral trophoblastic giant cell zone develops in the endometrial zone. The placenta is labyrinthine, has a hemotrichorial fine-structure, and is implanted above the mesometrial uterine side (de Rijk et al. 2002). There are three cell layers between the maternal and fetal circulations: an outer layer of cytotrophoblast cells and two inner layers of syncytial trophoblast cells (Aoki et al. 1978). Litter sizes are usually 10-20 pups.

2.5 Biomarkers of fetal wellbeing

2.5.1 Natriuretic peptides

Natriuretic peptides are essential for normal fetal cardiac development and are produced during cardiac distress to protect the myocardium. Atrial natriuretic peptide

(ANP) (Flynn et al. 1983) and brain B-type natriuretic peptide (BNP) (Sudoh et al. 1988) are produced by the cardiomyocytes. Cardiomyocyte stretch and cardiac wall stress due to pressure or volume load first launches ANP from atrial storage granules (de Bold et al. 1996). Continued stimuli to produce natriuretic peptides leads to increased gene expression within one day for ANP from the atrial and ventricular myocytes (Kinnunen et al. 1992) and within one hour for BNP from ventricular myocytes (Mäntymaa et al. 1993). In the developing human fetal heart at 17 and 19 weeks of gestation, ANP but not BNP, is produced in the ventricular myocytes (Takahashi et al. 1992). However, in pregnancies with cardiac stress fetal ventricular BNP mRNA is significantly increased (Mäkikallio et al. 2006b). In human T1DM pregnancies, elevated umbilical cord serum levels of NT-proANP and NT-proBNP, ANP and BNP cleavage products, have been reported (Russell et al. 2009; Girsén et al. 2008; Halse et al. 2005).

In adults, potential stimuli to ANP release are atrial stretch, hypoxia (Lew & Baertschi 1989), increased heart rate (de Bold et al. 1996), sympathetic stimulus (Lew & Baertschi 1989), and several humoral factors such as endothelin-1 (Uusimaa et al. 1992), nitric oxide (Leskinen et al. 1995), acetylcholine, angiotensin, prostaglandins, glucocorticoids, and thyroid hormones (Rosenzweig et al. 1991). Increased secretion of BNP is always preceded by increased expression of BNP mRNA, whereas ANP, since it is stored in intracellular granules, can be released rapidly by exocytosis in response to physiological or pathophysiological stimuli. Both natriuretic peptides relax vascular smooth muscle. They act on the kidney to reduce extracellular fluid volume and decrease blood pressure. In the developing fetus, ANP has a role in controlling mitotic activity (Thornburg et al. 2011). In adult animals, ANP depresses hypertrophic growth responses in cardiomyocytes (Horio et al. 2000).

2.5.2 Troponin T

Troponin T (TnT) is a cardiospecific protein that is released during myocardial ischemia (Boo et al. 2005). Cardiac TnT is a thin filament protein involved in cardiac contraction in the sarcomere-binding Z-zones as troponin-tropomyosin bound complexes. During relaxation troponin-tropomyosin inhibits actin-myosin-interaction. After cardiomyocyte damage, TnT is detected in serum within 3–12 hours, and returns to baseline in 5–14 days (Donnelly & Millar-Craig 1998). TnT gene mutations in humans lead to hypertrophic cardiomyopathy, which in animal models seem to affect myosin crossbridges within the myocardial structure (Gollapudi & Chandra 2016). Cord blood TnT concentration does not change with advancing gestation, mode of delivery, nor fetal weight or sex (Clark et al. 2001). Increased TnT levels have been reported in newborn umbilical cord serum in pregnancies complicated by severe placental insufficiency combined with increased afterload (Mäkikallio et al. 2000), and in T1DM pregnancies with increased myocardial growth and poor perinatal outcome (Russell et al. 2009).

2.5.3 Erythropoietin

In human T1DM pregnancies, increased amniotic fluid erythropoietin level are associated with chronic fetal asphyxia, and fetal and neonatal morbidity (Escobar et al. 2013). Erythropoietin is already produced in the embryonal yolk sac (Yasuda et al. 2002), and is assumed to have a role in feto-placental development. Maternal erythropoietin is not transported across the placenta (Malek et al. 1994) and after the embryonal period it is produced in the fetal liver, kidney, spleen, bone marrow (Dame et al. 1998), and in the placental trophoblast cells (Conrad et al. 1996). However, in normoxemia, the placenta does not contribute to the circulating erythropoietin levels, whereas in chronic hypoxia both the placenta and kidneys produce large quantities of erythropoietin with placental production surpassing the renal (Davis et al. 2003). A major stimulus for erythropoietin production is tissue hypoxia (Pagel et al. 1991). An acute hypoxic response increases erythropoietin production within a few hours (Turner et al. 2016; Widness et al. 1981), but the severity of hypoxia is not reflected in erythropoietin levels (Turner et al. 2016). Erythropoietin stimulates erythroblast formation, erythrocyte maturation, and decreases cell death (Koury & Bondurant 1990). It may also protect tissues from ischemic damage as in the myocardium (Lipsic et al. 2006) and in paracrine activated erythropoietin/erythropoietin-receptor in the brain (Sakanaka et al. 1998).

Interestingly, circulating erythropoietin is not stored and after a prolonged hypoxic insult, circulating levels reflect transcriptional level stimuli (Goldberg et al. 1991). *In vitro*, endogenous erythropoietin levels of the amniotic fluid and plasma retain 70% of the original activity after incubation of 21 days (Schmidt et al. 2004). However, not all erythropoietin stimuli are hypoxia-induced, since erythropoietin is produced by the kidneys even in the absence of hypoxia (Halt et al. 2016). Inflammation increases hepcidin synthesis which may lead to erythropoietin resistance or a blunted response, as seen in hemodialysis patients responding poorly to high recombinant human erythropoietin therapy (Ribeiro et al. 2016). Similarly nitric oxide, an oxidative stress product, stimulates erythropoietin in isolated perfused rat kidneys (Yoshioka & Fisher 1995) and increases gene expression *in vivo* (Todorov et al. 2000). Retinoic acid has antioxidant properties and increases erythropoietin production in embryonal carcinoma cell lines (Kambe et al. 2000) and in murine yolk sacs (Yasuda et al. 1996).

In women with T1DM high antenatal amniotic fluid erythropoietin levels have been associated with increased birth weight, high UA pCO₂ levels, increased maternal gHbA1c%, low UA pH, neonatal hypoglycemia, and low UA pO₂ (Teramo et al. 2004b). Umbilical cord serum erythropoietin levels have been shown to increase with worsening placental circulatory compromise (Girsén et al. 2007).

2.5.4 Activin A

Activin A is produced by the gonads, pituitary gland and placenta. It is expressed in the placental maternal-fetal interface and induces trophoblast invasion. It seems to in-

crease human trophoblast cell endothelial-like tube formations by up-regulating VEGF-A production (Li et al. 2015). Activin A has fibroblast activator potential and its neonatal serum and cerebrospinal fluid concentrations have predictive value in hypoxic-ischemic encephalopathy (Lv et al. 2015).

2.5.5 Soluble vascular endothelial growth factor receptor-1 (sFlt-1)

sFlt1 is the soluble form of vascular endothelial growth factor (VEGF) receptor-1, an antiangiogen. VEGF is a mitogen that stimulates endothelial cell proliferation. It is a key regulator of angiogenesis. Two receptor tyrosine kinases, VEGFR-1 (Flt-1) and VEGFR-2, mediate its activity, and Flt-1 has a soluble form (sFlt-1) produced by endothelial cells by differential splicing of the gene. Therefore Flt-1 activity is antagonized by sFlt-1 (Hornig et al. 1999). sFlt-1 is produced by endothelial cells and only 5% is detectable as free kinase whereas the rest is bound by ligands i.e. VEGF-A and placental growth factor (PlGF). Hypoxia induces sFlt-1 production from endothelial cells. sFlt1 appears to reduce the transmembrane availability of the bound ligands, and consequently functions as an antagonist of VEGF action (Hornig et al. 2000). Higher levels of sFlt-1 and lower levels of PlGF have been reported in pre-eclampsia (Palomaki et al. 2015). Similarly in diabetic pregnancies, PlGF and sFlt-1 function as predictors of increased risk for developing pre-eclampsia (Cohen et al. 2014).

3 AIMS OF THE STUDY

Previous studies have investigated the effect of maternal hyperglycemia on fetal circulation. Results have been conflicting. Based on these studies, we hypothesized that STZ-induced maternal hyperglycemia in a rat model affects fetal cardiac function and hemodynamics resulting in cardiac dysfunction. We also hypothesized that maternal pregestational hyperglycemia leads to placental, morphologic, inflammatory, and gene expression changes with hemodynamic consequences. Furthermore, we estimated that the effects of hyperglycemia on the fetal myocardium extend to the cellular and gene expression levels in fetuses and offspring of rats with pregestational maternal hyperglycemia. In human fetuses of diabetic mothers the aim was to investigate, whether maternal insulin therapy ameliorates fetal cardiac, hemodynamic, and placental abnormalities.

The specific aims of the study were:

1. To find out how maternal pregestational hyperglycemia in a rat model affects cardiac function and structure of the fetus (I) and cardiac gene expression and structure of the offspring (III).
2. To characterize placental hemodynamics, morphology, gene expression, and inflammatory biomarkers in a rat model of maternal hyperglycemia, and their effect (II).
3. To investigate changes in fetal cardiac function, biochemical markers of fetal well-being, and placental gene expression in human T1DM pregnancies (IV).

4 MATERIALS AND METHODS

4.1 Subject characteristics and study design

4.1.1 Rat model of maternal hyperglycemia (I-III)

The study protocol was approved by the University of Turku Laboratory Animal Care and Use Committee (permission no. 1664/06). Animal care at the university conforms with the European Community Council Directions 86/609/EC and follows the principles of laboratory animal care set down by the Council. All rats were purchased from the University of Turku Central Animal Laboratory and housed in dedicated pathogen-free conditions in room air with a 14:10-h light-dark cycle. The animals had free access to standard laboratory rodent food and water.

To induce hyperglycemia, female Sprague-Dawley (SD) rats were injected before mating intraperitoneally with streptozotocin (STZ) 35 mg/kg (Sigma, St Louis, MO) dissolved in citrate buffer (0.01 mol/l, pH 4.5) (Rees & Alcolado 2005). When necessary, 1–4 additional doses of 15 mg/kg STZ were given every two days. The tail vein blood glucose levels were collected 2 days after STZ-injection with an Elite glucometer (Bayer, Leverkusen, Germany) before noon (Table 3). All female rats were caged overnight with a male. Gestational day (GD) 1 was the day of a positive vaginal smear. Maternal blood samples during gestation were collected under general anesthesia under ultrasonographic examinations apart from GD 1 when the dams were conscious. Maternal pregestational samples were collected from conscious animals.

Table 3. Maternal glucose concentrations (mmol/l) in control and maternal hyperglycemia groups.

Variable	n	Control	n	Hyperglycemia
Studies I and II				
Pregestation			10	25.0 (5.3)
GD 13-14	20	6.2 (1.2)	9	29.6 (4.6)*
GD 16-17	20	4.4 (0.8)	9	29.3 (3.3)*
GD 19-21	20	4.0 (0.8)	10	29.6 (4.5)*
Study III				
Pregestation	2	5.1 (0.2)	7	20.9 (2.1)*
GD 15	3	4.0 (0.5)	7	25.0 (3.8)*
Postnatal feeder	4	5.4 (2.1)		

GD, gestational day. All values are mean (SD). * $p \leq 0.05$.

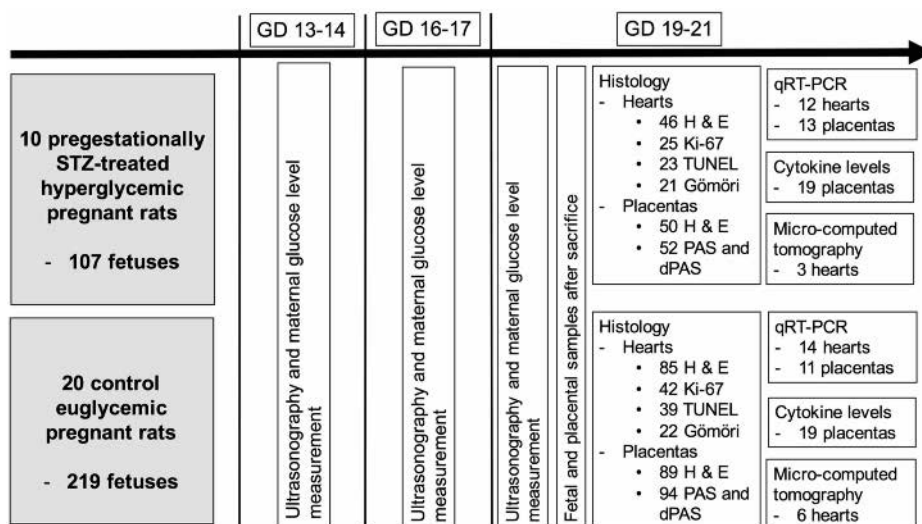


Figure 6. Rat pregnancy protocol flow chart.

4.1.2 Rat model of maternal hyperglycemia and pregnancy (I, II)

The protocol is shown in Figure 6. Ultrasonography was performed serially under isoflurane-induced (3–4%) anesthesia in an oxygen-air mixture into a chamber and maintained with 1.5–2% isoflurane-oxygen-air mixture via a mask. The lack of withdrawal reflexes was recorded as a measure of the depth of anesthesia, and loss of toe and tail-pinch reflexes marked full unconsciousness. After the last ultrasonographic examinations, the unconscious dam was humanely euthanized in a CO₂ chamber followed by cervical dislocation. A V-shaped incision was used to access the maternal abdomen, and the uterine horns and fetuses were identified by their location on the ultrasonography. Instant fetal decapitation was performed with specially designed sharp blades. The number of fetuses in hyperglycemic dams varied from 9 to 12 and in control dams from 10 to 16. From each dam, fetuses were randomly assigned for histological analyses, micro-computed tomography (CT), or gene expression analyses of the hearts, and either to histological or gene expression analyses of the placenta.

4.1.3 Rat model of maternal hyperglycemia and the rat neonatal heart (III)

Study protocol is in Figure 7. SD rats with STZ-induced hyperglycemia prior to mating and healthy pregnant female SD rats delivered spontaneously at term (approximately 22 days after conception). After birth, newborn pups from both groups were instantly separated from their own dam and weaned by healthy euglycemic dams. Glucose samples were collected from conscious animals using an Elite glucometer (Bayer, Leverkusen, Germany).

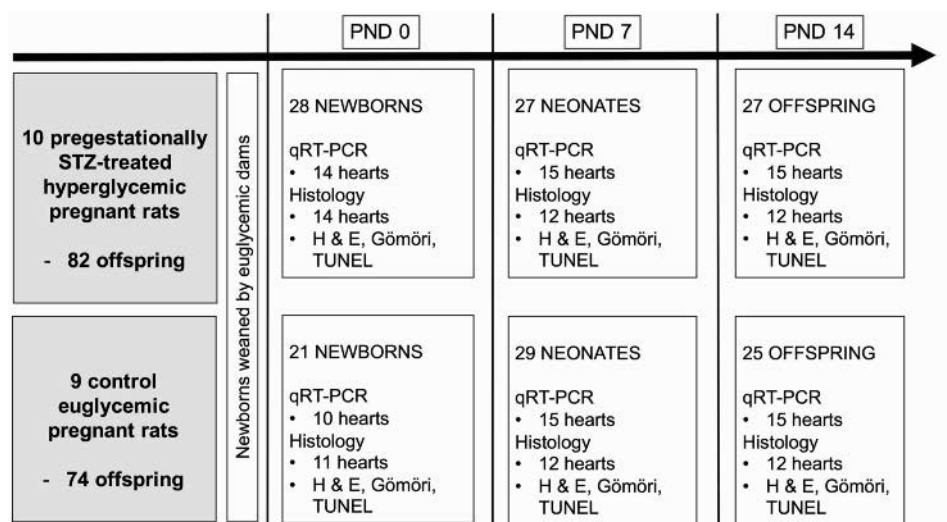


Figure 7. Rat offspring protocol flow chart.

All pups from the same litter were sacrificed simultaneously under rapid intraperitoneal injection of pentobarbital sodium (200 mg/kg) anesthesia and euthanized by cervical dislocation. PND 14 was selected as the last day of the experiment because newborn lungs complete alveolarization and the cardio-respiratory system is mature (Burri 2006). Hearts and bodies were weighed and randomly processed for analyses. The heart and lung blocks were randomly divided for histological or gene assays.

4.1.4 Human T1DM pregnancies (IV)

The Ethics Committee of the Hospital District of Southwest Finland approved the research protocol (167/2005 §183). Study IV included T1DM and healthy control women with singleton pregnancies (Figure 8). The women were attended by the department of obstetrics and gynecology of the Turku and Oulu University Hospitals, Finland.

Table 4. Characteristics of control and T1DM pregnancy groups.

Variable	Control	T1DM
n	67	33
Maternal prepregnancy characteristics		
Maternal age (years)	28.0 (4.0)	28.5 (4.9)
Prepregnancy BMI (kg/m ²)	23.2 (3.4)	26.1 (4.9)*
Smoking	2 (3.0 %)	5 (15.2 %)**
Nulliparous	42 (62.7 %)	17 (51.5 %)
White class		
B		6 (18.2 %)
C		8 (24.2 %)
D		6 (18.2 %)
R		8 (24.2 %)
F		1 (3.0 %)
D+R		1 (3.0 %)
R+F		4 (12.1 %)
gHbA1c%		7.9 (1.6)
Basal insulin dose		26.8 (19.9)
Prandial insulin dose		26.8 (19.9)
Previous illness		
Essential hypertension	3 (4.5 %)	5 (15.2 %)*
Thyroid dysfunction	2 (3.0 %)	6 (18.2 %)*
Asthma	2 (3.0 %)	3 (9.1 %)
Polycystic ovary syndrome	2 (3.0 %)	2 (6.1 %)
Hypercholesterolemia	1 (1.5 %)	1 (3.0 %)
Pregnancy characteristics		
gHbA1c% (32 weeks)		6.4 (0.9)
Hypoglycemia during pregnancy (plasma glucose <2,6 mmol/l)		15 (45.5 %)
Basal insulin dose (30 weeks, IU)		49.0 (20.5)
Prandial insulin dose (30 weeks, IU)		42.6 (19.5)
Retinopathy during pregnancy		20 (60.6 %)
Nephropathy during pregnancy		5 (15.2 %)
Neuropathy during pregnancy		1 (3.0 %)
Hypertensive disorders		
Hypertension (with labetalol or nifedipin medication)	3 (4.5 %)	3 (9.1 %)*
Pre-eclampsia	3 (4.5 %)	8 (24.2 %)*

Values are either mean (SD) or no. and (% of total). *p<0.05, **p<0.0001.

Demographic data is presented in Table 4. All women underwent Doppler ultrasonography and a serum sample collection. The ultrasound examination was performed at gestational week 35+5 (13 days) in T1DM and 37+3 (13 days) in the control group (p<0.0001). The time interval from the ultrasound to birth was similar in diabetic 12 (4 days) and 14 (8) control pregnancies. The ultrasonography was performed between the years 2006-2010. Amniocentesis was performed in T1DM women (n=24) for clinical indications. The amniotic fluid was tested for EPO concentrations in the laboratories of the university hospital (Oulu, n=5; Turku, n=19). After delivery, umbilical cord blood and placental samples were collected. Near the placental umbilical cord insertion, a 1 cm² placental segment of the whole placenta was cut sharply and fast-frozen in liquid nitrogen. Umbilical cord blood samples were centrifuged. All samples were stored at -80 C. Clinical data concerning pregnancies were obtained from hospital records.

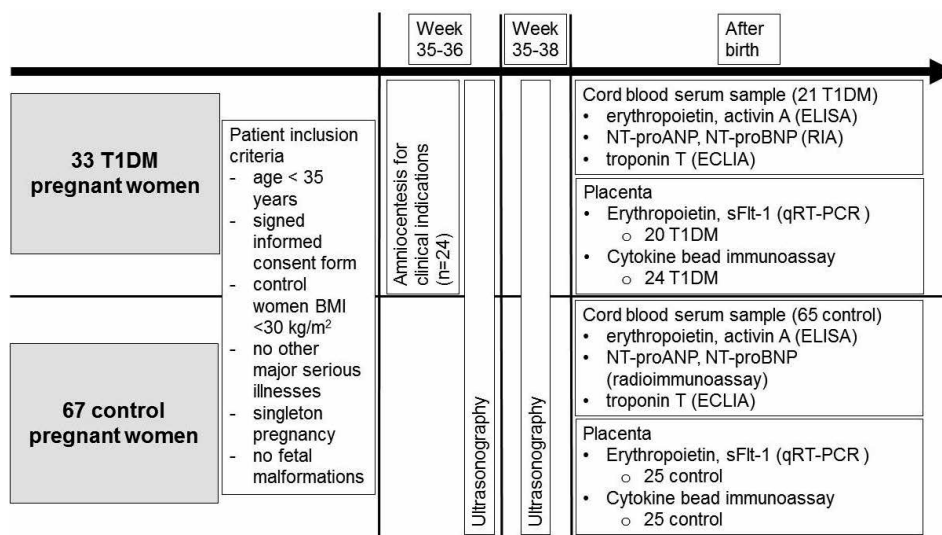


Figure 8. Human pregnancy follow-up flow chart.

4.2 Gene expression analysis (I-V)

4.2.1 RNA isolation

All tissue samples were initially fast-frozen in liquid nitrogen and stored at -80°C . Total ribonucleic acid (RNA) isolation was performed for gene expression analyses. Sample sizes are shown in Figures 6–8. RNA was isolated from each tissue homogenate using TissueLyser and purified with RNeasy mini kit and RNase-free DNase I (Qiagen, Hilden, Germany).

4.2.2 qRT-PCR analysis (I-IV)

For all studies, cDNA first strand was synthesized from RNA using Moloney murine leukemia virus reverse transcriptase. Real-time PCR reactions were performed with an ABI 7300 Real-Time PCR Systems (Applied Biosystems, CA) using TaqMan chemistry.

Table 5. Sequences of primers and bifunctional fluorogenic probes [6-carboxyfluorescein (5'-FAM), tetramethylrhodamine (3'-TAMRA)] used in qRT-PCR analyses.

<i>Adrb1</i> (rat)	Forward primer Reverse primer Probe	GGATCGCCTTTCGTCTTCTT TGCGGAGTAGATGATGGG CTGGGCTACGCCAACTCGGCCTT	<i>Slc2a3</i> (rat)	Forward primer Reverse primer Probe	GGTGCCATTTGGCAGCTAA CAAAGACTGAGCCACAAGGA CCAGCTGGGCATCGTTGTGGG
<i>Atp2a2</i> (rat)	Forward primer Reverse primer Probe	AACATCTGGCTCGTGGGC TGGCAAAGGTTCCACGATAGG TGCTTGCCATGTCCTTCAC-	<i>Slc2a4</i> (rat)	Forward primer Reverse primer Probe	TGTGGCCTCTTTGAGATTGG CTGAAGAGCTGGCCACAA CTGGCCCATCCCTGGTTG
TTCTTGA			<i>Tnfrsf12a</i> (rat)	Forward primer Reverse primer Probe	GACCACACAGCCACTTCTGC CATAGCATCCTGAAGTGGGA TGGGATGCGCAGCAGCACCT
<i>Bmpr1A</i> (rat)	Forward primer Reverse primer Probe	GCCCCCTGTCTTATAGC GCCATAGAGATGACACAGCC CATTCTTTGATGGCAGCGTCCGATG	<i>Ucp2</i> (rat)	Forward primer Reverse primer Probe	CTTCTGACCACCGCTCATTG GGCCCAAGGCAGAGTTCATA TCCCCTGTGATGGTCAAGACC
<i>Capza1</i> (rat)	Forward primer Reverse primer Probe	TCAGACACCAGTTCAAGGC TCGATTTTGGTGGCGGTAA TTGCGCCGGCAGCTTCCA	<i>Ucp3</i> (rat)	Forward primer Reverse primer Probe	AGCCTGTTTTGCTGATCTCCTC GGATCTGCAGGGGCACT CCTTCCCCTGGACACCCGC
<i>Cdkn1b</i> (rat)	Forward primer Reverse primer Probe	CCGGGACTTGGAGAAAGC AGTCGAAATGCCATTCGCGC TGCCGAGATGGAAGAAGCGAGCC	<i>Vegfa</i> (rat)	Forward primer Reverse primer Probe	GATCCGCAAGCTGTAATGTTTC TTAACTCAAGCTCCTCCGC TGCAAAAAACACAGACTCGCGTTGCA
<i>Flt1</i> (human)	Forward primer Reverse primer Probe	TCAGTACTGGGACACCGG CCTGACTAGATCCTGTGAGAAGCA TCCTGCTGTGCGCGCTGCTC			
<i>Egfr</i> (rat)	Forward primer Reverse primer Probe	CCTTAGCCGCTCCTGCCAAC TGTAAGTCCGCATGGGCA ATGGAAC-			
CAACAAAAGCTGGCTTAGGGA					
<i>Egln3</i> (rat)	Forward primer Reverse primer Probe	CCTCGGCTCTGTGAGCGA GGCGGATCTTCTCAGATC ATGCCCTGGGACACATCATGAGGC			
<i>Epo</i> (human)	Forward primer Reverse primer Probe	GGGACAGATGACCAGGTGTG GGCACAAGCAATGTTGGTG CCACCTGGGCATATCCA			
<i>Gpx3</i> (rat)	Forward primer Reverse primer Probe	AAGAACTTGGCCATTCGG GCTCCTGTTGCCAAATTTGG CTGTGCTATCTGGGCTCCCTTGCA			
<i>Hcn2</i> (rat)	Forward primer Reverse primer Probe	AGGGAATCGACTCCGAGGTC GAGGATCTGGTGAACGCAC AGACGGCCGTGCACTACGCA			
<i>Hsl</i> (rat)	Forward primer Reverse primer Probe	ACGGGCTCAGTGTGACTG GCAACTCTGGTCTATGGGG AAGTCCCTCTTTACGGGTGGCCGA			
<i>Igf2bp3</i> (rat)	Forward primer Reverse primer Probe	TCTCCGCTCGTCCCTTTTG TGTGCCATGCGTAGCTTGAG CGCCGCCCTTGCTACTTTG			
<i>Igfbp6</i> (rat)	Forward primer Reverse primer Probe	TCCTGCTGGTGTGGAT CTTCCCTGGCCATCTGGAG CGATGGCCAGCCTTTGCCAG			
<i>Kcnip2</i> (rat)	Forward primer Reverse primer Probe	CAGCAACTATGC-			
<i>Ldha</i> (rat)	Forward primer Reverse primer Probe	AGCCACAAGTCTCAAACCTGA CCTTTGACACCAACCAGTAGCTCT			
TTCA					
<i>Myh2</i> (rat)	Forward primer Reverse primer Probe	GCCAGAATAGCCCTTTTATG CGTCTTTGCTGCTGATGGTTCC CGGAGCCCAAGGATCCTTTGTCA			
<i>Myh3</i> (rat)	Forward primer Reverse primer Probe	ACAAGATCGAGGACATGGCC ACGTGTATCGTCTTGAAGTT TGACCCACCTGAACGAGCCTGCT			
<i>Myh6</i> (rat)	Forward primer Reverse primer Probe	AGTGCAGTGAACCGGAG GATTGCATCCTCTGCCGGA AGGGCTTCCCAACCGCATTCTTTAT			
<i>Nppa</i> (rat)	Forward primer Reverse primer Probe	GAAAAGCAAAGTGAAGGCTCTG CCTACCCCGCAAGCAGCT TCGCTGGCCCTCGGAGCCT			
<i>Nppb</i> (rat)	Forward primer Reverse primer Probe	TGGCAGAAGATAGACCGGA ACAACCTCAGCCGCTCAGC CGGGCAGTCAAGTGCCTTG			
<i>Pdgfr</i> (rat)	Forward primer Reverse primer Probe	AATATGAGTGGTGAGCACGC CATACACCCACTGACAGTGG CGCTCGCTCAGCTGACCA			
<i>Pgdh</i> (rat)	Forward primer Reverse primer Probe	TCATGCCCTGTTGCACAGCA GCTGAGCGTGTGAATCCGAT CCTGTTATTTGTGCCTCAA-			
GCATGGCA					
<i>Pdk2</i> (rat)	Forward primer Reverse primer Probe	GGCAGGAGCTGCCCGT CCCGTCAAGGAGCAGGT CGCCTGGCCAAATCATGAAAGA-			
GATC					
<i>Ptgs2</i> (rat)	Forward primer Reverse primer Probe	CATGATCTACCCTCCCCACG CAGACCAAAGACTCCTGCC CCCTGAGCACCTGCGGTTGCG			

Adrb1, β_1 -adrenergic receptor; *Hcn2*, hyperpolarization-activated cyclic nucleotide-gated potassium channel 2; *Atp2a2*, sarcoplasmic reticulum Ca^{2+} -ATPase; *Bmpr1A*, bone morphogenetic protein receptor type 1A; *Capza1*, Z-line actin-capping protein- α 1; *Cdkn1b/P27kip1*, cyclin-dependent kinase inhibitor 1B; *Flt1*, FMS-related tyrosine kinase 1; *Egfr*, epidermal growth factor receptor; *Egln3*, hypoxia-inducible factor prolyl hydroxylase 3; *Epo*, erythropoietin; *Gpx3*, glutathione peroxidase 3; *Hcn2*, hyperpolarization-activated cyclic nucleotide-gated potassium channel; *Hsl*, hormone-sensitive lipase; *Igf2bp3*, insulin-like growth factor 2 mRNA binding protein 3; *Igfbp6*, insulin-like growth factor binding protein 6; *Kcnip2*, kv-channel interacting protein; *Ldha*, lactate dehydrogenase A; *Myh2*, adult skeletal myosin heavy chain 2; *Myh3*, embryonic skeletal myosin heavy chain 3; *Myh6*, α -cardiac myosin heavy chain 6; *Nppa*, atrial natriuretic peptide; *Nppb*, brain natriuretic peptide; *Pdgfrb*, platelet derived growth factor receptor beta polypeptide; *Pdk2*, pyruvate dehydrogenase kinase, isozyme 2; *Pgdh*, hydroxyprostaglandin dehydrogenase 15; *Ptgs2*, cyclo-oxygenase 2; *Slc2a3*, facilitated glucose transporter 3; *Slc2a4*, insulin-responsive glucose transporter 4; *Tnfrsf12a*, tumor necrosis factor receptor superfamily member 12a; *Ucp2*, uncoupling protein 2; *Ucp3*, uncoupling protein 3; *Vegfa*, vascular endothelial growth factor A.

Quantification was performed using the standard curve method and the results were normalized to the housekeeping gene 18S RNA measured from the same sample. Primers and bifunctional fluorogenic probes (6-carboxyfluorescein and tetramethylrhodamine) for analyzed genes were designed with Primer Express software (Applied Biosystems, CA) (I-IV). Primers and probes are listed in Table 5.

4.3 Histological, tomographic, and biochemical analyses

4.3.1 Morphometric analysis (I-III)

Tissue samples were fixed in 10% buffered formalin for 24–48 hours and embedded in paraffin. Rat fetal thorax blocks (I) were scanned as whole, but all other samples were cut into sections with a thickness of 5 μm (I-III), stained, and examined under UV light at a x40 times magnification unless stated differently.

4.3.1.1 Hematoxylin & Eosin staining (I-III)

Hematoxylin & eosin (H & E) staining was used for morphological analysis in studies I–III. Rat cardiac morphology was examined for apoptosis and mitosis in late term fetuses (I) and offsprings (III) by either two (JL, LL) or one (JL) investigators blinded to the study group. A grid was set as a standard area inside the myocardial wall near the apex of the heart. Epithelium, endothelium, septal walls, and trabeculae were excluded. The apoptotic cells were identified by the dense, hyperchromatic, fragmented nuclei, eosinophilic cytoplasm, and the halo sign separating the cell (Mandarim-de-Lacerda & Pessanha 1995). Mitosis in a cell was identified by dividing chromatin figures; metaphase and anaphase easiest to identify. Apoptotic and mitotic cell activity was estimated by counting the cells (number of cells/ mm^2). In study III, the mitosis-karyorrhexis index (MKI) was calculated by adding mitotic and apoptotic cells together to estimate the general cell activity. For study I, the number of erythroblasts per 100 erythrocytes (ERBL/ERYT) ratio was calculated.

In study II, the H & E stained rat placental sections were examined for size, maternal arteries, villi, and vein thrombosis by a single investigator blinded to the study group (JL). The placental area was measured from the cross-sectional sagittal view of the placenta from the umbilical cord insertion area. Setting the grid as a standard area, the number of cysts, villi, venous thrombosis formations, and maternal artery diameter and wall thickness were measured.

4.3.1.2 Gömöri methenamine silver staining (I, III)

To study cardiac cell turnover, width, and number Gömöri methenamine silver staining was performed (I, III). Apoptotic and mitotic cells were identified in a similar fashion as in H & E stained samples. The number of cardiomyocyte nuclei per mm^2 and cardio-

myocyte width measurements from the narrowest nucleus crossing dimension were calculated by a single investigator blinded to the experimental group (JL).

4.3.2 Periodic acid-Schiff (PAS) and PAS diastase stainings (II)

Placental samples were stained with Periodic acid-Schiff (PAS) and PAS diastase (dPAS) (II). PAS stains all cells and glycogen, whereas dPAS erases staining with glycogen. The location of PAS positive staining in the placenta was recorded. Glycogen positive cells were calculated by the following formula: Glycogen positive cells = PAS positive cells – (PAS positive cells – dPAS positive cells). A standard x20 magnification was used and all the analyses were performed by a single investigator blinded to the experimental group (LL).

4.3.3 In situ detection of apoptotic cells (I, III)

Apoptotic myocardial cells were identified by terminal deoxynucleotide transferase-mediated dUTP nick-end labeling (TUNEL) from paraffin-embedded samples by a single investigator blinded to the study group (VK). First, samples in sodium citrate solution were heated and then digested with proteinase-K to expose DNA. Second, terminal transferase with digoxigenin-conjugated dideoxyuridine triphosphate was used to label DNA strand breaks and, finally, alkaline phosphatase immunohistochemistry was used for visualization. Adjacent sections were treated with DNaseI to verify a positive sample for apoptosis.

4.3.4 Immunohistochemistry for Ki-67 staining (I)

Ki-67 immunostaining was performed to estimate the proliferative activity of the fetal rat myocardium near the apex. Ki-67 is expressed in the cell nuclei in G1, S, G2, and M phases of the cell cycle (Fidaleo et al. 2011). Several staining dilutions were used and the most optimal was 1:1000 dilution for the primary antibody to stain all mitotic nuclei and some round nuclei (prophase and telophase) with a dark brown color. Light brown was occasionally seen in non-dividing nucleus but was disregarded. The protocol was adopted from Reis et al (Reis et al. 2010). The analyses were performed by a single investigator (LL) blinded to the study group.

4.3.5 Micro-computed tomography analysis (I)

Micro-computed tomography analysis was used to measure fetal rat late term ventricular chamber, free wall, and interventricular septal volumes. It was performed on a 1072 Desktop X-ray microtomograph (SkyScan, Kontich, Belgium). Excess material was cut out from paraffin embedded thorax blocks and thereafter the blocks were scanned with a x45 magnification with settings of 6.51 μm pixel resolution, 3.9 sec exposure time (50 kV, 150 μA), 0.45 rotation step (180°), and 0.25 mm aluminium filter. Volumetric recon-

struction software (NRecon version 1.4.4., SkyScan) and 3-dimensional image volume analysis with CT Analyzer software (version 1.7.05, SkyScan) were used for image creation.

4.3.6 Cytokine bead array analysis (II, IV)

In study II, frozen rat placentas were weighed and immersed in PBS pH 7,5 (100 mg of tissue to 100 ml) containing 0,1% Igepal CA-630 nonionic detergent (Sigma-Aldrich, MO). Ultra-Turrex was used to homogenize sample mixtures on ice, and samples were centrifuged at 6000 x g for 30 minutes. Supernatants were stored at -80 °C for cytokine assay. After defrosting, samples were centrifuged at 13000 x g for 30 min for excess cell removal. The concentrations were analyzed using Milliplex Map Rat Cytokine/Chemokine Magnetic Bead Panel assay kit (Merck Millipore, MA). Supernatants were diluted with a 1:5 to assay buffer. Duplicate sample assays were performed with Luminex 200 system and analyzed with xPONENT software (build 3.1.579.0) (Luminex Corporation, TX).

For study IV, placental cytokine concentrations of interleukins (IL) 1 β , IL2, IL4, IL6, IL8, IL10, monocyte chemoattractant protein 1 (MCP1), and tumor necrosis factor α (TNF α) (Bio-Plex Pro Human Cytokine 8-Plex Immunoassay, Bio-Rad, Hercules, CA) were measured. The assay was done in duplicate according to manufacturer's instructions using Bio-Plex MAGPIX Multiplex Reader.

4.3.7 Umbilical cord serum immunoassays (IV)

4.3.7.1 Erythropoietin

Umbilical cord serum erythropoietin concentrations were analyzed in duplicates by a quantitative enzyme linked immunosorbent assay (ELISA) (Quantikine IVD Human Epo Immunoassay, R & D Systems, MN). The detection limit for erythropoietin was 2.5 mIU/ml. ELISA is a method that employs antigen-antibody binding to detect a certain substance that is analyzed spectrophotometrically and given a numerical estimation. The analysis was performed in Research Centre of Applied and Preventive Cardiovascular Medicine, CAPC, University of Turku.

Amniotic fluid erythropoietin concentration was analyzed by a two-site sandwich immunoassay with chemiluminescent detection on an automated random access immunoassay analyzer (TYKSLAB and NordLab, Finland).

4.3.7.2 Activin A

Activin A serum concentrations were analyzed in duplicates using solid-phase ELISA assay according to manufacturers instructions (Quantikine Human/Mouse/Rat Activin A Immunoassay, R & D Systems, MN) in CAPC. The detection limit was 15.6 pg/ml.

4.3.7.3 Natriuretic peptides

Cardiac ANP and BNP are synthesized as inactive prohormones and cleaved in equimolar amounts to ANP and BNP, and inactive N-terminal fragments (NT-proANP, NT-proBNP) (Hunt et al. 1997; Rosenzweig et al. 1991). Circulating fetal umbilical serum concentrations of NT-proANP and NT-proBNP were measured by radioimmunoassay (Ala-Kopsala et al. 2004). The sequences for NT-proANP and NT-proBNP antisera recognition were proANP₄₆₋₇₉ and proBNP₁₀₋₂₉. The detection limit was 60 pmol/l for NT-proANP and 40 pmol/l for NT-proBNP.

4.3.7.4 Troponin T

Umbilical cord serum cardiac troponin T (TnT) concentrations were measured with electrochemiluminescence immunoassay (ECLIA) (TYKSLAB, Finland). The lowest detection limit was set at <0.014 ng/ml.

4.4 Ultrasonographic assessment (I, II, IV)

4.4.1 Animal models of maternal hyperglycemia and pregnancy (I, II)

Ultrasonographic examinations were performed longitudinally (Figure 8). Dams were placed in a dorsal position, and the lower abdomen was shaved after adequate anesthesia. The body temperature was maintained at 38°C with a heat pad. Acuson Sequoia 512 equipment (Mountain View, CA) with a 15L8W linear array probe (frequency 14.0 MHz, dynamic range contrast 74 dB, edge 0, color frame rate 28/sec, space-time temporal resolution 68%, wall motion filter set 3) was used with a lowest high-pass filter setting (Gui et al. 1996). Starting from the top, all fetuses were localized in each uterine horn. Color-Doppler was used to identify the fetal heart. The pulsed Doppler sample volume was adjusted to cover the heart or the vessel of interest. The fetal heart was examined from different directions to minimize the angle. Cardiac inflow (IF) and outflow (OF) areas were identified to record their maximal velocities during several cardiac cycles with a sweep speed of 100 mm/s (Figure 9). From the fetal sagittal view, descending aorta and DV were located with color Doppler and blood flow velocity waveforms were obtained by pulsed Doppler US with an angle less than 30–40° between the vessel and the Doppler beam. UA blood flow velocity waveforms were collected from the umbilical cord free loop. The ultrasonographic examinations were videotaped and analyzed offline.

4.4.2 Maternal T1DM and pregnancy (IV)

In human pregnancy, transabdominal ultrasound (Acuson Sequoia 512, Mountain View, CA) was performed with an 5-8 MHz convex transducer by two investigators (MH, LL). The high pass filter was set at its minimum. An angle of < 20° degrees be-

tween the vessel and the Doppler beam was accepted for further analysis. The mean value was calculated from three consequent cardiac cycles. Mechanical and thermal indices were kept <1.0. The examinations were videotaped and later analyzed offline.

The four-chamber view of the heart was used to obtain mitral and tricuspid valve blood velocity waveforms, as well as PPA and pulmonary veins (Pulm V). Tricuspid regurgitation (TR) was noted if present. Outflow blood flow velocity waveforms were recorded at the level of pulmonary and aortic valves. Valve diameters were measured using leading-edge-to-leading edge method during systole. CSA was calculated with the assumption that the annuli are circular. VTI were calculated by planimetry of the area of the Doppler spectrum. M-mode recordings were obtained from the four-chamber view. M-mode was used to measure the ventricular wall thicknesses obtained at the atrioventricular valve level during end-diastole.

From the fetal sagittal view, DAo, IVC, left hepatic vein, and DV blood flow velocity waveforms were obtained. AoI blood flow velocity waveforms were obtained from the sagittal aortic arch view. UA blood velocity waveforms from free loops of the umbilical cord and FHR were measured. MCA blood flow velocity waveform was acquired. The blood flow velocity waveforms from the uterine arteries (AUt) were recorded.

4.5 Statistics

In studies I–II, data were analyzed using mixed-model approach, with the dam as a random effect. Analyses tested mean differences of the outcome variables. Repeated measurements of ultrasonographic data were analyzed using time, maternal hyperglycemia, and interaction between these two as independent variables. In morphologic, microcomputed-tomography, and mRNA data analyses, hyperglycemia was used as an independent variable. Interactions between ultrasound measurements in peripheral vessels were analyzed with factorial two-way ANOVA. Correlation between parameters was examined using either Spearman's correlation coefficient or Pearson's test. Intraobserver variability was estimated with Bland-Altman analysis on two measurements of UA and descending aorta PI, as well as DV PIV. Bias was defined as the geometric mean of all PI value ratios and precision as 95% confidence limits of agreement.

In study III, data were analyzed with one-way ANOVA (gene and histologic analyses) or either with Student's t-test or Mann-Whitney U-test (glucose levels, differences within a group). Analyses were used to test mean differences of the outcome variables. Measurements of gene and histologic data were analyzed with time, maternal hyperglycemia, and interaction between both as independent variables.

Study IV used Kruskal-Wallis H test for three-way comparisons. The categorical variables were tested for significance using Mantel-Haenszel's X^2 or Fisher's exact test (for variables with 5 or fewer entries). Student's t-test or Mann-Whitney U-test was used for

two-way comparisons. Associations were tested using Spearman's correlation coefficient (Rs) and for categorical variables with logistic or multinomial logistic regression analysis. The following limits were regarded for associations: 0.40–0.59 moderate, 0.60–0.79 strong, and 0.80–1.00 very strong.

For all studies, statistical significance was set at $p \leq 0.05$. When required by the statistical distribution, logarithmic or \sqrt{x} conversion was utilized. Analyses were performed with SAS (version 9.2; SAS Institute, Cary, NC) or IBM SPSS Statistics (version 19.0; IBM Analytics, Armonk, NY). The results are given as means standard deviation (SD), confidence interval (CI) 95%, or median (range).

5 RESULTS

5.1 Rat model of maternal hyperglycemia (I-III)

5.1.1 Fetal rat cardiac function during the second half of pregnancy

At GD 13 and 14, rat fetuses in the maternal hyperglycemia group had AVVR more often and decreased outflow V_{mean} than control group fetuses (Figure 9, Table 6). Furthermore, E/A VTI ratio and ICT% were increased. Later in pregnancy no valve regurgitation was seen but E/A VTI ratio and IRT% remained increased in the maternal hyperglycemia group. Throughout pregnancy, the rat fetuses in the maternal hyperglycemia group had lower FHR and increased vascular impedance in the descending aorta and UA.

5.1.2 Intraobserver variability in the experimental rat model

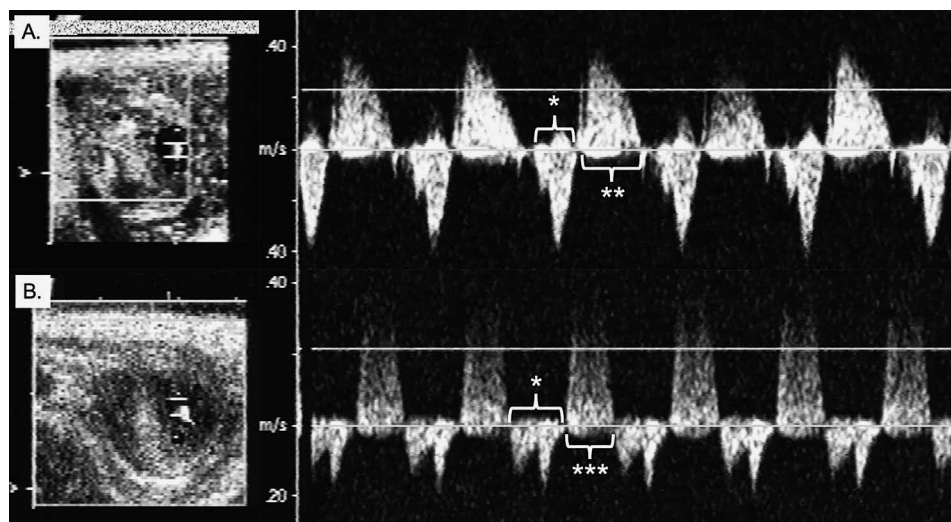


Figure 9. Pulsed Doppler sonography of the fetal heart at 13–14 GD. The inflow blood flow velocity waveform is below the baseline (*). Top figure represents inflow-outflow blood flow velocity waveforms from the control fetus. Bottom figure represents inflow blood velocity waveform with holosystolic AVVR at the end of diastole in a fetus in the hyperglycemic group.

Table 6. Fetal cardiac and peripheral hemodynamics in the control and maternal hyperglycemia groups.

Variable	Control	Hyperglycemia	Control	Hyperglycemia	Control	Hyperglycemia
	GD 13-14		GD 16-17		GD 19-21	
n ^{fp}	219	98	208	99	199	104
n ^d	20	10	20	10	20	10
Central hemodynamics						
AVVR	57/219 (26 %)	98/100 (98 %)	0/208 (0 %)	0/99 (0 %)	0/199 (0 %)	0/104 (0 %)
FHR	195 (30)	154 (17)***	203 (32)	188 (18)*	218 (33)	191 (24)**
OF Vmean	9.6 (2.8)	3.8 (1.5)***	11.9 (2.5)	11.1 (2.0)	11.4 (2.1)	10.5 (1.9)
E/A VTI	0.11 (0.19)	1.17 (0.52)***	0.10 (0.09)	0.11 (0.08)	0.27 (0.16)	0.42 (0.20)***
IRT%	10.5 (5.5)	NA	12.5 (2.5)	14.1 (2.9)	11.4 (2.9)	13.2 (2.9)*
ICT%	4.9 (2.1)	5.3 (2.2)***	4.7 (1.7)	6.6 (3.4)***	5.9 (2.2)	5.0 (1.6)*
MPI	0.31 (0.15)	NA	0.35 (0.07)	0.43 (0.11)*	0.37 (0.11)	0.39 (0.09)
Peripheral hemodynamics						
UA PI	2.68 (0.85)†	3.70 (0.75)***†	2.51 (0.42)‡	2.94 (0.54)***‡	2.32 (0.47)§	2.98 (0.43)***
DAO PI	2.73 (0.48)†	3.83 (0.73)***†	2.60 (0.37)‡	3.07 (0.41)***‡	2.36 (0.51)§	2.85 (0.67)***§
DV PIV			0.85 (0.19)	0.99 (0.15)***	0.83 (0.21)	1.27 (0.32)***

Data are mean (SD). * $p < 0.05$, ** $p \leq 0.001$, *** $p \leq 0.0001$, † $p \leq 0.05$ (GD 13-14 to GD 16-17 within a group), ‡ $p \leq 0.05$ (GD 13-14 to GD 19-21 within a group), § $p \leq 0.05$ (GD 16-17 to GD 19-21 within a group). GD, gestational day; n^f, number of fetuses; n^d, number of dams; AVVR, atrioventricular valve regurgitation; FHR, fetal heart rate; OF Vmean, outflow mean velocity; E/A VTI, early-ventricular-filling-to-atrial contraction wave/velocity-time integral ratio; IRT%, proportion of isovolumetric relaxation time of total cardiac cycle; ICT%, proportion of isovolumetric contraction time of total cardiac cycle; MPI, index of myocardial performance; NA, not applicable.

In the rat model of maternal hyperglycemia, the fetal intraobserver variability for UA PI was 9.9% (95% CI 7.0, 12.9%), for DAO PI 6.7% (95% CI 4.3, 9.2%), and for DV PIV 6.4% (95% CI 4.4, 8.3%). Paired correlation coefficients were significant for UA PI ($p < 0.00001$, $R = 0.883$), DAO PI ($p < 0.00001$, $R = 0.942$), and DV PIV ($p < 0.00001$, $R = 0.977$).

5.1.3 Fetal rat cardiac morphology at term gestation

In the maternal hyperglycemia group, fetal rat hearts at term gestation were larger, had increased number of apoptotic and mitotic cells, but had a similar amount of cell nuclei per view when compared to the control group (Tables 7 & 8). At term gestation, fetal rat erythroblast to erythrocyte ratio was greater ($p = 0.0001$) in the maternal hyperglycemia group [3.7 (4.5), $n = 48$] than in the control group [0.6 (0.7), $n = 58$].

Table 7. Cardiac characteristics in the control and maternal hyperglycemia groups in the experimental animal model.

Variable	GD 19-21		PND 0		PND 7		PND 14	
	Control	Hyperglycemia ⁱⁱ	Control	Hyperglycemia	Control	Hyperglycemia	Control	Hyperglycemia
	94	52	10	10	8	8	9	9
n ^{fp}	17	10	2	3	3	3	4	4
n ^d								
Cardiac characteristics								
Heart weight, mg			30.3 (4.7)	39.0 (4.2)**	81.6 (9.5)	75.8 (9.1)	150.7 (13.7)	148.2 (11.8)
Body weight, mg			5770 (250)	6160 (420)	14350 (830)	12550 (650)***	27330 (2060)	26710 (1670)***
Heart/body weight ratio			0.0053 (0.0008)	0.0064 (0.0009)*	0.0057 (0.0007)	0.0060 (0.0006)	0.0055 (0.0004)	0.0056 (0.0004)
CA/TA ratio	0.20 (0.03)	0.25 (0.05)*						
Cardiac muscle, mm	3.19 (0.69)	3.87 (0.60)						
Septum, mm	0.60 (0.41)	0.84 (0.26)						
Left ventricle, mm	0.57 (0.30)	0.92 (0.39)						
Right ventricle, mm	0.77 (0.37)	0.85 (0.44)						

Data are presented as mean (SD). * p<0.05, ** p<0.001, *** p<0.0001. GD, gestational day; PND, postnatal day; n^{fp}, number of fetuses/pups; n^d, number of dams; CA/TA ratio, cardiac area to thoracic area ratio.

Table 8. Cardiac histology in the control and maternal hyperglycemia groups in the experimental animal model.

Variable	Control		Hyperglycemia		Control		Hyperglycemia		Control		Hyperglycemia	
	GD	GD 19-21	PND 0	PND 7	PND 0	PND 7	PND 0	PND 7	PND 0	PND 7	PND 0	PND 7
n ^{fp}	85	46	11	14	15	12	10	14				
n ^d	17	10	2	3	3	2	3	3				3
H & E												
apoptotic cells	36.0 (27.5)	55.0 (30.5)***	1.27 (1.17)	0.82 (0.75)	0.57 (0.56)	0.67 (0.62)	0.30 (0.26)	0.64 (0.66)				
mitotic cells	183.4 (79.6)	254.3 (103.7)***	5.36 (4.10)	5.44 (3.16)	6.17 (3.41)	6.58 (2.94)	1.50 (0.97)	2.86 (1.85)*				
MKI			6.64 (4.92)	6.26 (3.55)	6.73 (3.65)	7.25 (3.14)	1.80 (1.14)	3.50 (1.75)*				
Gömöri												
mitotic cells	318.5 (176.3)	427.2 (153.7)*										
cell size	8.3 (1.1)	8.1 (1.3)	7.06 (1.10)	6.50 (0.64)	7.36 (0.50)	6.96 (0.55)	8.44 (1.26)	7.84 (0.89)				
nuclear count	5720 (1040)	5760 (820)	5900 (733)	6025 (910)	5321 (759)	5691 (554)	5357 (1370)	4818 (794)				
TUNEL												
apoptotic cells	0.036 (0.023)	0.11 (0.045)**	0.17 (0.13)	0.12 (0.06)	0.02 (0.03)	0.08 (0.04)**	0.05 (0.05)	0.05 (0.04)				
nuclear count	5870 (460)	5710 (470)										
Ki-67												
mitotic cells	83.8 (37.1)	200.3 (87.9)***										

Data are presented as mean (SD). * p<0.05, ** p<0.001, *** p<0.0001. Results are no. of nuclei/mm² apart from TUNEL (%total nuclei) and Gömöri cell sizes (width in m). GD, gestational day; PND, postnatal day; n^{fp}, number of fetuses/pups; n^d, number of dams; H & E, hematoxylin and eosin; MKI, mitosis-karyorrhexis index.

5.1.4 Fetal rat cardiac gene expression

5.1.4.1 Cardiac contractility

At late term rat gestation, the expression of Kv channel-interacting protein 2 (*Kcnp2*), a key regulator of electrical cardiac function, was downregulated in the maternal hyperglycemia group (Table 9). Expression of other genes involved in cardiac contractility was similar to the control group fetuses.

5.1.4.2 Natriuretic peptides, myosins, and associated to actin

In the maternal hyperglycemia fetuses, cardiac natriuretic peptide gene expression was increased at near term (Table 9). Furthermore, embryonic and adult skeletal myosin heavy chain gene expression was greater than in the control group fetuses.

5.1.4.3 Cardiac metabolism, hypoxia, and growth

At term gestation, fetal rat cardiac expression of uncoupling proteins (*Ucp2*, *Ucp3*) was upregulated and the expression of insulin-responsive glucose transporter 4 (*Slc2a4*) was downregulated when compared to control group fetuses. At near term, hypoxia-related gene expression of HIF-prolyl hydroxylase 3 (*Egln3*) was lower in rat fetal hearts of the maternal hyperglycemia group at near term (Table 9). Tumor necrosis factor receptor superfamily member 12a (*Tnfrsf12a*) is an indicator of cardiomyocyte proliferation, and was upregulated in the maternal hyperglycemia group rat fetal hearts.

5.1.5 Newborn and offspring rat heart

In the newborn rats of the maternal hyperglycemia group, the heart to body weight ratios were increased at birth (Table 7). By one to two weeks of age, the heart weights and heart to body weight ratios were comparable in the control and maternal hyperglycemia groups. However, the body weight was lower in the maternal hyperglycemia offspring than in the control group.

Table 9. Fetal and offspring rat cardiac gene expression (gene/18S) in the control and maternal hyperglycemia groups.

Variable	Control		Hyperglycemia		Control		Hyperglycemia		Control		Hyperglycemia	
	GD 19-21	GD 19-21	PND 0	PND 0	PND 7	PND 7	PND 14	PND 14	PND 14	PND 14	PND 14	PND 14
n ^{f/p}	14	12	10	14	13	15	15	15	15	15	15	13
n ^d	5	5	2	3	3	3	4	3	4	4	3	3
Contractility												
<i>Aubr1</i>	1.11 (0.10)	1.12 (0.10)										
<i>Atp2a2</i>	1.11 (0.07)	0.92 (0.07)	0.99 (0.22)	0.74 (0.19)*	1.44 (0.49)	1.17 (0.34)	1.15 (0.25)	1.83 (0.43)***				
<i>Hcn2</i>	1.64 (0.19)	1.02 (0.12)										
<i>Kcnip2</i>	1.08 (0.11)	0.71 (0.12)**	0.91 (0.27)	0.49 (0.18)†	1.35 (0.55)	1.51 (0.60)	1.13 (0.41)	2.35 (0.76)**				
Natriuretic peptides												
<i>Nppa</i>	0.90 (0.08)	1.58 (0.19)*	0.89 (0.46)	1.29 (0.70)	1.68 (1.57)	1.44 (1.14)	0.77 (0.65)	0.80 (0.86)				
<i>Nppb</i>	0.91 (0.04)	1.58 (0.14)**	2.08 (1.31)	3.50 (1.69)*	2.23 (1.60)	2.93 (1.69)	0.66 (0.43)	1.35 (0.66)***				
Myosins and actin-associated genes												
<i>Myh2</i>	0.86 (0.07)	1.36 (0.12)*	1.28 (0.83)	0.71 (0.50)*	0.95 (0.50)	1.00 (0.37)	0.56 (0.22)	0.95 (0.27)*				
<i>Myh3</i>	0.76 (0.07)	1.04 (0.08)*	1.40 (0.47)	2.07 (1.74)	2.56 (2.46)	0.94 (0.92)*	0.26 (0.17)	0.50 (0.56)				
<i>Myh6</i>	0.99 (0.10)	1.24 (0.10)	1.32 (0.35)	0.92 (0.33)*	1.36 (0.65)	1.22 (0.36)	0.89 (0.26)	1.66 (0.51)***				
<i>Capza</i>	0.82 (0.06)	0.95 (0.07)										
Metabolism												
<i>Pdk2</i>	1.03 (0.11)	0.76 (0.05)										
<i>Sic2a3</i>	0.73 (0.06)	0.83 (0.04)	1.63 (0.29)	0.93 (0.35)***	1.73 (0.83)	1.46 (0.39)	0.88 (0.29)	1.48 (0.18)***				
<i>Sic2a4</i>	1.23 (0.09)	0.92 (0.04)*	0.64 (0.15)	0.47 (0.27)*	1.55 (0.52)	1.00 (0.43)*	1.28 (0.38)	2.47 (0.72)**				
<i>Ucp2</i>	0.85 (0.06)	1.13 (0.07)*	1.24 (0.65)	1.01 (0.35)	1.46 (0.76)	1.35 (0.62)	1.13 (0.26)	2.12 (0.54)**				
<i>Ucp3</i>	0.55 (0.08)	0.96 (0.18)*	0.26 (0.12)	0.18 (0.07)*	0.47 (0.48)	0.42 (0.25)	2.36 (1.33)	4.36 (1.53)*				
Hypoxia and inflammation												
<i>Egln3</i>	1.08 (0.11)	0.83 (0.05)*	1.06 (0.34)	0.95 (0.32)	2.07 (0.86)	1.81 (0.64)	0.94 (0.31)	1.87 (0.52)***				
<i>Vegfa</i>	0.88 (0.06)	0.84 (0.06)										
Growth												
<i>Cdkn1b</i>	0.80 (0.05)	0.88 (0.06)										
<i>Tnfrsf12a</i>	1.18 (0.09)	1.55 (0.10)*	2.82 (1.14)	1.79 (0.96)*	1.52 (0.74)	1.58 (0.81)	0.44 (0.23)	0.85 (0.28)***				

Data are presented as mean (SD). * p<0.05, ** p<0.001, *** p<0.0001. mRNA concentrations as arbitrary unit (AU). GD, gestational day; PND, postnatal day; n^{f/p}, number of fetuses/pups; n^d, number of dams; *Aubr1*, β_1 -adrenergic receptor; *Atp2a2*, sarcoplasmic reticulum Ca²⁺-ATPase; *Hcn2*, hyperpolarization-activated cyclic nucleotide-gated potassium channel 2; *Kcnip2*, kv-channel interacting protein; *Mppa*, atrial natriuretic peptide; *Mppb*, brain natriuretic peptide; *Myh2*, adult skeletal myosin heavy chain 2; *Myh3*, embryonic skeletal myosin heavy chain 3; *Myh6*, α -cardiac myosin heavy chain 6; *Capza1*, Z-line actin-capping protein- α 1; *Pdk2*, pyruvate dehydrogenase kinase, isozyme 2; *Sic2a3*, facilitated glucose transporter 3; *Sic2a4*, insulin-responsive glucose transporter 4; *Ucp2*, uncoupling protein 2; *Ucp3*, uncoupling protein 3; *Egln3*, hypoxia-inducible factor prolyl hydroxylase 3; *Vegfa*, vascular endothelial growth factor; *Cdkn1b*, cyclin-dependent kinase inhibitor 1B; *Tnfrsf12a*, tumor necrosis factor receptor superfamily member 12a.

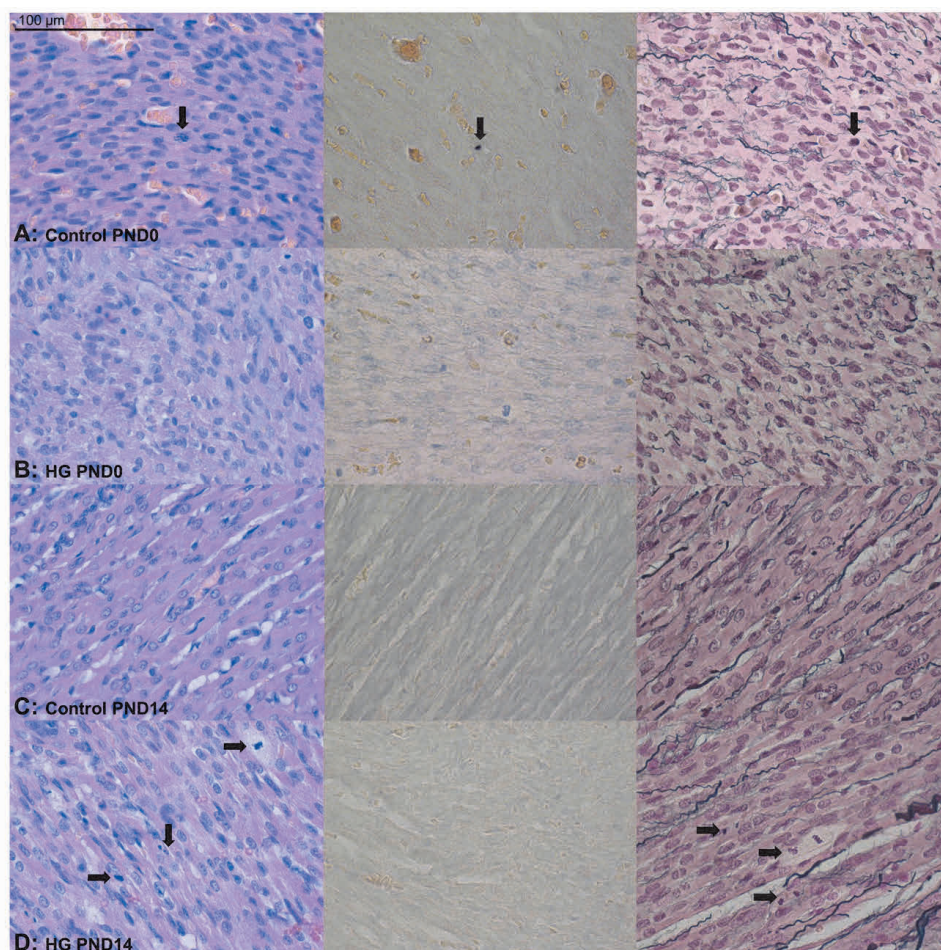


Figure 10. Stainings from left to right: H & E, TUNEL immunohistochemistry, Gömori methenamine silver. **A.** Control newborn heart at postnatal day (PND) 0. A mitotic cell is seen (arrow). **B.** Newborn heart at PND 0 from the maternal hyperglycemia group. The nuclei are disorganized compared to the control newborn heart. **C.** Offspring heart from the control group with clearly structured cardiomyocyte walls in the Gömori stain at PND 14. **D.** Offspring heart from the maternal hyperglycemia group at PND 14. Mitosis (arrows) are seen, cellular structure is better organized than at PND 0.

5.1.6 Newborn and offspring rat cardiac morphology

At birth, no differences in cell turnover parameters were seen between the control and maternal hyperglycemia groups (Table 8, Figure 10). At the age of one week, increased cardiac cell apoptosis and at the age of two weeks, increased cardiac cell mitosis, were observed in the neonates of maternal hyperglycemia group when compared to the neonates of the control group.

5.1.7 Newborn and offspring rat cardiac gene expression

5.1.7.1 Cardiac contractility

In newborn rat hearts, sarcoplasmic reticulum Ca²⁺-ATPase (*Atp2a2*), involved in cardiomyocyte relaxation and contraction, and *Kcnip2* were downregulated in the maternal hyperglycemia group when compared to the control group. At the age of two weeks, both gene expressions were greater in the maternal hyperglycemia offspring rat hearts.

5.1.7.2 Natriuretic peptides and myosins

In newborns of the maternal hyperglycemia group, increased expression of *Nppb* and decreased expression of adult skeletal myosin (*Myh2*) and α -cardiac myosin heavy chain (*Myh6*) were observed (Table 9). At the age of one week, neonates in the maternal hyperglycemia group had decreased expression of embryonic skeletal myosin (*Myh3*) when compared to the control neonates. At the age of two weeks, *Nppb*, *Myh2*, and *Myh6* had increased expression in the maternal hyperglycemia group when compared to the control group.

5.1.7.3 Cardiac metabolism, hypoxia, and growth

In newborns (PND 0), gene expression levels of glucose transporters and uncoupling proteins were lower in the maternal hyperglycemia than in the control group (Table 9). At the age of two weeks, the expression of these genes was increased in the offspring of maternal hyperglycemia compared to controls. Also in newborns, no differences were seen in *Egln3* and *Tnfrsf12a* gene expressions between the groups. However, at the age of two weeks, hypoxia-related *Egln3* had increased expression in the offspring of the maternal hyperglycemia group compared to the control group (Table 9). At the same time, proliferation indicator *Tnfrsf12a* gene expression was greater in the maternal hyperglycemia offspring.

5.1.8 Rat placenta

5.1.8.1 Structure and growth

Placental area, width, and thickness were increased in the maternal hyperglycemia group when compared to the control group (Table 10). Placental weight was similar in both groups. Peripheral sinus veins with thrombosis (60 % vs. 20% of veins), homogeneous colloid type fluid containing cysts and interstitial fluid (37% vs. 11% of basal zone area), and glycogen-containing cells in the basal zone in cystic cytotrophoblasts were observed more often in the placentas of the maternal hyperglycemia group than in the control group (Table 10, Figure 11). Umbilical artery PI correlated with interstitial fluid accumulation ($p < 0.00001$, $R = 0.47$) and the number of glycogen-containing cells ($p = 0.002$, $R = 0.56$).

Table 10. Placental characteristics in the control and maternal hyperglycemia groups in the experimental animal model.

Variable	Control	Hyperglycemia
	GD 19-21	GD 19-21
n ^p	94	52
n ^d	17	10
Placental characteristics		
Weight, mg	411.5 (109.0)	451.5 (91.9)
Area, mm ²	177.4 (4.5)	217.3 (8.5)*
Thickness, mm	4.0 (0.1)	4.3 (0.1)*
Width, mm	11.0 (0.2)	12.1 (0.3)*
Thrombosis, % of placentas (no thrombi/placenta)	12 (4)	60 (11)***
Cysts (% of basal zone area)	10.9 (0.6)	36.8 (2.1)***
Villi (n per placenta)	13.9 (0.8)	16.8 (1.4)
Maternal artery diameter (mm)	0.50 (0.01)	0.50 ± (0.01)
Maternal artery wall (µm)	113.3 (6.8)	88.1 (6.8)
Glycogen positive cells (n/plac)	45.2 (85.8)	361.5 (204.1)***

Data are mean (SD). * p<0.05, ** p≤0.001, *** p≤0.0001. GD, gestational day; n^p, number of placentas; n^d, number of dams; Maternal art diam, maternal central placental vessel diameter; glycogen positive cells, number of glycogen positive cells in PAS-dPAS staining.

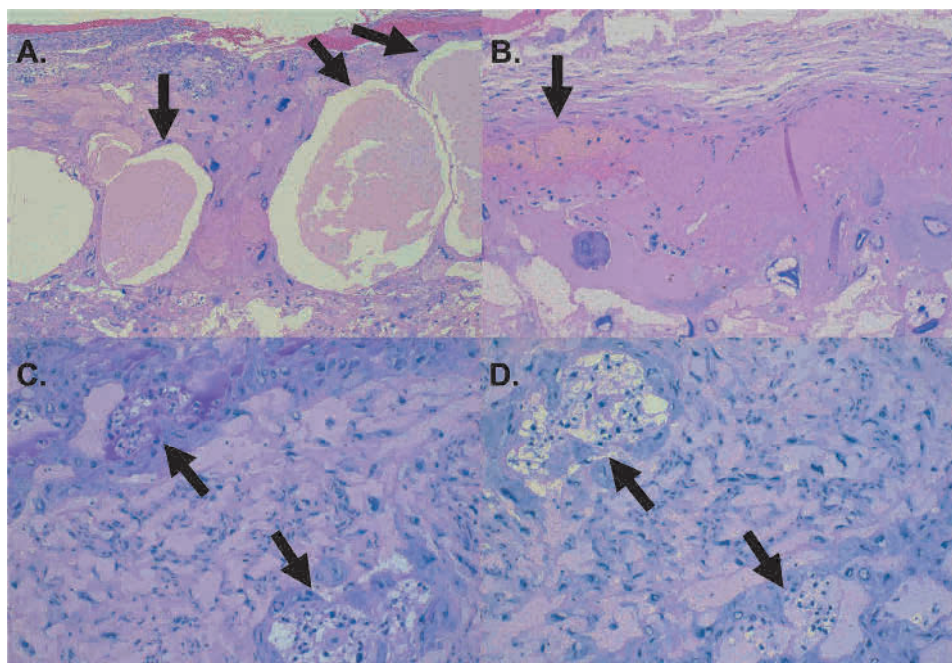


Figure 11. Placental histology at late term rat pregnancy from a maternal hyperglycemia group placenta. A. Placental basal zone with cysts containing homogenous colloid type fluid (arrows). B. Placental sinus vein with a small thromboembolic mass (arrow) on the left side. C. Placental PAS staining. Two placental villi are depicted on top left and bottom right (arrows). Glycogen appear dark purple. D. Placental dPAS staining, where the glycogen is removed. Glycogen in villi is a normal finding. The abnormal glycogen accumulation in the maternal hyperglycemia group occurred in the decidual layer. Arrows point to the villi without glycogen.

5.1.8.2 Gene expression

5.1.8.2.1 Metabolism, hypoxia and inflammation

In the maternal hyperglycemia rat placentas, direct glucose transporter and uncoupling protein 2 genes had increased expression when compared to the control group (Table 11). Genes involved in hypoxia (*Egln3*, glutathione peroxidase 3) and inflammation regulation had decreased expression in rat placentas of the maternal hyperglycemia group when compared to controls (Table 11).

Table 11. Placental gene expression (gene/18S) in the control and maternal hyperglycemia groups.

	Control	Hyperglycemia
n ^p	11	13
n ^d	5	5
Metabolism		
<i>Slc2a3</i>	0.69 (0.05)	1.34 (0.10)**
<i>Slc2a4</i>	0.60 (0.07)	0.75 (0.05)
<i>Ucp2</i>	0.93 (0.06)	1.13 (0.05)*
<i>Ucp3</i>	0.79 (0.14)	0.77 (0.10)
Hypoxia and inflammation		
<i>Egln3</i>	0.71 (0.18)	0.29 (0.06)*
<i>Gpx3</i>	1.06 (0.15)	0.70 (0.17)*
<i>Hsl</i>	0.99 (0.08)	1.00 (0.07)
<i>Ldha</i>	0.95 (0.06)	0.98 (0.05)
<i>Pgdh</i>	1.47 (0.12)	0.44 (0.04)***
<i>Ptgs2</i>	1.50 (0.12)	0.71 (0.07)*
<i>Vegfa</i>	11.40 (1.10)	11.30 (0.90)
Growth		
<i>Atp2a2</i>	0.92 (0.05)	0.95 (0.05)
<i>Bmpr1A</i>	1.01 (0.08)	0.96 (0.08)
<i>Cdkn1b</i>	1.08 (0.41)	0.85 (0.31)*
<i>Egfr</i>	1.20 (0.07)	0.78 (0.05)***
<i>Igf2bp3</i>	1.09 (0.07)	1.09 (0.07)
<i>Igfbp6</i>	0.91 (0.13)	0.56 (0.10)
<i>Pdgfrb</i>	1.08 (0.04)	0.90 (0.05)*
<i>Tnfrsf12a</i>	1.15 (0.12)	0.79 (0.07)*

Data are presented as mean (SD). * p<0.05, ** p<0.001, *** p<0.0001. mRNA concentrations as arbitrary unit (AU). n^p, number of placentas; n^d, number of dams; *Slc2a3*, facilitated glucose transporter 3; *Slc2a4*, insulin-responsive glucose transporter 4; *Ucp2*, uncoupling protein 2; *Ucp3*, uncoupling protein 3; *Egln3*, hypoxia-inducible factor prolyl hydroxylase 3; *Gpx3*, glutathione peroxidase 3; *Hsl*, hormone-sensitive lipase; *Ldha*, lactate dehydrogenase A; *Pgdh*, hydroxyprostaglandin dehydrogenase 15; *Ptgs2*, cyclooxygenase 2 or prostaglandin-endoperoxidase 15; *Vegfa*, vascular endothelial growth factor; *Atp2a2*, sarcoplasmic reticulum Ca²⁺-ATPase; *Bmpr1A*, bone morphogenetic protein receptor type 1A; *Cdkn1b*, cyclin-dependent kinase inhibitor 1B; *Egfr*, epidermal growth factor receptor; *Igf2bp3*, insulin-like growth factor 2 mRNA binding protein 3; *Igfbp6*, insulin-like growth factor binding protein 6; *Pdgfrb*, platelet derived growth factor receptor beta polypeptide; *Tnfrsf12a*, tumor necrosis factor receptor superfamily member 12a.

5.1.8.2.2 Growth

In the maternal hyperglycemia group, placental gene expression of cell cycle controller cyclin-dependent kinase inhibitor 1B (*Cdkn1b*) and placental proliferation inducing *Tnfrsf12a* was increased, and decreased for genes involved in normal placental growth (epidermal growth factor receptor, platelet derived growth factor receptor beta polypeptide) and apoptosis regulation (insulin-like growth factor binding protein 6) when compared to control placentas (Table 11). Umbilical artery PI values had a negative correlation with epidermal growth factor receptor (*Egfr*) ($p=0.002$, $R=-0.62$) and platelet derived growth factor receptor (*Pdgfrb*) ($p=0.03$, $R=-0.45$).

5.1.8.2.3 Placental cytokines

In the maternal hyperglycemia group, placental concentration of proinflammatory IL1 was increased and anti-inflammatory IL2 and IL4 were decreased when compared to the control group (Table 12). Umbilical artery PI values showed a negative correlation with IL4 ($p=0.004$, $R=-0.35$).

Table 12. Placental cytokine and chemokine levels in control and maternal hyperglycemia groups.

Variable	Animal model	
	Control	Hyperglycemia
n ^p	19	19
n ^d	17	9
IL1β	879.8 (357.6)	1827.0 (1378.0)*
IL2	80.7 (25.1)	59.0 (20.8)*
IL4	117.5 (4.8)	85.63 (8.5)*
IL6	<366.0	454.2 (379.1)
IL10	<36.5	<36.5
IL13	<24.5	<24.5
MCP1	<36.50	<36.50
TNFα	<12	<12
G-CSF	<24.5	<24.5
GM-CSF	<61.0	<61.0
IFNγ	<73.0	<73.0
GRO-KC	1659.0 (1017.0)	1283.0 (1084.0)

Data are presented as mean (SD). * $p \leq 0.05$. Results are given as pg/ml/g. IL, interleukin; MCP1, monocyte chemo attractant protein 1; TNF, tumor necrosis factor; G-CSF, granulocyte colony-stimulating factor; GM-CSF, granulocyte macrophage colony-stimulating factor; IFN γ , interferon- γ ; GRO-KC, chemokine C-X-C motif ligand 1.

5.2 Maternal T1DM and the human fetus at near term (IV)

5.2.1 Human pregnancy demographics

The ultrasonography was performed at gestational week 35+5 (13 days) in T1DM women and 37+3 (13 days) for the control group ($p<0.0001$). The time interval from the ultrasound examination to delivery was similar with 12 (4) days in the diabetic group and 14 (8) days in control pregnancies, respectively.

T1DM women had a greater BMI, and increased incidence of smoking, hypertensive disorders, induction of labor, and shorter duration of gestation (Table 13). An operative vaginal delivery or cesarean section, treatment for neonatal jaundice, and neonatal intensive care unit admission were more common among T1DM newborns than in the controls.

Table 13. Obstetric outcome in control and T1DM groups.

Variable	Control	T1DM
n	67	33
Delivery		
Prematurity (<37 gestational weeks)	6 (9.0 %)	11 (33.3 %)*
GA at delivery (weeks)	39.5 (1.9)	37.4 (1.5)**
Induction of labor	15 (22.4 %)	14 (42.4 %)*
Mode of delivery		
Vaginal	50 (74.6 %)	13 (39.4 %)**
Vaginal operative	7 (10.4 %)	2 (6.1 %)
Cesarean section	10 (14.9 %)	18 (54.5 %)**
Elective	3 (4.5 %)	13 (39.4 %)
Acute	7 (10.4 %)	5 (15.2 %)
Neonatal characteristics		
Apgar score at 5 min	8.9 (0.8)	8.6 (0.8)*
Umbilical artery pH	7.3 (0.1)	7.3 (0.1)
Birth weight (g)	3505.0 (555.8)	3685.6 (599.1)
IUGR	3 (4.5 %)	-
LGA	2 (3.0 %)	11 (33.3 %)
Gender male	35 (52.2 %)	16 (78.8 %)
Neonatal jaundice	9 (13.4 %)	9 (27.3 %)*
NICU admission	7 (10.4 %)	24 (72.7 %)**

Values are either mean (SD) or no. and (% of total). * $p\leq 0.05$, ** $p\leq 0.0001$.

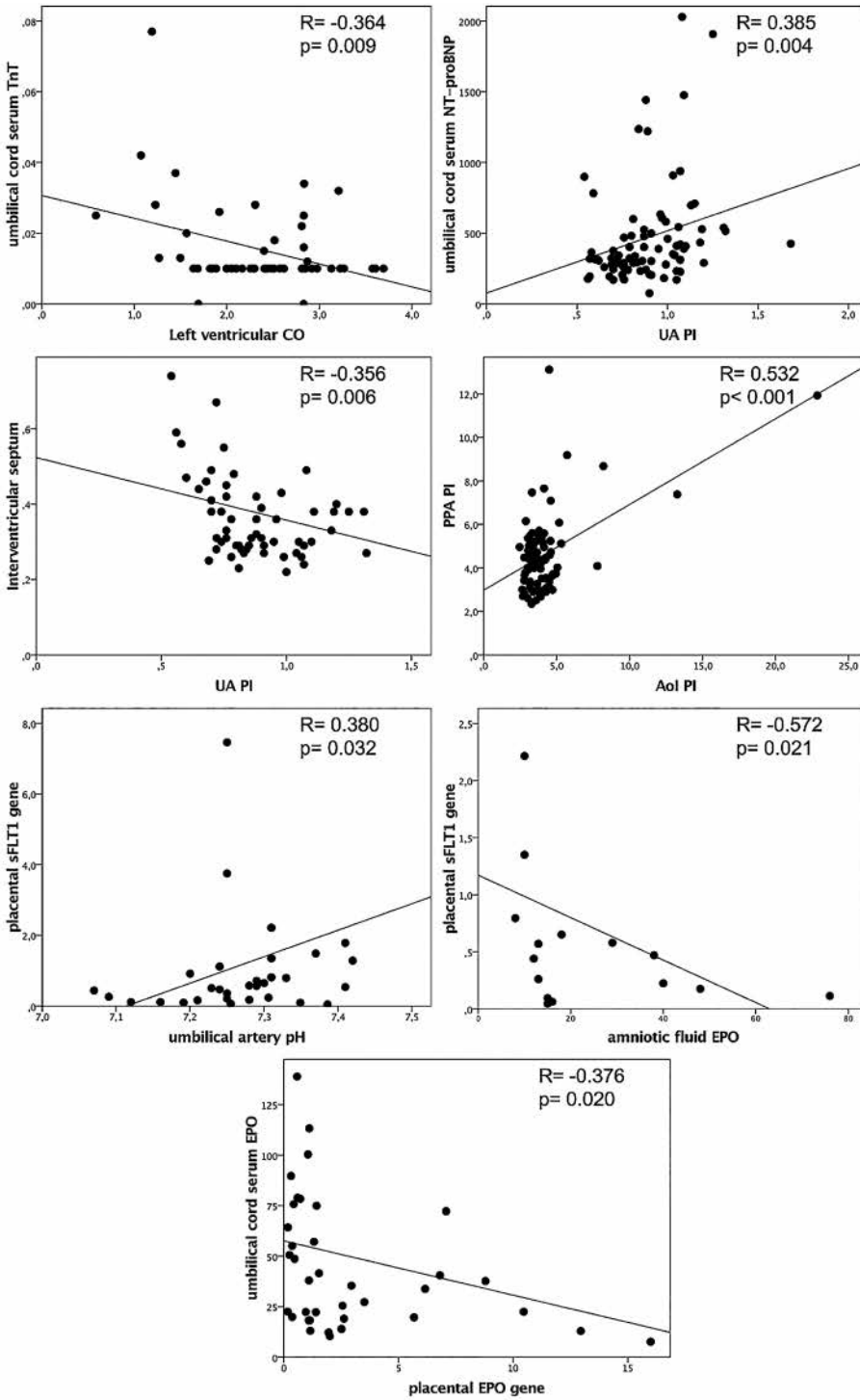


Figure 12. Correlation parameters in control and T1DM pregnancies.

5.2.2 Human fetal heart, and cardiovascular and peripheral hemodynamics

Fetal cardiac ventricular wall and interventricular septal thicknesses were increased in T1DM pregnancies compared to control fetuses (Table 14). In T1DM fetuses, decreased weight-adjusted cardiac output and increased aortic isthmus and inferior vena cava blood flow velocity waveform pulsatilities, and elevated fetal heart rate, were observed. There was a positive correlation between umbilical artery PI values and umbilical cord serum NT-proBNP concentrations and a negative correlation to interventricular septal wall thickness (Figure 12). Umbilical cord serum TnT levels had a negative correlation with left ventricular CO, aortic isthmus PI, and PPA PI had a positive correlation.

Table 14. Fetal hemodynamic data of the control and T1DM pregnancies.

Variable	Control	T1DM
n	67	33
Central hemodynamics		
FHR (bpm)	137.4 (10.7)	144.3 (13.4)*
MPI (LV)	0.43 (0.10)	0.43 (0.09)
TV E/A-ratio	0.66 (0.22)	0.63 (0.30)
MV E/A-ratio	0.83 (0.29)	0.66 (0.27)*
RVCO (ml/min*kg)	369.1 (85.5)	220.1 (93.4)***
LVCO (ml/min*kg)	247.9 (61.5)	162.3 (65.9)***
CCO (ml/min*kg)	619.2 (129.5)	405.9 (184.5)**
RVW diastole (mm)	3.5 (0.69)	5.6 (2.6)***
IVS diastole (mm)	3.5 (0.9)	5.8 (3.0)***
LVW diastole (mm)	3.5 (0.7)	4.5 (0.8)***
Peripheral hemodynamics		
A Ut mean PI	0.63 (0.26)	0.61 (0.17)
UA PI	0.88 (0.20)	0.73 (0.41)
MCA PI	1.58 (0.47)	1.67 (0.71)
AoI PI	3.77 (0.76)	7.23 (4.42)*
DAo PI	1.97 (0.44)	1.92 (0.41)
PPA PI	4.51 (1.73)	6.08 (2.64)
IVC PIV	1.70 (0.43)	2.01 (0.34)**
DV PIV	0.50 (0.18)	0.53 (0.10)

Data are presented as mean (SD). * $p \leq 0.05$, ** $p \leq 0.001$, *** $p \leq 0.0001$. FHR, fetal heart rate; MPI, index of myocardial performance; TV, tricuspid valve; E/A-ratio, atrial E-wave to A-wave ratio; MV, mitral valve; R/LV/CCO, right/left ventricular/combined cardiac output; R/LVW, right/left ventricular wall; IVS, interventricular septum; AUt, uterine artery; PI, pulsatility index; UA, umbilical artery; MCA, middle cerebral artery; AoI, aortic isthmus; DAo, descending aorta; PPA, proximal pulmonary artery; IVC, inferior vena cava; PIV, pulsatility index for veins; DV, ductus venosus.

5.2.3 Newborn human biochemical markers of cardiac function

In the T1DM pregnancies, the newborn umbilical cord serum concentrations of NT-proANP, NT-proBNP, and cTnT were increased when compared to controls (Table 15). No differences were seen in the umbilical cord serum erythropoietin concentrations between the groups.

Table 15. Biochemical markers in control and T1DM pregnancies.

Variable	Control	T1DM
n	67	33
Amniotic fluid		
EPO (U/l) (n=24)		30.8 (54.2)
Umbilical cord blood serum		
EPO (U/l)	41.61 (42.62)	66.43 (106.65)
NT-proANP (pmol/l)	2134.0 (945.6)	2956.7 (1304.4)*
NT-proBNP (pmol/l)	383.8 (267.7)	710.4 (488.4)**
TnT (μ g/ml)	0.014 (0.008)	0.033 (0.032)**
Activin A (pg/ml)	836.1 (801.9)	1038.2 (1174.4)
Placenta		
<i>Epo</i> mRNA (/18S)	3.26 (3.67)	1.79 (3.31)
<i>sFlt1</i> mRNA (/18S)	2.72 (2.83)	0.73 (0.88)*

Data as mean (SD). * $p \leq 0.05$, ** $p \leq 0.0001$. EPO, erythropoietin; NT-proANP/BNP, N-terminal pro-atrial/B-type natriuretic peptide; TnT, troponin T; sFlt1, soluble Fms Related Tyrosine Kinase 1.

5.2.4 Human placenta

Placental gene expression of soluble vascular endothelial growth factor receptor (*sFlt1*) was lower in the T1DM group than in the control group (Table 15). The placental gene expression and umbilical cord serum *Epo*, and cytokine concentrations (Table 16) were similar in both groups. Placental sFlt1 showed a positive correlation to umbilical artery pH and a negative correlation to amniotic fluid EPO (Figure 12).

Table 16. Human placental cytokine levels in control and T1DM pregnancies.

Variable	Human data	
	Control	T1DM
n	67	33
IL1 β	< 6.58	< 6.58
IL2	< 6.65	< 6.65
IL4	7.93 (1.08)	<7.60
IL6	20.63 (29.44)	31.89 (77.61)
IL8	41.64 (38.40)	76.74 (223.12)
IL10	< 7.08	< 7.08
MCP1	333.17 (266.60)	642.94 (1776.80)
TNF α	6.13 (0.46)	6.18 (0.78)

Data are mean (SD). * $p \leq 0.05$. Results are given as pg/ml/g. IL, interleukin; MCP1, monocyte chemo attractant protein 1; TNF, tumor necrosis factor.

6 DISCUSSION

6.1 Validation and limitations of methodology

6.1.1 *Rat model of maternal hyperglycemia (I-III)*

The duration of rat pregnancy is only approximately 22 days, much shorter than human pregnancy. Nevertheless, the mode of placentation – discoid uniplacenta – and the main principles of fetal development are close to that of humans. After birth, neonatal rats mature rapidly, and a postnatal age of 14 days of the rat is the equivalent of 3–6 months of human infant age, depending on the organ investigated. Therefore, it is obvious that a chronic human disease with organ complications developing over several decades cannot be studied solely by experimental animal models.

Administration of STZ before or after the commencement of pregnancy creates different types of hyperglycemic models. Rodents are the most commonly used laboratory animals, since they are economical to use, have a short biological life span and are small in size. Animal models enable researchers to examine diseases with invasive methods, and this increases our fundamental knowledge on disease processes. On the other hand, an artificial model can never completely reproduce the complex immunological, inflammatory, and metabolic processes taking place in human disease, information on which we need to be able to understand the pathophysiologic consequences for the fetus during maternal hyperglycemia (Jawerbaum & White 2010). STZ has a half-life of <6 hours. It is cytotoxic, and since it targets pancreatic β -cells through glucose transporter 2 (*Slc2a2*, GLUT2 protein), it may be harmful to tissues expressing *Slc2a2* (Schnedl et al. 1994). Since the heart does not express *Slc2a2*, it is protected from direct cytotoxicity, whereas the liver and kidneys are affected (Jurysta et al. 2013). In this study, STZ was administered prior to pregnancy to avoid direct fetal cytotoxic effects.

A limitation in this study is that we did not measure fetal and offspring glucose or insulin levels. We tried to collect fetal blood samples at late term gestation, but the volumes were too small for analysis. Furthermore, there is bound to be some limitations due to the processing of samples. The interval between tissue removal and freezing affects the tissue size – the longer the interval, the smaller the tissue (Larsson & Skogsberg 1988). Volume analysis in the animal studies were performed on previously frozen samples and this is likely to affect volumes. However, micro-CT samples in both study groups were processed similarly.

6.1.2 *Human data (IV)*

A limitation on human study is the selection of patients. Study IV was a prospective observational study. T1DM women regardless of their White classification status were

consequently recruited at the outpatient maternity department. The control women had an inclusion criteria for BMI < 30 kg/m².

6.1.3 Ultrasonography (I, II, IV)

Doppler ultrasonography is a widely used non-invasive method to assess fetal and maternal hemodynamics during pregnancy. Ultrasound creates energy while travelling through tissues. The forms of energy are usually classified as thermal, cavitation and radiation pressure streaming effects. Thermal energy created by the transducer on fetal tissues may be harmful for the fetus because of hyperthermia (Abramowicz et al. 2002). Each ultrasound equipment used in human studies must have information about thermal and mechanical indexes. The mechanical index describes the cavitation potential of the tissue that increases with increasing pulse amplitudes. Cavitation is the formation of gas bubbles at high negative pressure. Radiation pressure is generally thought to be insignificant with modern Doppler ultrasound techniques. Cynomolgus monkey (*Macaca fascicularis*) shows no long-term harmful effects after repeated (1–5 times /week) ultrasonographies (Tarantal et al. 1993; Tarantal & Hendrickx 1989b; Tarantal & Hendrickx 1989a). In humans, there were no significant differences after multiple mid- to late-term sonographic examinations in children followed-up for 8 years (Newnham et al. 2004). However, a meta-analysis with follow-up data on nearly 8900 children until age 8–14 years did show an association between pregnancy ultrasound screening and being non-right handed later in life (Salvesen 2011).

The main limitations of pulsed wave Doppler ultrasonography are in the maximum detectable blood flow velocity and the depth of penetration; the preceding pulse needs to return to the transducer before a new pulse can be emitted. Color-coded pulsed Doppler adds information on the direction and speed of the blood flow, but it has the same limitations as pulsed wave Doppler ultrasonography. However, previous animal experiments have found that Doppler ultrasonography derived volume flow measurements correlate well with those measured by invasive methods (Acharya et al. 2004). In the present rat model, we could not distinguish between right and left ventricular inflow and outflow. In humans, atrioventricular valves form during gestational week 7 (de Vlaming et al. 2012). In mice, the valves are formed by gestational day 15 (Gui et al. 1996; Witte et al. 1994). Data on rat valve embryology was not available. However, we extrapolate from mice pregnancy that the valve leak found in fetuses with maternal hyperglycemia originated from a common AV-valve structure before its separation to TV and MV. Cardiac inflow and outflow blood flow velocity waveform patterns in mice from 15 gestational days correspond to human fetal patterns recorded at gestational week 20. In both species, developing fetal cardiac inflow patterns signify increasing cardiac compliance and blood flow. However, outflow tract peak blood flow velocities are controlled with developing AV and semilunar valves that decrease the cardiac work needed to eject blood (Gui et al. 1996). Fetal circulation works in parallel due to the ductus arteriosus

and the foramen ovale, and the systemic pressure in the right and left ventricle is equal. Finally, we were compelled to use anesthesia during ultrasonographic examination. Nevertheless, fetal ultrasonography would be impossible and not ethically acceptable to perform without anesthesia in animals, and invasive measurements have been performed under similar anesthesia.

Repeatability of the measured parameters is crucial for assessing validity. Intra-observer variability of Doppler-derived parameters was tested for fetal peripheral vessels in the rat model and it was found to vary between 6.4 and 9.9%. Previously, a mouse model experiment has shown that the intraobserver variability of inflow and outflow VTIs range from 6.0 to 6.5% and of time interval measures from 2.5 to 15.9% (Rounioja et al. 2003). Slight and insignificant inter- and intraobserver variability was recorded in mice pregnancies. However, the peak outflow velocity was susceptible to error (Gui et al. 1996). In humans, the intraobserver variability of volume blood flow calculations is < 9% and < 4% for vascular impedance measurements (Rasanen et al. 1998). Altogether, these studies demonstrate that ultrasonography is a repeatable and reliable method in both animal and clinical studies.

6.1.4 Histological and biochemical assays (I-IV)

Histological and biochemical assays have been well validated in cardiac (McCormick et al. 2014) and placental examinations (Mayhew & Burton 1988). In histological and some biochemical assays fetal and neonatal tissues are highly active and common staining methods used in adult tissue can give falsely positive results. For example, Ki67 immunostaining proved to be highly complex and the appropriate dilution was tested intensively. Since histological analyses are performed by humans bias is possible. To reduce this risk, most of the histologic analyses were performed independently by two investigators blinded to the study group.

6.2 Fetal and neonatal cardiac development and function in maternal hyperglycemia

One of the most consistently documented complications related to pregnancies of women with T1DM is fetal cardiomegaly (Aman et al. 2011; Russell et al. 2008; Veille et al. 1992). This holds true also for several animal models (Dowling et al. 2014; Corrigan et al. 2013). Cardiac enlargement can be associated with increased cardiac work load, *i.e.*, afterload or preload, and has been reported in fetuses of T1DM mothers estimated from cardiac sonographic parameters (Russell et al. 2008; Rizzo et al. 1991; Räsänen & Kirkinen 1987). Based on previous studies, we hypothesized that rat fetal cardiac function is compromised in maternal hyperglycemia. We also hypothesized that, in human T1DM pregnancies with maternal insulin treatment, fetal cardiac function

and hemodynamics, placental morphology, placental gene expression, and cytokine production are similar to those of control pregnancies.

In the fetus of hyperglycemic rats, one of the most interesting findings was the presence of holosystolic AV-valve regurgitation in almost all fetuses and a significantly decreased outflow V_{mean} at 13–14 days of gestation. Although this may indicate fetal cardiac functional compromise, it is likely to reflect immature development as this finding was transient. By later gestation the incidence of AV regurgitation and outflow V_{mean} were comparable to those of control group fetuses. Fetuses of hyperglycemic rats also had an increased E/A VTI ratio reflecting diastolic functional impairment and increased atrial workload. Sudden changes in fetal cardiac loading conditions, such as preload and afterload, increase the incidence of AVVR that resolves after the heart has adjusted to these changes (Respondek et al. 1994). In humans, fetal diastolic and systolic function improve between gestational weeks 7 to 10 and fetal AVVR is very common in healthy fetuses at gestational weeks 9 to 10, which probably reflects the significant increase in placental volume blood flow (Mäkikallio et al. 2005). Maternal pregestational hyperglycemia leads to abnormal cardiac function at gestational weeks 11 to 14 (Turan et al. 2011). Still, maternal hyperglycemia might remodel the myocardium and reduce its capacity to adapt to rapid changes in cardiac loading conditions. This could partially explain the increased occurrence of miscarriages in T1DM women during early pregnancy. In human early pregnancy, the umbilicoplacental volume blood flow increases with no changes in umbilical artery vascular impedance (Mäkikallio et al. 2005). In the present rat model of maternal hyperglycemia, vascular impedance in the descending aorta and UA was increased. DV pulsatility increased towards term in the maternal hyperglycemia group, suggesting cardiac diastolic impairment in accordance with the increased E/A VTI ratio.

In human T1DM pregnancies near term, a striking finding was the decreased weight-adjusted RVCO, LVCO, and CO. Furthermore, the thickness of the right and left ventricle wall and the interventricular septum was significantly greater in T1DM fetuses than controls. Despite insulin treatment during pregnancy as opposed to the experimental animals in this study, there was an increase in umbilical cord serum natriuretic peptides and TnT in the T1DM fetuses at birth, as has been observed previously (Russell et al. 2009). This might indicate fetal myocardial strain or ischemia (Boo et al. 2005). In addition, we saw an increase in the pulsatility of IVC and Aol in fetuses of T1DM women when compared to the fetuses of healthy control women. Increased Aol pulsatility correlates with a poor fetal outcome, especially if fetal growth is restricted (Del Río et al. 2008; Mäkikallio et al. 2003). In human fetuses of mothers with varying types and treatments of diabetes, the Aol isthmus flow index is decreased indicating increased pulsatility (Zielinsky et al. 2011). Aol blood flow velocity waveform is affected by a difference in the upper and lower body and placental vascular resistances. Furthermore, central hemodynamics may play a crucial role in the regulation of blood flow across the

AoI, and it seems that adequate LVCO is important for maintaining antegrade flow across the aortic isthmus. In fetuses of T1DM mothers, there was a reduction in the weight-indexed LVCO which could contribute to the increased pulsatility in the AoI. The AoI pulsatility index correlated positively with the PPA pulsatility index, suggesting that pulmonary vascular impedance in PPA is involved in regulating the AoI blood flow velocity waveform. In fact, the increased pulsatility index in PPA indicates, at least indirectly, increased pulmonary vascular resistance and decreased lung volume blood flow. Fetal LVCO is the sum of the blood flow volume across the foramen ovale and the lung circulation. Thus, a reduction in volume blood flow or reduced foramen shunting due to increased left ventricle end-diastolic pressure would lead to a reduction in LVCO and contribute to increased pulsatility in the AoI blood flow velocity waveform. The UA and MCA PI values were comparable between the groups. However, the reduction in LVCO may be detrimental to cerebral blood flow and perfusion pressure. The concentration of TnT correlated negatively with LVCO, indicating that the leak of TnT from the myocardium correlates with left ventricular cardiac performance. In human neonates, TnT concentrations are elevated in newborns with cardiorespiratory morbidity (Clark et al. 2001). Increased IVC pulsatility may be a sign of augmented atrial contraction or increased ventricular end-diastolic pressure.

The fetuses of a hyperglycemic mothers have an increased cardiac work load (Turan et al. 2011; Russell et al. 2008; Tsutsumi et al. 1999; Räsänen & Kirkinen 1987). We demonstrated excess ventricular and septal wall growth in humans, and heavier hearts in rats. Both of these develop when cardiac work load is increased. In the animal model, we found an increase in cell turnover activity at late term gestation with evidence of cardiac hyperplastic growth. Similar growth patterns have been reported in other studies on maternal hyperglycemia of the rat (Han et al. 2015), while the mouse may exhibit a hypertrophic growth pattern (Dowling et al. 2014). During pregnancy, fetal cardiac growth occurs mainly via proliferation (Thornburg et al. 2011). This changes to a hypertrophic growth pattern after birth, in rats at 3–4 postnatal days (Li et al. 1996). In the present rat study, the cell turnover activity decreased after birth in both study groups compared to the cell turnover rates during pregnancy. In the offspring to rats with hyperglycemia cardiomyocyte apoptosis was increased at one week postnatally, and two weeks after birth an increase in cardiomyocyte mitosis was seen. The fetal heart weight was similar in both groups, but the body weight was lower in the maternal hyperglycemia group. Despite a similar euglycemic diet to both groups after birth, the offspring to the rats in the maternal hyperglycemia group were programmed to conserve cardiac growth at the expense of other organs.

The fetal rat hearts in the maternal hyperglycemia group demonstrated increased gene expression of cardiomyocyte proliferation, *Tnfrsf12a*, and natriuretic peptides (*Nppa*, *Nppb*), important regulators also during pregnancy for maintaining homeostasis and vasodilation (Cameron & Ellmers 2003). In human fetuses of T1DM mothers the con-

centrations of natriuretic peptides were increased in umbilical cord sera, which is in agreement with previous findings (Russell et al. 2009; Girsen et al. 2008). This shows that despite insulin treatment of maternal hyperglycemia, natriuretic peptide concentrations are increased in T1DM fetuses. Natriuretic peptides have several functions, e.g., regulation of cell mitosis, extracellular fluid volume, electrolyte balance, and blood pressure through vasodilation, and to provide cardioprotection (Das et al. 2009). It has been suggested that ANP treatment should be provided to patients with acute myocardial infarction, since it improves myocardial function and survival (Lyu et al. 2014).

Fetuses of the mothers with T1DM in this study had a statistically significantly increased FHR compared to the control group. However, the clinical significance of this observation is questionable because in both groups the mean is well within limits. A study on hyperglycemic murine pregnancies found increased FHR, as well (Aasa et al. 2013). Increased FHR in T1DM pregnancies occurs during hyperglycemic episodes (Cypryk et al. 2015). Increased fetal heart rate variability in T1DM fetuses is regarded as a sign of fetal sympathetic dominance (Russell et al. 2016). Increased norepinephrine concentrations have been reported in hyperglycemic rats (Paulson & Light 1981), and it seems that catecholamines can be transferred across the placenta (Eisenhofer 2001). In fetal monkeys, hyperglycemia decreases the catecholamine response to stress, whereas insulin increases the catecholamine response (Cohn et al. 1992). Hyperglycemic fetuses live in an environment similar to type 2 diabetes, and in adult type 2 diabetic mice, the dobutamine stress test results in an accentuated cardiac inotropic and lusitropic response (Daniels et al. 2010). However, the *Kcnip2* gene, which mediates improved contractility and systolic function through increased action potential duration (Sah et al. 2003), is downregulated in rat fetuses at near term. At term, in fetuses of rats with hyperglycemia, decreased expression of the *Kcnip2* gene suggests a role for this gene in decreasing FHR.

After birth, cardiac gene expression patterns in the newborns to rats with maternal hyperglycemia differed from the control offspring. In the offspring to rats with hyperglycemia, most genes were downregulated on the day of birth and reached normal levels at one week of postnatal life. After birth, gene expression patterns respond to the sudden increase in cardiac work load, the fall in glucose levels, and the changes in oxygen supply. The fetus needs to adapt quickly to the new metabolic environment. Cardiac gene expression patterns reflect the changes in previous cardiac loading and metabolic conditions. The genes involved in cardiac contractility, *Atp2a2* and *Kcnip2*, and growth, *Tnfrsf12a*, were downregulated. *Atp2a2*, previously known as *Serca2*, recirculates Ca^{2+} into the sarcoplasmic reticulum, and in decreased levels contributes to diastolic dysfunction in adult hyperglycemic mice (Yue et al. 2007). Decreased concentrations of *Atp2a2* protein promote arrhythmias after myocardial injury in adult rats (Matus et al. 2015). Lack of *Kcnip2* in knock-out mice increases the risk of ventricular tachycardia, as the plateau phase of the cardiac action potential is prolonged (Kuo et al. 2001). Both

Atp2a2 and *Kcnp2* improve contractility. Furthermore, the expression of genes regulating natriuretic peptide expression were increased. Natriuretic peptides have several functions and participate in fetal cardiac development (Cameron & Ellmers 2003), e.g. ANP induces apoptosis (Thornburg et al. 2011), but mainly works to protect the heart (Das et al. 2009). At PND 14 *Atp2a2*, *Kcnp2*, *Tnfrsf12a*, and *Nppb* expression levels were increased. This may be in response as the environment normalizes. Increased NT-proBNP levels are found in human newborns, and associated with interventricular septal thickness (Mert et al. 2016). Human newborns of mothers with T1DM had increased NT-proANP and NT-proBNP umbilical cord serum concentrations (IV). This could be a sign of cardioprotection and an attempt to improve cardiac compliance as suggested by the rat model of maternal hyperglycemia.

6.3 Placental function in maternal hyperglycemia

Our experimental animal model showed several abnormalities in placental structure, hemodynamics, and gene expression in the maternal hyperglycemia group near term. Although the placental weights were not statistically different between the maternal hyperglycemia and control groups, they were larger in dimension (Table 10, study II). The placental structure was disrupted by peripheral sinus vein thrombi, interstitial fluid, and basal zone cysts containing collagenous fluid. Previously, Padmanabhan and Shafiullah (Padmanabhan & Shafiullah 2001) found that placentas of STZ-treated dams developed abnormally: There were extensive glycogen formations especially in the decidua and glycogen in the basal zone of the placenta had degenerated into an eosinophilic mass containing cysts and a porous labyrinthine layer at gestational day 18. In the present study (II), in addition to the abnormalities described by Padmanabhan & Shafiullah (2001), near term gestation interstitial fluid formation, thrombosis, and large cysts throughout the basal zone had emerged. These morphologic abnormalities were associated with increased UA vascular impedance. The vascular resistance of the umbilical artery reflects the number of tertiary villous arterioles in the placenta (Fadda et al. 2001; Trudinger et al. 1985). However, increased vascular resistance in the placenta does not necessarily increase placental vascular impedance (Junno et al. 2013). Still, vascular impedance in the UA increases once 60% of the placental arterioles are obstructed (Trudinger et al. 1985). There was no association between the vascular impedance of the UA and the number or density of placental villi. These findings indicate that fluid and glycogen accumulation and increased thrombosis formations affect placental circulation negatively.

Interestingly, the placentas derived from rats with STZ-induced hyperglycemia demonstrated signs of inflammation. Proinflammatory IL-1 β was increased and anti-inflammatory interleukins were decreased. Also, the expression of genes involved in prostaglandin synthesis and metabolism of the placenta were increased. UA PI values, again, correlated negatively with the concentration of anti-inflammatory interleukin IL-

1 β and to the placental expression of cyclo-oxygenase 2 (Tables 11 & 12). Previously, a maternal high-fat diet during pregnancy has been linked with increased placental IL-1 β levels in a primate model with decreased umbilical venous volume blood flow (Frias et al. 2011). Although it seems that morphological changes of the placenta affect umbilicoplacental vascular impedance, it is unlikely that gas diffusion in and through the placenta is affected, since the transfer of glucose and amino acids across the placenta occur mainly through other means than simple diffusion (Hay 1994). However, our findings with a rat model of maternal hyperglycemia demonstrate that morphological changes in the placenta may contribute to the development of placental insufficiency in the hyperglycemic rat and possibly increase the risk for intrauterine fetal death.

Near term, placental growth-related gene expressions were decreased in the maternal rat hyperglycemia group, apart from the IGF-related genes. *Egfr* and *Pdgfr* are essential for normal development of the placenta. *Egfr* deficiency leads to a small placental size and fetal multi-organ failure (Miettinen et al. 1995), whereas *Pdgfr* is needed for normal development of the placental vasculature (Nystrom et al. 2006). *Egfr* and *Cdkn1b* enhance normal villous structural maturation and if their gene expression is low, increased proliferation but not differentiation of the cytotrophoblast ensues (Abdou et al. 2013). UA PI values correlated negatively with *Egfr* and *Pdgfr* further strengthening the concept that the maternal hyperglycemia group exhibited placental insufficiency.

Human placental histologic findings are well described in type 1 diabetic pregnancies. The abnormalities include increased placental volume and branching of villous capillaries (Jirkovska et al. 2012), placental glycogen content and weight (Desoye et al. 1992), and vessel chorangiomas, villous immaturity, and fibrinoid necrosis (Evers et al. 2003). In the present study (study IV), there were no signs of increased umbilical or uterine artery vascular impedance in T1DM fetuses at term perhaps implying redundancy in placental functional capacity.

We investigated several cytokines and chemokines based on our previous results in rat term placentas. Previous studies have reported that placentas of T1DM women have increased invasion of pro-inflammatory macrophages (Sisino et al. 2013) and elevated cytokine levels (Hiden et al. 2008). High cytokine levels are also present in maternal and umbilical blood in type 2 diabetes mellitus and gestational diabetes (Hara et al. 2016). Primates fed with a high-fat diet, present with increased placental levels of pro-inflammatory cytokines (Frias et al. 2011). Obesity alone affects the placental transcriptome, the pathways involved in placental inflammation and immune responses, lipid metabolism, cancer pathways, and angiogenesis (Altmäe et al. 2017). However, we did not find any differences in placental cytokine levels between T1DM and control women (Table 16, study IV). Perhaps insulin counteracts hyperglycemia sufficiently on the placental level, and other harmful substances such as fatty acids are transported further

into the fetus. Furthermore, placental storage capacity may protect the placenta to some extent.

6.4 Fetal cardiac metabolism and hypoxia in maternal hyperglycemia

The fetuses of rats with maternal hyperglycemia were exposed to severe hyperglycemia throughout pregnancy. Metabolism-associated genes were affected in the heart. *Slc2a4*, the insulin- and contraction-responsive glucose transporter, is found in high amounts in striated muscle where it controls glucose uptake in adults. Decreased levels lead to insulin resistance, glucose intolerance, cardiac hypertrophy, and heart failure (Zisman et al. 2000). At late term pregnancy and at birth rat fetuses and newborns of rats with maternal hyperglycemia had decreased levels of *Slc2a4*, but by 2 weeks after birth the expression of this gene was increased. The downregulation of *Slc2a4* is probably due to the excess availability of glucose. After birth, its expression increased in the group of rats with STZ-induced hyperglycemia as the newborns become hypoglycemic. Also, the excessive growth of the myocardium may require more glucose postnatally. In the maternal hyperglycemia offspring, the levels of the facilitated glucose transporter, *Slc2a3*, were decreased at PND 0 and increased at PND 14. These changes apparently reflect the circulating glucose levels in the offspring. At PND 0, *Slc2a3* gene expression reflects glucose concentrations during pregnancy. Later cardiac expression levels reflect hypoglycemia in the newborn, which reacts by increasing the expression. These results are in agreement with some previous studies (Garcia et al. 2016).

Uncoupling proteins participate in mitochondrial respiration and protect the mitochondria from lipid-induced oxidative stress (Chan & Harper 2006). There are signs of increased oxidative stress in the fetus of mothers with T1DM (Escobar et al. 2013; Loukovaara et al. 2005). Maternal hyperglycemia affects fetal and neonatal rat heart *Ucp* expressions. Myocardial expressions of *Ucp2* and 3 were upregulated at term pregnancy and at PND 14, but downregulated at PND 0 in the maternal hyperglycemia group (Table 9, study III). *Ucp2* expression is increased in neonates, and this probably reflects the switch of energy source from carbohydrates to fatty acids (Van Der Lee et al. 2000). The expression of *Ucp3* is induced, in turn, when fatty acids are supplied in excess and the oxidative capacity of the cell is exceeded (Cole et al. 2011). Cardiac excess growth and maternal hyperglycemia delay the switch from carbohydrates to fatty acids in cardiomyocytes (Kantor et al. 1999); insulin resistance further increases the fatty acid uptake to mitochondria (Cole et al. 2011). However, upregulation of uncoupling proteins may not always be beneficial, since the uncoupling proteins may produce heat rather than ATP, and ATP *per se* is produced less than during normal aerobic respiration based on glucose availability (Cole et al. 2011). Hyperglycemic adult mice require increased amounts of cardiac oxygen, because the expression of genes regulating basal metabolism and excitation-contraction coupling are less efficient and

this reduced the metabolic efficiency of the myocardial tissue (Boardman et al. 2009). Perhaps due to energy-expenditure reasons, fetal and neonatal rat cardiac myosin expressions were disturbed in maternal hyperglycemia in this study (I, III). By late term pregnancy, the skeletal type heavy-chain myosin increases. After a transient reduction in the expression of myosin at birth, adult skeletal type and α -cardiac heavy chain myosin expression is regained. However, expression of myocardial skeletal type myosins are slower, but less energy-consuming (Rajabi et al. 2007). Furthermore, even during hyperglycemia in the myocardium, EPO protects the tissue from ischemia-reperfusion injuries (Jun et al. 2014). However, during pregnancy the hearts were not hypoxic (I). In maternal hyperglycemia, expression of *Egln3*, a cardiac hypoxia marker, in the myocardium of rat offspring is increased. *Egln3* seems to enhance cardiac function (Xia et al. 2015), but may also be triggered by inflammation (Salas et al. 2017). Perhaps this increase in *Egln3* gene expression is caused by inflammatory reactions rather than by frank myocardial ischemia.

6.5 Placental metabolism and hypoxia in maternal hyperglycemia

Rat maternal hyperglycemia pregnancies revealed placental expression of certain genes at term gestation. The levels of *Slc2a3*, a facilitated glucose transporter with a higher affinity for glucose than other glucose transporters, and of *Ucp2* were increased. *Slc2a3* reflects the availability of glucose in the placenta and is naturally upregulated in maternal hyperglycemia (Sciullo et al. 1997). *Ucp2* is a marker of oxidative stress, and its expression in the placenta from women with diabetes and obesity is increased (Martino et al. 2016).

EPO may serve as a marker of chronic fetal hypoxia in diabetic pregnancies (Escobar et al. 2013; Teramo et al. 2004b). However, some studies claim that umbilical cord serum EPO correlates better with fetal oxygen tension and pH at birth than with indicators of chronic hypoxia, such as fetal growth and hematocrit (Rollins et al. 1993). EPO induces erythropoiesis and protects tissues from ischemic damage (Lipsic et al. 2006). EPO production may also be triggered by fetal oxidative stress (Todorov et al. 2000). In study IV, no fetuses of T1DM mothers had an arterial pH <7.05 at birth, nor was there any difference between the groups regarding umbilical arterial pH or Apgar scores. Still, 29 % (7/24) of T1DM fetuses had EPO-levels in the amniotic fluid exceeding 27 U/l. The EPO concentrations in amniotic fluid and umbilical cord blood serum were not associated with arterial pH values or Apgar scores, and the same was true for placental *Epo* expression. The expression of placental *sFlt1* was, on the other hand, positively associated with arterial pH. In the rat model of maternal hyperglycemia, the number of nucleated red blood cells was increased, and this may be a sign of hypoxia. However, the gene-expression patterns in the placenta of the maternal hyperglycemia group indicate that the placentas were not hypoxic (II). Placental expression of *sFlt1* is lower in T1DM than control women. *sFlt1* has a detrimental effect on placental blood vessel

growth. Its maternal serum concentrations are higher in early pregnancy in women who develop pre-eclampsia later on than in women with uncomplicated pregnancies (Moore Simas et al. 2014). Altogether, EPO production may be a beneficial compensatory mechanism in a hemodynamically uncompensated fetus and the inability to increase EPO may be the true risk factor determinant. Furthermore, placental production of sFlt1 may be actively inhibited to enhance placental vascular function.

6.6 Clinical implications

The rat model of maternal pregestational hyperglycemia demonstrates the effects of constant maternal and fetal hyperglycemia on the developing fetal heart and placenta with evidence of long-term consequences on the neonate. These further emphasize the importance of optimal maternal glycemic control during pregnancy. In this study, maternal glycemic control during pregnancy was inadequate in human T1DM pregnancies, but still fetal cardiac function and central hemodynamics were abnormal compared to the control fetuses. In diabetic and other high-risk pregnancies, the worldwide surveillance protocol of fetal well-being includes the monitoring of umbilical artery and middle cerebral artery blood flow velocity waveform patterns. This study shows that in fetuses of human T1DM pregnancies, MCA and UA vascular impedances are comparable to those found in fetuses with uncomplicated pregnancies. Fetal monitoring based solely on these impedances may not reveal compromise in fetal well-being. However, major changes in central hemodynamics were observed in the human T1DM group fetuses. In the T1DM fetuses, pulsatility index values of Aoi and IVC blood flow velocity waveforms were increased and weight-adjusted cardiac outputs were decreased. These alterations in fetal central hemodynamics were present even with normal UA and MCA velocimetries. The results of this thesis suggest that the fetal surveillance strategy in diabetic pregnancies should include monitoring of fetal central hemodynamics though peripheral velocimetries may reveal other harmful processes occurring in the fetus such as placental insufficiency. This new strategy could potentially improve detection of fetal compromise in pregnancies complicated by maternal diabetes.

7 CONCLUSIONS

1. The experimental studies show that fetuses to rats with STZ-induced hyperglycemia present signs of cardiac enlargement and myocardial remodeling due to hyperplasia. Cardiomyocytes of these fetuses were used to show that expression patterns involve genes related to electrical, contractile, endocrine, and metabolic functions of the heart. There is a transient reduction in cardiac output and holosystolic atrio-ventricular valve regurgitation but a consistent reduction in the fetal heart rate. At term there are signs of cardiac diastolic dysfunction. Furthermore, fetal vulnerability to hypoxemic stress may be attenuated (I).
2. Throughout gestation, maternal STZ-induced hyperglycemia in the rat leads to compromised placental and fetal hemodynamics compared to healthy control pregnancies. Near term, umbilical artery vascular impedance correlates with structural abnormalities of the placenta in the maternal hyperglycemia group. In the maternal hyperglycemia group, this has detrimental effects on the placental hemodynamic capacity that may increase the incidence of intrauterine fetal death (II).
3. Maternal pregestational STZ-induced hyperglycemia in the rat associates with altered expression of genes regulating fetal cardiac growth, function, and metabolism. The gene expression patterns show decreased gene expression profiles on the day of delivery. At age 2 weeks, the gene expression profiles had increased again. Maternal pregestational hyperglycemia may reprogram gene expression of the myocardium of the offspring and establish long-term consequences in gene expression patterns (III).
4. In pregnant women with T1DM at term, fetal cardiac output decreases while the pulsatility of the aortic isthmus blood flow velocity waveform increases. Fetal serum concentrations of natriuretic peptides and troponin T increase, as well. The reduction in cardiac output of the fetus takes place concomitantly with biochemical evidence of myocardial dysfunction (IV).

8 ACKNOWLEDGEMENTS

This study was carried out at the Department of Obstetrics and Gynecology and at the Research Center of Applied and Preventive Cardiovascular Medicine (CAPC), University of Turku, and in the Biomedicine Unit, Physiology, and Nordlab, University of Oulu, during the years 2006-2017. I owe my gratitude to the women who participated in this study.

I sincerely thank Professor Juha Mäkinen, Head of the Obstetrics and Gynecology University unit and a fellow native of Pori, and Professor Seija Grenman, Head of the Department of Obstetrics and Gynecology, for creating excellent facilities and an environment that supports scientific research. I thank Professor Olli Raitakari, Head of the CAPC, for the opportunity to work and use the superb facilities in this institution.

My deepest and sincerest gratitude belongs to my three supervisors: Professor Juha Räsänen, MD, Docent Eeva Ekholm, MD, and Professor Olli Vuolteenaho, MD. I have the utmost respect and admiration for Juha and his scientific mind and skills relentlessly applied in this study, as well as in clinical practice. Juha is extremely hard-working, encouraging, patient, creative, and without him this study would not have been performed. He taught me the basics of ultrasound examination in both rats and humans. I am very grateful to Eeva for introducing me to this project. She has been the sound voice of reason and has kindly endured my high-flying ideas and sometimes impossible dead lines. Eeva's clinical skills and contacts in Turku are highly appreciated. Olli has been an inspiration to work with: he provided this study with a physiological point of view and up-to-date laboratory services. His interest in this study and instructive discussions on the function of genes in fetal life have been crucial.

I whole-heartedly thank my co-authors. Mervi Haapsamo, MD, PhD, has been instrumental in carrying out the patient protocol and has helped me immensely in understanding fetal hemodynamics. Mervi has invested in this study, and is a dear friend and my go-to problem solver. In CAPC, Anna Koskinen, MD, PhD, and Docent Hanna Soukka, MD, introduced me to the world of animal experiments. They have been my support group and friends throughout the years. I am very grateful for Docent Jukka Laine, MD, for his expertise and patience in teaching me some principles in the field of pathology. Docent Ville Kytö, MD, has been extremely helpful in performing and analyzing TUNEL assays in rat fetal and neonatal hearts. I am happy that Pertti Palo, MD, PhD, has been interested and a part in this study. I thank Docent Jorma Määttä, PhD, for his expertise in performing micro-CT assays in rat fetal thoraxes and Lauri Polari, PhD, for performing and analyzing the cytokine bead assays in study II.

I am especially grateful for the reviewers of this thesis. Professor Helena Gardiner, MD, from McGovern Medical School in UTHealth, and Professor Saemundur Gudmundsson, MD, from Lund University, gave excellent, valuable comments and corrections

very rapidly. I thank my steering group, Professor Emeritus Pertti Kirkinen, MD, and Docent Juha Koskenvuo, MD, for being interested in my work. I feel extremely honored that Professor Fionnuala McAuliffe, MD, Head of the Department of Gynaecology and Obstetrics, University College Dublin, has agreed to be my opponent. I am looking forward to hearing her views on the effect maternal hyperglycemia has on the developing heart and circulation.

I thank the following people at the Universities of Turku and Oulu, and Turku and Oulu University Hospitals. Firstly, the midwives in the maternity outpatient clinics and delivery wards for recruiting the patients and gathering samples. Secondly, from CAPC, I am grateful to Ms. Tiina Peromaa for her splendid laboratory work, Ms. Nina Aalto for the use of machinery, Ms. Niina Ruotsalainen for office assistance, and Ms. Soile Kotilainen for excellent roommate behavior and lovely company. Thirdly, I acknowledge laboratory technicians Ms. Tuula Taskinen from the University of Oulu and Ms. Sinikka Collanus from the Turku University Hospital for expert technical advice and performance. Fourthly, I commend the University of Turku Central Animal Laboratory staff for running this facility well. Fifthly, I am grateful to Docent Robert Paul, MD, for editing the language in this thesis. Finally, I express my gratitude to Professor Tapani Rönnemaa, MD, for advice on glucose and insulin homeostasis; Professor Matti Välimäki, MD, a family friend, for advice and pep talk; and Docent Tuomas Kiviniemi, MD, my brother-in-law and friend, for technical advice and his attempts at making me understand cardiology.

I am privileged to work with several inspiring and dedicated colleagues at the Turku University Hospital. I wish to acknowledge Kristiina Tertti, MD, PhD; Nanneli Pallasmaa, MD, PhD; Docent Mäkikallio-Anttila, MD; Outi Pellonperä, MD; my tutor Marjut Rintala, MD, PhD; Riikka Aaltonen, MD, PhD; Maria Malminen, MD, PhD; Sanna Oksjoki, MD, PhD; Docent Antti Perheentupa, MD; Docent Päivi Polo, MD; my fellow residents and Ms. Riitta Ulén just to name some. My former colleagues Mervi Haarala, MD, PhD, and Merja Huttunen, MD, have been essential for my clinical training and supported of this study.

For long friendships I thank Hanna and Sune Lilbaek, Pirkkoliisa Heinonen and her boys, Sanna Grönlund, Tommi "Paavo" Väyrynen, other friends, and former study mates from cursus Tumor. I would like to thank Farhia Mohamed, BM, for her interest in my work. I am also a proud godmother to these following charming personalities: Oiva, Lilli, Ruuben, Matias, Lili-Maria, Sisu, and Vellamo. You lovelies have been a joy in my life. I also thank Marasmus for not losing your nerve when I wouldn't take a no as an answer.

This thesis would never have been completed without my parents-in-law, Irmeli and Risto. They have provided childcare services 24/7 willingly, and have loved my children without reservations. This kind of selfless help can never be repayed. My own god-

mother Riitta has a quiet, unassuming presence and I am so lucky to have her as my friend and “Riitta-mamma” to my children. I acknowledge my aunt Heidi for her inspiring conversation and chauffeur services. I have enjoyed my cousin Laura’s friendship from her teen years into adulthood. My husband’s relatives have become my own and I have been happy for the company of Mari, Jonas, Matias, Ester, Leila, Jorma, Timo, Petra, Kenda, Kaapo, Juha, Leila, Kasimir, Lilli, and Leevi throughout the years.

My family is very dear to me. The other “pikkulikka” Aida is my best friend, and the funniest and smartest person. I fondly remember our TALT-days! Aida and Tuoski and their children Kauri, Vellamo, and Ellinoora are an adventurous and wild bunch. My elder sister Nora is also my best friend and the warmest and kindest sister. Nora, Stögö a.k.a. Professor Palindrome, Rebekka, Ruuben, and Rafu are all sporty, freethinking, and good-natured. My brother Rudi is a quick-witted and fun guy, and his wife Jenni and children Tomi, Lili, Lumi, and Dani are excellent and joyful company. Finally, my parents Paula and Ari are the best parents and grandparents in the world. Your love, trust, outlook on life, and appreciation of knowledge and a good meal have set an example in my life. Despite having 13 grandchildren, you have time for my worries and take care of my children with the same love as me. I thank you from the bottom of my heart for all these years, for caring for your children and grandchildren above yourselves, and for all the great holidays. This work would never have been finished were it not for you.

My love Tuomas has been my companion for nearly 20 years. I love your positive and quiet confidence, truthfulness, hard-working attitude, and of course your singing, though a little bit of rock would occasionally be fine. You take good care of our children, house, and me; and without you I would not have written this thesis. Finally, I thank the best children in the world for existing. My lovely, creative “Kissa Krumeluu” Louna, who appreciates all things beautiful and is a natural care-taker; my fierce Reino, who loves a fine sword but is a true mediator in crisis; and my baby Salme, the passionate, shrewd, loud little lady.

This work was financially supported by the Clinical Research funding (EVO) of Turku University Hospital, The Diabetes Research Foundation of The Finnish Diabetes Association, The Foundation for Pediatric Research, The Heart Research Foundation, The Varsinais-Suomi Regional Fund of The Finnish Cultural Foundation, The Aarne Koskelo Foundation, The Maud Kuistila Memorial Foundation, The Turku University Foundation, The Sigrid Juselius Foundation, and the National Graduate School of Clinical Investigation.

Turku, April 2nd, 2017,

Lara Lehtoranta

9 REFERENCES

- Aasa, K.L. et al., 2013. Analysis of Maternal and Fetal Cardiovascular Systems During Hyperglycemic Pregnancy in the Nonobese Diabetic Mouse. *Biology of Reproduction*, 88(6), pp.151–151.
- Abdou, A. et al., 2013. The diagnostic value of p27 in comparison to p57 in differentiation between different gestational trophoblastic diseases. *Fetal and pediatric pathology*, 32(6), pp.395–411.
- Abe, T. et al., 2002. Left ventricular diastolic dysfunction in type 2 diabetes mellitus model rats. *American journal of physiology. Heart and circulatory physiology*, 282, pp.H138–H148.
- Abramowicz, J.S. et al., 2002. Literature review by the ISUOG Bioeffects and Safety Committee. *Ultrasound in obstetrics & gynecology: the official journal of the International Society of Ultrasound in Obstetrics and Gynecology*, 19(3), pp.318–9.
- Acharya, G. et al., 2005. Doppler-derived umbilical artery absolute velocities and their relationship to fetoplacental volume blood flow: a longitudinal study. *Ultrasound in obstetrics & gynecology: the official journal of the International Society of Ultrasound in Obstetrics and Gynecology*, 25(5), pp.444–53.
- Acharya, G. et al., 2011. Effect of angiotensin II on the left ventricular function in a near-term fetal sheep with metabolic acidemia. *Journal of pregnancy*, 2011, p.634240.
- Acharya, G. et al., 2004. Relationships among Doppler-derived umbilical artery absolute velocities, cardiac function, and placental volume blood flow and resistance in fetal sheep. *American journal of physiology.Heart and circulatory physiology*, 286(4), pp.H1266–72.
- al-Ghazali, W. et al., 1989. Evidence of redistribution of cardiac output in asymmetrical growth retardation. *British journal of obstetrics and gynaecology*, 96(6), pp.697–704.
- Al-Matubsi, H.Y. et al., 2010. Activities of cyclooxygenases, and levels of prostaglandins E2 and F2alpha, in fetopathy associated with experimental diabetic gestation. *Diabetes & metabolism*, 36(1), pp.43–50.
- Ala-Kopsala, M. et al., 2004. Molecular heterogeneity has a major impact on the measurement of circulating N-terminal fragments of A- and B-type natriuretic peptides. *Clinical chemistry*, 50(9), pp.1576–88.
- Altmäe, S. et al., 2017. Maternal Pre-Pregnancy Obesity Is Associated with Altered Placental Transcriptome C. Torrents, ed. *PLOS ONE*, 12(1), p.e0169223.
- Aman, J. et al., 2011. Increased fat mass and cardiac septal hypertrophy in newborn infants of mothers with well-controlled diabetes during pregnancy. *Neonatology*, 100(2), pp.147–154.
- Anderson, M.S. et al., 2001. Glucose transporter protein responses to selective hyperglycemia or hyperinsulinemia in fetal sheep. *American journal of physiology. Regulatory, integrative and comparative physiology*, 281(5), pp.R1545–52.
- Anger, G.J. et al., 2012. Expression of ABC Efflux Transporters in Placenta from Women with Insulin-Managed Diabetes H. W. van Veen, ed. *PLoS ONE*, 7(4), p.e35027.
- American Diabetes Association, 2016. Standards of Medical Care in Diabetes-2016: Summary of Revisions. *Diabetes care*, 39 Suppl 1, pp.S4–5.
- Aoki, A. et al., 1978. Studies on the ultrastructure and permeability of the hemotrichorial placenta. II. Fetal capillaries and tracer administration into the fetal blood circulation. *Cell and tissue research*, 192(3), pp.409–22.
- Arduini, D. et al., 1992. Changes of pulsatility index from fetal vessels preceding the onset of late decelerations in growth-retarded fetuses. *Obstetrics and gynecology*, 79(4), pp.605–10.
- Arison, R.N. et al., 1967. Light and electron microscopy of lesions in rats rendered diabetic with streptozotocin. *Diabetes*, 16(1), pp.51–6.
- Atiq, M. et al., 2017. Assessment of Cardiac Function in Fetuses of Gestational Diabetic Mothers During the Second Trimester. *Pediatric cardiology*.
- Babic, I. et al., 2015. Intraplacental villous artery resistance indices and identification of placenta-mediated diseases. *Journal of perinatology: official journal of the California Perinatal Association*, 35(10), pp.793–8.
- Baschat, A.A. et al., 1997. Demonstration of fetal coronary blood flow by Doppler ultrasound in relation to arterial and venous flow velocity waveforms and perinatal outcome—the “heart-sparing effect”. *Ultrasound in obstetrics & gynecology: the official journal of the International Society of Ultrasound in Obstetrics and Gynecology*, 9(3), pp.162–72.
- Baschat, A.A. et al., 2004. Venous Doppler in the prediction of acid-base status of growth-restricted fetuses with elevated placental blood flow resistance. *American journal of obstetrics and gynecology*, 191(1), pp.277–84.
- Baschat, A.A. et al., 2001. The sequence of changes in Doppler and biophysical parameters as severe fetal growth restriction worsens. *Ultrasound in obstetrics & gynecology: the official journal of the International Society of Ultrasound in Obstetrics and Gynecology*, 18(6), pp.571–7.

- Van Bel, F. et al., 1991. Cerebral blood flow velocity and cardiac output in infants of insulin-dependent diabetic mothers. *Acta paediatrica Scandinavica*, 80(10), pp.905–10.
- Bewley, S. et al., 1989. Uteroplacental Doppler flow velocity waveforms in the second trimester. A complex circulation. *British journal of obstetrics and gynaecology*, 96(9), pp.1040–6.
- Beyerlein, A. et al., 2010. Improvement in pregnancy-related outcomes in the offspring of diabetic mothers in Bavaria, Germany, during 1987-2007. *Diabetic medicine: a journal of the British Diabetic Association*, 27(12), pp.1379–84.
- Björklund, A.O. et al., 1996. Effects of hypoglycaemia on fetal heart activity and umbilical artery Doppler velocity waveforms in pregnant women with insulin-dependent diabetes mellitus. *British journal of obstetrics and gynaecology*, 103(5), pp.413–20.
- Di Blasio, A.M. et al., 1997. Basic fibroblast growth factor messenger ribonucleic acid levels in human placentas from normal and pathological pregnancies. *Molecular human reproduction*, 3(12), pp.1119–23.
- Boardman, N. et al., 2009. Increased O₂ cost of basal metabolism and excitation-contraction coupling in hearts from type 2 diabetic mice. *AJP: Heart and Circulatory Physiology*, 296(5), pp.H1373–H1379.
- Boileau, P. et al., 1995. Overexpression of GLUT3 placental glucose transporter in diabetic rats. *The Journal of clinical investigation*, 96(1), pp.309–317.
- de Bold, A.J. et al., 1996. Mechanical and neuroendocrine regulation of the endocrine heart. *Cardiovascular research*, 31(1), pp.7–18.
- Bollepalli, S. et al., 2010. Asymmetric large-for-gestational-age infants of type 1 diabetic women: morbidity and abdominal growth. *American journal of perinatology*, 27(8), pp.603–10.
- Boo, N.-Y. et al., 2005. Comparison of serum cardiac troponin T and creatine kinase MB isoenzyme mass concentrations in asphyxiated term infants during the first 48 h of life. *Journal of paediatrics and child health*, 41(7), pp.331–7.
- Bui, Y.K. et al., 2013. Tissue Doppler is more sensitive and reproducible than spectral pulsed-wave Doppler for fetal right ventricle myocardial performance index determination in normal and diabetic pregnancies. *Journal of the American Society of Echocardiography: official publication of the American Society of Echocardiography*, 26(5), pp.507–14.
- Burri, P.H., 2006. Structural aspects of postnatal lung development - alveolar formation and growth. *Biology of the neonate*, 89(4), pp.313–22.
- Cameron, V.A. & Ellmers, L.J., 2003. Minireview: natriuretic peptides during development of the fetal heart and circulation. *Endocrinology*, 144(6), pp.2191–2194.
- Capponi, A. et al., 1997. Splenic artery velocity waveforms in small-for-gestational-age fetuses: relationship with pH and blood gases measured in umbilical blood at cordocentesis. *American journal of obstetrics and gynecology*, 176(2), pp.300–7.
- Cetin, H. et al., 2011. Polycythaemia in infants of diabetic mothers: β -hydroxybutyrate stimulates erythropoietic activity. *The Journal of international medical research*, 39(3), pp.815–21.
- Chan, C.B. & Harper, M.E., 2006. Uncoupling proteins: role in insulin resistance and insulin insufficiency. *Current diabetes reviews*, 2(3), pp.271–283.
- Chartrel, N.C. et al., 1990. Uteroplacental hemodynamic disturbances in establishment of fetal growth retardation in streptozocin-induced diabetic rats. *Diabetes*, 39(6), pp.743–6.
- Cheema, R. et al., 2009. Signs of fetal brain sparing are not related to umbilical cord blood gases at birth. *Early human development*, 85(7), pp.467–70.
- Clark, S.J. et al., 2001. Cardiac troponin T in neonates. *Acta paediatrica (Oslo, Norway: 1992)*, 90(8), p.957.
- Cohen, A.L. et al., 2014. The association of circulating angiogenic factors and HbA_{1c} with the risk of preeclampsia in women with preexisting diabetes. *Hypertension in pregnancy*, 33(1), pp.81–92.
- Cohn, H.E. et al., 1992. The effect of hyperglycemia on acid-base and sympathoadrenal responses in the hypoxemic fetal monkey. *Journal of developmental physiology*, 17(6), pp.299–304.
- Cole, M.A. et al., 2011. A high fat diet increases mitochondrial fatty acid oxidation and uncoupling to decrease efficiency in rat heart. *Basic research in cardiology*, 106(3), pp.447–457.
- Conrad, K.P. et al., 1996. Expression of erythropoietin by the human placenta. *FASEB journal: official publication of the Federation of American Societies for Experimental Biology*, 10(7), pp.760–8.
- Cook, G.A. et al., 2017. Streptozotocin diabetes increases mRNA expression of ketogenic enzymes in the rat heart. *Biochimica et Biophysica Acta (BBA) - General Subjects*, 1861(2), pp.307–312.
- Corrigan, N. et al., 2013. Cardiomyopathy and Diastolic Dysfunction in the Embryo and Neonate of a Type 1 Diabetic Mouse Model. *Reproductive Sciences*, 20(7), pp.781–790.

- Cowett, R.M. & Schwartz, R., 1979. The role of hepatic control of glucose homeostasis in the etiology of neonatal hypo- and hyperglycemia. *Seminars in perinatology*, 3(4), pp.327–40.
- Cox, E.J. & Marsh, S.A., 2014. A Systematic Review of Fetal Genes as Biomarkers of Cardiac Hypertrophy in Rodent Models of Diabetes S. Sadayappan, ed. *PLoS ONE*, 9(3), p.e92903.
- Cypryk, K. et al., 2015. Continuous Glucose Monitoring in Type 1 Diabetes Pregnancy Shows that Fetal Heart Rate Correlates with Maternal Glycemia. *Diabetes Technology & Therapeutics*, 17(9), pp.619–624.
- Dame, C. et al., 1998. Erythropoietin mRNA expression in human fetal and neonatal tissue. *Blood*, 92(9), pp.3218–25.
- Damm, P. et al., 2014. Poor pregnancy outcome in women with type 1 diabetes is predicted by elevated HbA1c and spikes of high glucose values in the third trimester. *The journal of maternal-fetal & neonatal medicine: the official journal of the European Association of Perinatal Medicine, the Federation of Asia and Oceania Perinatal Societies, the International Society of Perinatal Obstetricians*, 27(2), pp.149–54.
- Dandel, M. et al., 2009. Strain and strain rate imaging by echocardiography - basic concepts and clinical applicability. *Current cardiology reviews*, 5(2), pp.133–48.
- Daniels, A. et al., 2010. Impaired cardiac functional reserve in type 2 diabetic db/db mice is associated with metabolic, but not structural, remodelling. *Acta physiologica (Oxford, England)*, 200(1), pp.11–22.
- Das, B.B. et al., 2009. Natriuretic peptides in cardiovascular diseases of fetus, infants and children. *Cardiovascular & hematological agents in medicinal chemistry*, 7(1), pp.43–51.
- Davis, L.E. et al., 2003. Renal and placental secretion of erythropoietin during anemia or hypoxia in the ovine fetus. *American journal of obstetrics and gynecology*, 189(6), pp.1764–70.
- Desoye, G. et al., 1992. Insulin binding to trophoblast plasma membranes and placental glycogen content in well-controlled gestational diabetic women treated with diet or insulin, in well-controlled overt diabetic patients and in healthy control subjects. *Diabetologia*, 35(1), pp.45–55.
- DeVore, G.R. et al., 1984. Fetal echocardiography. IV. M-mode assessment of ventricular size and contractility during the second and third trimesters of pregnancy in the normal fetus. *American journal of obstetrics and gynecology*, 150(8), pp.981–8.
- Dicker, D. et al., 1990. Umbilical artery velocimetry in insulin dependent diabetes mellitus (IDDM) pregnancies. *Journal of perinatal medicine*, 18(5), pp.391–5.
- Dickey, R.P., 1997. Doppler ultrasound investigation of uterine and ovarian blood flow in infertility and early pregnancy. *Human reproduction update*, 3(5), pp.467–503.
- Donnelly, R. & Millar-Craig, M.W., 1998. Cardiac troponins: IT upgrade for the heart. *Lancet (London, England)*, 351(9102), pp.537–9.
- Dowling, D. et al., 2014. Cardiomyopathy in Offspring of Pregestational Diabetic Mouse Pregnancy. *Journal of Diabetes Research*, 2014, pp.1–6.
- Dubiel, M. et al., 2000. Fetal adrenal and middle cerebral artery Doppler velocimetry in high-risk pregnancy. *Ultrasound in obstetrics & gynecology: the official journal of the International Society of Ultrasound in Obstetrics and Gynecology*, 16(5), pp.414–8.
- Dubiel, M. et al., 1997. Middle cerebral artery velocimetry as a predictor of hypoxemia in fetuses with increased resistance to blood flow in the umbilical artery. *Early human development*, 47(2), pp.177–84.
- Dubiel, M. et al., 2002. Blood redistribution in the fetal brain during chronic hypoxia. *Ultrasound in obstetrics & gynecology: the official journal of the International Society of Ultrasound in Obstetrics and Gynecology*, 20(2), pp.117–21.
- Edelstone, D.I. et al., 1978. Liver and ductus venosus blood flows in fetal lambs in utero. *Circulation research*, 42(3), pp.426–33.
- Eisenhofer, G., 2001. The role of neuronal and extraneuronal plasma membrane transporters in the inactivation of peripheral catecholamines. *Pharmacology & therapeutics*, 91(1), pp.35–62.
- Erkinaro, T. et al., 2007. Divergent effects of ephedrine and phenylephrine on cardiovascular hemodynamics of near-term fetal sheep exposed to hypoxemia and maternal hypotension. *Acta anaesthesiologica Scandinavica*, 51(7), pp.922–8.
- Escobar, J. et al., 2013. Amniotic fluid oxidative and nitrosative stress biomarkers correlate with fetal chronic hypoxia in diabetic pregnancies. *Neonatology*, 103(3), pp.193–8.
- Evers, I.M. et al., 2003. Placental pathology in women with type 1 diabetes and in a control group with normal and large-for-gestational-age infants. *Placenta*, 24(8–9), pp.819–825.
- Fadda, G.M. et al., 2001. Umbilical artery pulsatility index in pregnancies complicated by insulin-dependent diabetes mellitus without hypertension. *Gynecologic and obstetric investigation*, 51(3), pp.173–177.
- Ferdous, Z. et al., 2016. Different Profile of mRNA Expression in Sinoatrial Node from Streptozotocin-Induced Diabetic Rat M. Rota, ed. *PLoS ONE*, 11(4), p.e0153934.
- Fidaleo, M. et al., 2011. A role for the peroxisomal 3-ketoacyl-CoA thiolase B enzyme in the control

- of PPAR α -mediated upregulation of SREBP-2 target genes in the liver. *Biochimie*, 93(5), pp.876–91.
- Flynn, T.G. et al., 1983. The amino acid sequence of an atrial peptide with potent diuretic and natriuretic properties. *Biochemical and biophysical research communications*, 117(3), pp.859–65.
- Fouron, J.-C. et al., 2005. The relationship between an aortic isthmus blood flow velocity index and the postnatal neurodevelopmental status of fetuses with placental circulatory insufficiency. *American Journal of Obstetrics and Gynecology*, 192(2), pp.497–503.
- Fouron, J.C. et al., 1994. Flow velocity profile of the fetal aortic isthmus through normal gestation. *The American journal of cardiology*, 74(5), pp.483–6.
- Fouron, J.C. et al., 1999. Relationship between flow through the fetal aortic isthmus and cerebral oxygenation during acute placental circulatory insufficiency in ovine fetuses. *American journal of obstetrics and gynecology*, 181(5 Pt 1), pp.1102–7.
- Fowelin, J. et al., 1993. Effect of prolonged hyperglycemia on growth hormone levels and insulin sensitivity in insulin-dependent diabetes mellitus. *Metabolism: clinical and experimental*, 42(3), pp.387–94.
- Frias, A.E. et al., 2011. Maternal high-fat diet disturbs uteroplacental hemodynamics and increases the frequency of stillbirth in a nonhuman primate model of excess nutrition. *Endocrinology*, 152(6), pp.2456–2464.
- Gaber, E.M. et al., 2014. Effects of a sucrose-enriched diet on the pattern of gene expression, contraction and Ca²⁺ transport in Goto-Kakizaki type 2 diabetic rat heart. *Experimental Physiology*, 99(6), pp.881–893.
- Gaither, K. et al., 1999. Diabetes Alters the Expression and Activity of the Human Placental GLUT1 Glucose Transporter¹. *The Journal of Clinical Endocrinology & Metabolism*, 84(2), pp.695–701.
- Garcia, N.A. et al., 2016. Cardiomyocyte exosomes regulate glycolytic flux in endothelium by direct transfer of GLUT transporters and glycolytic enzymes. *Cardiovascular Research*, 109(3), pp.397–408.
- Georgieff, M.K. et al., 1990. Abnormal iron distribution in infants of diabetic mothers: spectrum and maternal antecedents. *The Journal of pediatrics*, 117(3), pp.455–61.
- Giles, W.B., Trudinger, B.J. & Baird, P.J., 1985. Fetal umbilical artery flow velocity waveforms and placental resistance: pathological correlation. *British journal of obstetrics and gynaecology*, 92(1), pp.31–8.
- Gill, R.W., 1987. Doppler ultrasound—physical aspects. *Seminars in perinatology*, 11(4), pp.292–9.
- Girsen, A. et al., 2008. Increased fetal cardiac natriuretic peptide secretion in type-1 diabetic pregnancies. *Acta Obstetrica et Gynecologica Scandinavica*, 87(3), pp.307–312.
- Girsen, A. et al., 2007. The relationship between human fetal cardiovascular hemodynamics and serum erythropoietin levels in growth-restricted fetuses. *American journal of obstetrics and gynecology*, 196(5), p.467.e1-6.
- Goldberg, M.A. et al., 1991. Erythropoietin mRNA levels are governed by both the rate of gene transcription and posttranscriptional events. *Blood*, 77(2), pp.271–7.
- Gollapudi, S.K. & Chandra, M., 2016. The effect of cardiomyopathy mutation (R97L) in mouse cardiac troponin T on the muscle length-mediated recruitment of crossbridges is modified divergently by α - and β -myosin heavy chain. *Archives of biochemistry and biophysics*.
- Gordon, E.E. et al., 2015. Maternal Hyperglycemia Directly and Rapidly Induces Cardiac Septal Overgrowth in Fetal Rats. *Journal of diabetes research*, 2015, p.479565.
- Groen, B. et al., 2015. Impaired trophoblast invasion and increased numbers of immune cells at day 18 of pregnancy in the mesometrial triangle of type 1 diabetic rats. *Placenta*, 36(2), pp.142–9.
- Grunewald, C. et al., 1996. Doppler velocimetry in last trimester pregnancy complicated by insulin-dependent diabetes mellitus. *Acta obstetrica et gynecologica Scandinavica*, 75(9), pp.804–8.
- Gudmundsson, S. et al., 1996. Venous Doppler in the fetus with absent end-diastolic flow in the umbilical artery. *Ultrasound in obstetrics & gynecology: the official journal of the International Society of Ultrasound in Obstetrics and Gynecology*, 7(4), pp.262–7.
- Gudmundsson, S. et al., 1991. Venous Doppler ultrasonography in the fetus with nonimmune hydrops. *American journal of obstetrics and gynecology*, 164(1 Pt 1), pp.33–7.
- Gui, Y.H. et al., 1996. Doppler echocardiography of normal and abnormal embryonic mouse heart. *Pediatric research*, 40(4), pp.633–642.
- Gustafson, T.A. et al., 1987. Hormonal regulation of myosin heavy chain and alpha-actin gene expression in cultured fetal rat heart myocytes. *The Journal of biological chemistry*, 262(27), pp.13316–22.
- Gutierrez, J.C. et al., 2009. Late-gestation ventricular myocardial reduction in fetuses of hyperglycemic CD1 mice is associated with increased apoptosis. *Birth Defects Research Part B: Developmental and Reproductive Toxicology*, 86(5), pp.409–415.

- Halse, K.G. et al., 2005. Increased plasma pro-B-type natriuretic peptide in infants of women with type 1 diabetes. *Clinical chemistry*, 51(12), pp.2296–2302.
- Halt, K.J. et al., 2016. CD146(+) cells are essential for kidney vasculature development. *Kidney international*.
- Han, J. et al., 2007. Rat maternal diabetes impairs pancreatic beta-cell function in the offspring. *American journal of physiology. Endocrinology and metabolism*, 293(1), pp.E228–36.
- Han, S. et al., 2015. Investigating the Mechanism of Hyperglycemia-Induced Fetal Cardiac Hypertrophy D. K. Singla, ed. *PLOS ONE*, 10(9), p.e0139141.
- Hara, C. de C.P. et al., 2016. Characterization of Natural Killer Cells and Cytokines in Maternal Placenta and Fetus of Diabetic Mothers. *Journal of Immunology Research*, 2016, pp.1–8.
- Harjutsalo, V. et al., 2013. Incidence of type 1 diabetes in Finland. *JAMA*, 310(4), pp.427–8.
- Harvey, W., 1628. Movement of the Heart and Blood in Animals, T. Translated from the original Latin by K.J. Franklin. *Oxford, Blackwell Scientific Publications* 1957, pp. 44–60.
- Hawkins, J. et al., 1989. Effects of increasing afterload on left ventricular output in fetal lambs. *Circulation research*, 65(1), pp.127–34.
- Hay, W.W., 1994. Placental transport of nutrients to the fetus. *Hormone research*, 42(4–5), pp.215–22.
- He, M. et al., 2016. Nrf2 signalling and autophagy are involved in diabetes mellitus-induced defects in the development of mouse placenta. *Open Biology*, 6(7), p.160064.
- Hecher, K. et al., 1995. Fetal venous, intracardiac, and arterial blood flow measurements in intrauterine growth retardation: relationship with fetal blood gases. *American journal of obstetrics and gynecology*, 173(1), pp.10–5.
- Hecher, K. et al., 1994. Reference ranges for fetal venous and atrioventricular blood flow parameters. *Ultrasound in obstetrics & gynecology: the official journal of the International Society of Ultrasound in Obstetrics and Gynecology*, 4(5), pp.381–90.
- Hernandez-Andrade, E. et al., 2005. A modified myocardial performance (Tei) index based on the use of valve clicks improves reproducibility of fetal left cardiac function assessment. *Ultrasound in Obstetrics and Gynecology*, 26(3), pp.227–232.
- Hidden, U. et al., 2008. MT1-MMP Expression in First-Trimester Placental Tissue Is Upregulated in Type 1 Diabetes as a Result of Elevated Insulin and Tumor Necrosis Factor- Levels. *Diabetes*, 57(1), pp.150–157.
- Higgins, M. & Mc Auliffe, F., 2010. A review of maternal and fetal growth factors in diabetic pregnancy. *Current diabetes reviews*, 6(2), pp.116–125.
- Hofstaetter, C. et al., 2001. Two types of umbilical venous pulsations and outcome of high-risk pregnancy. *Early human development*, 61(2), pp.111–7.
- Horio, T. et al., 2000. Inhibitory regulation of hypertrophy by endogenous atrial natriuretic peptide in cultured cardiac myocytes. *Hypertension*, 35(1 Pt 1), pp.19–24.
- Hornig, C. et al., 1999. Detection and quantification of complexed and free soluble human vascular endothelial growth factor receptor-1 (sVEGFR-1) by ELISA. *Journal of immunological methods*, 226(1–2), pp.169–77.
- Hornig, C. et al., 2000. Release and complex formation of soluble VEGFR-1 from endothelial cells and biological fluids. *Laboratory investigation; a journal of technical methods and pathology*, 80(4), pp.443–54.
- Horowitz, K. et al., 2011. Full-term neonatal intensive care unit admission in an urban community hospital: the role of respiratory morbidity. *The journal of maternal-fetal & neonatal medicine: the official journal of the European Association of Perinatal Medicine, the Federation of Asia and Oceania Perinatal Societies, the International Society of Perinatal Obstetricians*, 24(11), pp.1407–10.
- Hui, H.P. et al., 2006. [Adeno-associated viral gene transfer of SERCA2a improves heart function in chronic congestive heart failure rats]. *Zhonghua Xin Xue Guan Bing Za Zhi*, 34(4), pp.357–362.
- Hunt, P.J. et al., 1997. Immunoreactive amino-terminal pro-brain natriuretic peptide (NT-PROBNP): a new marker of cardiac impairment. *Clinical endocrinology*, 47(3), pp.287–96.
- Husain, S.M. et al., 1994. Effect of Diabetes Mellitus on Maternofetal Flux of Calcium and Magnesium and Calbindin9K mRNA Expression in Rat Placenta. *Pediatric Research*, 35(3), pp.376–380.
- Iciek, R. et al., 2013. Placental leptin and its receptor genes expression in pregnancies complicated by type 1 diabetes. *Journal of physiology and pharmacology: an official journal of the Polish Physiological Society*, 64(5), pp.579–85.
- Jaeggi, E.T. et al., 2001. Fetal cardiac performance in uncomplicated and well-controlled maternal type I diabetes. *Ultrasound in obstetrics & gynecology: the official journal of the International Society of Ultrasound in Obstetrics and Gynecology*, 17(4), pp.311–315.
- Janota, J. et al., 2003. Expression of angiopoietic factors in normal and type-I diabetes human placenta: a pilot study. *European journal of obstetrics, gynecology, and reproductive biology*, 111(2), pp.153–6.

- Jauniaux, E. & Burton, G.J., 2006. Villous histomorphometry and placental bed biopsy investigation in Type I diabetic pregnancies. *Placenta*, 27(4–5), pp.468–474.
- Jawerbaum, A. & White, V., 2010. Animal Models in Diabetes and Pregnancy. *Endocrine Reviews*, 31(5), pp.680–701.
- Jirkovska, M. et al., 2012. The branching pattern of villous capillaries and structural changes of placental terminal villi in type 1 diabetes mellitus. *Placenta*, 33(5), pp.343–351.
- Johnson, P. et al., 2000. Intracardiac pressures in the human fetus. *Heart (British Cardiac Society)*, 84(1), pp.59–63.
- Johnstone, F.D. et al., 1992. Doppler umbilical artery flow velocity waveforms in diabetic pregnancy. *British journal of obstetrics and gynaecology*, 99(2), pp.135–40.
- Jun, J.H. et al., 2014. Erythropoietin protects myocardium against ischemia–reperfusion injury under moderate hyperglycemia. *European Journal of Pharmacology*, 745, pp.1–9.
- Junno, J. et al., 2013. Fetal sheep left ventricle is more sensitive than right ventricle to progressively worsening hypoxemia and acidemia. *European journal of obstetrics, gynecology, and reproductive biology*, 167(2), pp.137–141.
- Junod, A. et al., 1969. Diabetogenic action of streptozotocin: relationship of dose to metabolic response. *The Journal of clinical investigation*, 48(11), pp.2129–2139.
- Jurysta, C. et al., 2013. Comparison of GLUT1, GLUT2, GLUT4 and SGLT1 mRNA Expression in the Salivary Glands and Six Other Organs of Control, Streptozotocin-Induced and Goto-Kakizaki Diabetic Rats. *Cellular Physiology and Biochemistry*, 31(1), pp.37–43.
- Kambe, T. et al., 2000. Retinoic acid stimulates erythropoietin gene transcription in embryonal carcinoma cells through the direct repeat of a steroid/thyroid hormone receptor response element half-site in the hypoxia-response enhancer. *Blood*, 96(9), pp.3265–71.
- Kantor, P.F. et al., 1999. Volume overload hypertrophy of the newborn heart slows the maturation of enzymes involved in the regulation of fatty acid metabolism. *Journal of the American College of Cardiology*, 33(6), pp.1724–1734.
- Kappen, C. et al., 2012. Maternal Diet Modulates Placenta Growth and Gene Expression in a Mouse Model of Diabetic Pregnancy C. Penha-Goncalves, ed. *PLoS ONE*, 7(6), p.e38445.
- Kapusta, L. et al., 2013. Changes in Fetal Left and Right Ventricular Strain Mechanics during Normal Pregnancy. *Journal of the American Society of Echocardiography*, 26(10), pp.1193–1200.
- Kekäläinen, P. et al., 2016. Continuous Subcutaneous Insulin Infusion During Pregnancy in Women with Complicated Type 1 Diabetes Is Associated with Better Glycemic Control but Not with Improvement in Pregnancy Outcomes. *Diabetes technology & therapeutics*, 18(3), pp.144–50.
- Kenny, J.F. et al., 1986. Changes in intracardiac blood flow velocities and right and left ventricular stroke volumes with gestational age in the normal human fetus: a prospective Doppler echocardiographic study. *Circulation*, 74(6), pp.1208–16.
- Kinnunen, P. et al., 1992. Passive mechanical stretch releases atrial natriuretic peptide from rat ventricular myocardium. *Circulation research*, 70(6), pp.1244–53.
- Kiserud, T. et al., 2000a. Effect of NO, phenylephrine, and hypoxemia on ductus venosus diameter in fetal sheep. *American journal of physiology. Heart and circulatory physiology*, 279(3), pp.H1166–71.
- Kiserud, T. et al., 2006. Fetal cardiac output, distribution to the placenta and impact of placental compromise. *Ultrasound in obstetrics & gynecology: the official journal of the International Society of Ultrasound in Obstetrics and Gynecology*, 28(2), pp.126–36.
- Kiserud, T. et al., 1999. Validation of diameter measurements by ultrasound: intraobserver and interobserver variations assessed in vitro and in fetal sheep. *Ultrasound in obstetrics & gynecology: the official journal of the International Society of Ultrasound in Obstetrics and Gynecology*, 13(1), pp.52–7.
- Kiserud, T. et al., 2000b. Blood flow and the degree of shunting through the ductus venosus in the human fetus. *American journal of obstetrics and gynecology*, 182(1 Pt 1), pp.147–53.
- Kiserud, T. et al., 2005. Physiology of the fetal circulation. *Seminars in Fetal and Neonatal Medicine* 10(6), pp. 493–503.
- Klemetti, M. et al., 2012. Trends in maternal BMI, glycaemic control and perinatal outcome among type 1 diabetic pregnant women in 1989–2008. *Diabetologia*, 55(9), pp.2327–2334.
- Klemetti, M.M. et al., 2013. Blood pressure levels but not hypertensive complications have increased in Type 1 diabetes pregnancies during 1989–2010. *Diabetic medicine: a journal of the British Diabetic Association*, 30(9), pp.1087–93.
- Klemetti, M.M. et al., 2015. White's classification and pregnancy outcome in women with type 1 diabetes: a population-based cohort study. *Diabetologia*.
- Klemetti, M.M. et al., 2016. White's classification and pregnancy outcome in women with type 1 diabetes: a population-based cohort study. *Diabetologia*, 59(1), pp.92–100.

- Knorr, S. et al., 2015. Multisystem Morbidity and Mortality in Offspring of Women With Type 1 Diabetes (the EPICOM Study): A Register-Based Prospective Cohort Study. *Diabetes care*, 38(5), pp.821–6.
- Konje, J.C. et al., 2005. Normative values of Doppler velocimetry of five major fetal arteries as determined by color power angiography. *Acta obstetrica et gynecologica Scandinavica*, 84(3), pp.230–7.
- Korgun, E.T. et al., 2011. Expression of glucocorticoid receptor and glucose transporter-1 during placental development in the diabetic rat. *Folia histochemica et cytobiologica / Polish Academy of Sciences, Polish Histochemical and Cytochemical Society*, 49(2), pp.325–334.
- Koskinen, A. et al., 2015. Maternal diabetes induces changes in the umbilical cord gene expression. *Placenta*, 36(7), pp.767–74.
- Koskinen, A. et al., 2010. Maternal hyperglycemia modifies extracellular matrix signaling pathways in neonatal rat lung. *Neonatology*, 98(4), pp.387–96.
- Kosseljans, W. et al., 2000. Role of peroxynitrite in altered fetal-placental vascular reactivity in diabetes or preeclampsia. *American journal of physiology. Heart and circulatory physiology*, 278(4), pp.H1311-9.
- Koury, M.J. & Bondurant, M.C., 1990. Control of red cell production: the roles of programmed cell death (apoptosis) and erythropoietin. *Transfusion*, 30(8), pp.673–4.
- Kowalczyk, M. et al., 2002. Psychomotor development in the children of mothers with type 1 diabetes mellitus or gestational diabetes mellitus. *Journal of pediatric endocrinology & metabolism: JPEM*, 15(3), pp.277–81.
- Kremkau, F.W., 1992a. Doppler color imaging. Principles and instrumentation. *Clinics in diagnostic ultrasound*, 27, pp.7–60.
- Kremkau, F.W., 1992b. Doppler principles. *Seminars in roentgenology*, 27(1), pp.6–16.
- Kuo, H.C. et al., 2001. A defect in the Kv channel-interacting protein 2 (KCHIP2) gene leads to a complete loss of I(to) and confers susceptibility to ventricular tachycardia. *Cell*, 107(6), pp.801–13.
- Kurjak, A. et al., 1997. Intervillous circulation in all three trimesters of normal pregnancy assessed by color Doppler. *Journal of perinatal medicine*, 25(4), pp.373–80.
- Kurtz, M. et al., 2014. PPAR ligands improve impaired metabolic pathways in fetal hearts of diabetic rats. *Journal of Molecular Endocrinology*, 53(2), pp.237–246.
- LaGamma, E.F. et al., 1982. Effects of naloxone on fetal circulatory responses to hypoxemia. *American journal of obstetrics and gynecology*, 143(8), pp.933–40.
- Landon, M.B. et al., 1989. Doppler umbilical artery velocimetry in pregnancy complicated by insulin-dependent diabetes mellitus. *Obstetrics and gynecology*, 73(6), pp.961–5.
- Larger, E. et al., 2004. Hyperglycemia-induced defects in angiogenesis in the chicken chorioallantoic membrane model. *Diabetes*, 53(3), pp.752–61.
- Larsson, L. & Skogsberg, C., 1988. Effects of the interval between removal and freezing of muscle biopsies on muscle fibre size. *Journal of the neurological sciences*, 85(1), pp.27–38.
- Van Der Lee, K.A. et al., 2000. Effects of fatty acids on uncoupling protein-2 expression in the rat heart. *FASEB journal: official publication of the Federation of American Societies for Experimental Biology*, 14(3), pp.495–502.
- Leiva, M.C. et al., 1999. Fetal cardiac development and hemodynamics in the first trimester. *Ultrasound in obstetrics & gynecology: the official journal of the International Society of Ultrasound in Obstetrics and Gynecology*, 14(3), pp.169–74.
- Leskinen, H. et al., 1995. Role of nitric oxide on cardiac hormone secretion: effect of NG-nitro-L-arginine methyl ester on atrial natriuretic peptide and brain natriuretic peptide release. *Endocrinology*, 136(3), pp.1241–9.
- Leturque, A. et al., 1987. Hyperglycemia and hyperinsulinemia increase glucose utilization in fetal rat tissues. *The American journal of physiology*, 253(6 Pt 1), pp.E616-20.
- Leung, K.Y. et al., 2006. A new strategy for prenatal diagnosis of homozygous α_0 -thalassemia. *Ultrasound in Obstetrics and Gynecology*, 28(2), pp.173–177.
- Lew, R.A. & Baertschi, A.J., 1989. Mechanisms of hypoxia-induced atrial natriuretic factor release from rat hearts. *The American journal of physiology*, 257(1 Pt 2), pp.H147-56.
- Li, F. et al., 1996. Rapid transition of cardiac myocytes from hyperplasia to hypertrophy during postnatal development. *Journal of Molecular and Cellular Cardiology*, 28(8), pp.1737–1746.
- Li, Y. et al., 2015. Vascular Endothelial Growth Factor-A (VEGF-A) Mediates Activin A-Induced Human Trophoblast Endothelial-Like Tube Formation. *Endocrinology*, 156(11), pp.4257–68.
- Lindegaard, M.L.S. et al., 2006. Placental triglyceride accumulation in maternal type 1 diabetes is associated with increased lipase gene expression. *The Journal of Lipid Research*, 47(11), pp.2581–2588.
- Lindegaard, M.L.S. & Nielsen, L.B., 2008. Maternal diabetes causes coordinated down-regulation of genes involved with lipid metabolism in the murine fetal heart. *Metabolism*, 57(6), pp.766–773.

- Lingman, G. et al., 1984. Haemodynamic assessment of fetal heart arrhythmias. *British journal of obstetrics and gynaecology*, 91(7), pp.647–52.
- Lipsic, E. et al., 2006. Protective effects of erythropoietin in cardiac ischemia: from bench to bedside. *Journal of the American College of Cardiology*, 48(11), pp.2161–7.
- Lisowski, L.A. et al., 2003. Altered fetal circulation in type-1 diabetic pregnancies. *Ultrasound in obstetrics & gynecology: the official journal of the International Society of Ultrasound in Obstetrics and Gynecology*, 21(4), pp.365–369.
- Locci, M. et al., 1992. Fetal cerebral haemodynamic adaptation: a progressive mechanism? Pulsed and color Doppler evaluation. *Journal of perinatal medicine*, 20(5), pp.337–43.
- Loukovaara, M.J. et al., 2005. Endothelium-derived nitric oxide metabolites and soluble intercellular adhesion molecule-1 in diabetic and normal pregnancies. *European journal of obstetrics, gynecology, and reproductive biology*, 118(2), pp.160–5.
- Lv, H. et al., 2015. Neonatal hypoxic ischemic encephalopathy-related biomarkers in serum and cerebrospinal fluid. *Clinica chimica acta; international journal of clinical chemistry*, 450, pp.282–97.
- Lyu, T. et al., 2014. Natriuretic peptides as an adjunctive treatment for acute myocardial infarction: insights from the meta-analysis of 1,389 patients from 20 trials. *International heart journal*, 55(1), pp.8–16.
- Macklon, N.S. et al., 1998. Fetal cardiac function and septal thickness in diabetic pregnancy: a controlled observational and reproducibility study. *British journal of obstetrics and gynaecology*, 105(6), pp.661–666.
- Madsen, H. & Ditzel, J., 1984. Blood-oxygen transport in first trimester of diabetic pregnancy. *Acta obstetrica et gynecologica Scandinavica*, 63(4), pp.317–20.
- Malek, A. et al., 1994. Lack of transport of erythropoietin across the human placenta as studied by an in vitro perfusion system. *Pflügers Archiv: European journal of physiology*, 427(1–2), pp.157–61.
- Mandarim-de-Lacerda, C.A. & Pessanha, M.G., 1995. Stereology of the myocardium in embryos, fetuses and neonates of the rat. *Acta Anatomica*, 154(4), pp.261–266.
- Manderson, J.G. et al., 2003. Preprandial versus postprandial blood glucose monitoring in type 1 diabetic pregnancy: A randomized controlled clinical trial. *American Journal of Obstetrics and Gynecology*, 189(2), pp.507–512.
- Mari, G. et al., 1996. Adrenal artery velocity waveforms in the appropriate and small-for-gestational-age fetus. *Ultrasound in obstetrics & gynecology: the official journal of the International Society of Ultrasound in Obstetrics and Gynecology*, 8(2), pp.82–6.
- Mari, G. et al., 1995. Blood flow velocity waveforms of the abdominal arteries in appropriate- and small-for-gestational-age fetuses. *Ultrasound in obstetrics & gynecology: the official journal of the International Society of Ultrasound in Obstetrics and Gynecology*, 6(1), pp.15–8.
- Mari, G. & Deter, R.L., 1992. Middle cerebral artery flow velocity waveforms in normal and small-for-gestational-age fetuses. *American journal of obstetrics and gynecology*, 166(4), pp.1262–70.
- Mari, G. et al., 1993. Fetal renal artery flow velocity waveforms in normal pregnancies and pregnancies complicated by polyhydramnios and oligohydramnios. *Obstetrics and gynecology*, 81(4), pp.560–4.
- Marsál, K. et al., 1987. Blood flow in the fetal descending aorta. *Seminars in perinatology*, 11(4), pp.322–34.
- Martino, J. et al., 2016. Maternal Body Weight and Gestational Diabetes Differentially Influence Placental and Pregnancy Outcomes. *The Journal of clinical endocrinology and metabolism*, 101(1), pp.59–68.
- Maruotti, G.M. et al., 2014. Are there any relationships between umbilical artery Pulsatility Index and macrosomia in fetuses of type I diabetic mothers? *The journal of maternal-fetal & neonatal medicine: the official journal of the European Association of Perinatal Medicine, the Federation of Asia and Oceania Perinatal Societies, the International Society of Perinatal Obstetricians*, 27(17), pp.1776–81.
- Matsui, H. et al., 2011. Temporal and spatial performance of vector velocity imaging in the human fetal heart. *Ultrasound in Obstetrics & Gynecology*, 37(2), pp.150–157.
- Matus, M. et al., 2015. Upregulation of SERCA2a following short-term ACE inhibition (by enalaprilat) alters contractile performance and arrhythmogenicity of healthy myocardium in rat. *Molecular and Cellular Biochemistry*, 403(1–2), pp.199–208.
- Maunu, J. et al., 2007. Antenatal Doppler Measurements and Early Brain Injury in Very Low Birth Weight Infants. *The Journal of Pediatrics*, 150(1), p.51–56.e1.
- Mayhew, T.M. & Burton, G.J., 1988. Methodological problems in placental morphometry: apologia for the use of stereology based on sound sampling practice. *Placenta*, 9(6), pp.565–81.
- McCormick, N. et al., 2014. Validity of Heart Failure Diagnoses in Administrative Databases: A Systematic Review and Meta-Analysis Y. Guo, ed. *PLoS ONE*, 9(8), p.e104519.
- Mert, M.K. et al., 2016. Troponin T and NT ProBNP Levels in Gestational, Type 1 and Type 2

- Diabetic Mothers and Macrosomic Infants. *Pediatric Cardiology*, 37(1), pp.76–83.
- Mestas, J. & Hughes, C.C.W., 2004. Of Mice and Not Men: Differences between Mouse and Human Immunology. *The Journal of Immunology*, 172(5), pp.2731–2738.
- Meyer, W.W. et al., 1978. Structure and closure mechanism of the human umbilical artery. *European Journal of Pediatrics*, 128(4), pp.247–259.
- Miettinen, P.J. et al., 1995. Epithelial immaturity and multiorgan failure in mice lacking epidermal growth factor receptor. *Nature*, 376(6538), pp.337–341.
- Milley, J.R., et al., 1986. Effect of insulin on uptake of metabolic substrates by the sheep fetus. *The American journal of physiology*, 251(3 Pt 1), pp.E349–56.
- Moazzen, H. et al., 2014. N-Acetylcysteine prevents congenital heart defects induced by pregestational diabetes. *Cardiovascular Diabetology*, 13(1), p.46.
- Moore Simas, T.A. et al., 2014. Angiogenic biomarkers for prediction of early preeclampsia onset in high-risk women. *The Journal of Maternal-Fetal & Neonatal Medicine*, 27(10), pp.1038–1048.
- Mori, A. et al., 2007. Evaluation of cardiac function of the fetus by inferior vena cava diameter pulse waveform. *American heart journal*, 154(4), pp.789–94.
- Mori, A. et al., 2011. Noninvasive measurement of fetal augmentation index by fetal aortic diameter pulse and flow velocity waveforms. *Acta Obstetrica et Gynecologica Scandinavica*, 90(8), pp.839–845.
- Murakoshi, T. et al., 1996. Uterine and spiral artery flow velocity waveforms in pregnancy-induced hypertension and/or intrauterine growth retardation. *Ultrasound in obstetrics & gynecology: the official journal of the International Society of Ultrasound in Obstetrics and Gynecology*, 7(2), pp.122–8.
- Mäkikallio, K. et al., 2000. Association of severe placental insufficiency and systemic venous pressure rise in the fetus with increased neonatal cardiac troponin T levels. *American journal of obstetrics and gynecology*, 183(3), pp.726–31.
- Mäkikallio, K. et al., 2010. Ductus venosus velocimetry in acute fetal acidemia and impending fetal death in a sheep model of increased placental vascular resistance. *American journal of physiology. Heart and circulatory physiology*, 298(4), pp.H1229–34.
- Mäkikallio, K. et al., 2006b. Fetal cardiac natriuretic peptide expression and cardiovascular hemodynamics in endotoxin-induced acute cardiac dysfunction in mouse. *Pediatric research*, 59(2), pp.180–4.
- Mäkikallio, K. et al., 2006a. Fetal oxygenation and Doppler ultrasonography of cardiovascular hemodynamics in a chronic near-term sheep model. *American journal of obstetrics and gynecology*, 194(2), pp.542–50.
- Mäkikallio, K. et al., 2002a. Ultrasonographic and biochemical markers of human fetal cardiac dysfunction in placental insufficiency. *Circulation*, 105(17), pp.2058–63.
- Mäkikallio, K. et al., 2005. Human fetal cardiac function during the first trimester of pregnancy. *Heart (British Cardiac Society)*, 91(3), pp.334–8.
- Mäkikallio, K. et al., 2003. Retrograde aortic isthmus net blood flow and human fetal cardiac function in placental insufficiency. *Ultrasound in obstetrics & gynecology: the official journal of the International Society of Ultrasound in Obstetrics and Gynecology*, 22(4), pp.351–7.
- Mäkikallio, K. et al., 2002b. Retrograde net blood flow in the aortic isthmus in relation to human fetal arterial and venous circulations. *Ultrasound in obstetrics & gynecology: the official journal of the International Society of Ultrasound in Obstetrics and Gynecology*, 19(2), pp.147–52.
- Mäntymaa, P. et al., 1993. Atrial stretch induces rapid increase in brain natriuretic peptide but not in atrial natriuretic peptide gene expression in vitro. *Endocrinology*, 133(3), pp.1470–3.
- Nelson, S.M. et al., 2009. Placental structure in type 1 diabetes: relation to fetal insulin, leptin, and IGF-I. *Diabetes*, 58(11), pp.2634–41.
- Nessa, A. et al., 2016. Hyperinsulinemic Hypoglycemia - The Molecular Mechanisms. *Frontiers in endocrinology*, 7, p.29.
- Newnham, J.P. et al., 2004. Effects of repeated prenatal ultrasound examinations on childhood outcome up to 8 years of age: follow-up of a randomised controlled trial. *Lancet (London, England)*, 364(9450), pp.2038–44.
- Nold, J.L. & Georgieff, M.K., 2004. Infants of diabetic mothers. *Pediatric clinics of North America*, 51(3), p.619–37, viii.
- Nystrom, H.C. et al., 2006. Platelet-derived growth factor B retention is essential for development of normal structure and function of conduit vessels and capillaries. *Cardiovascular research*, 71(3), pp.557–565.
- Oberhoffer, R. et al., 1997. Cardiac and extracardiac complications in infants of diabetic mothers and their relation to parameters of carbohydrate metabolism. *European journal of pediatrics*, 156(4), pp.262–5.
- Olofsson, P. et al., 1987. Fetal blood flow in diabetic pregnancy. *Journal of perinatal medicine*, 15(6), pp.545–53.
- Onkamo, P. et al., 1999. Worldwide increase in incidence of Type I diabetes--the analysis of the data on published incidence trends. *Diabetologia*, 42(12), pp.1395–403.

- Oparil, S. et al., 1984. Myocardial cell hypertrophy or hyperplasia. *Hypertension*, 6(6 Pt 2), p.III38-43.
- Padmanabhan, R. & Shafiullah, M., 2001. Intrauterine growth retardation in experimental diabetes: possible role of the placenta. *Archives of Physiology and Biochemistry*, 109(3), pp.260-271.
- Pagel, H. et al., 1991. Isolated serum-free perfused rat kidneys release immunoreactive erythropoietin in response to hypoxia. *Endocrinology*, 128(5), pp.2633-8.
- Pallasmaa, N. et al., 2015. The impact of maternal obesity, age, pre-eclampsia and insulin dependent diabetes on severe maternal morbidity by mode of delivery-a register-based cohort study. *Archives of gynecology and obstetrics*, 291(2), pp.311-8.
- Palomaki, G.E. et al., 2015. Modeling risk for severe adverse outcomes using angiogenic factor measurements in women with suspected preterm preeclampsia. *Prenatal diagnosis*, 35(4), pp.386-93.
- Paulson, D.J. & Light, K.E., 1981. Elevation of serum and ventricular norepinephrine content in the diabetic rat. *Research communications in chemical pathology and pharmacology*, 33(3), pp.559-62.
- Pedersen, J., 1954. Weight and length at birth of infants of diabetic mothers. *Acta endocrinologica*, 16(4), pp.330-42.
- Peeters, L.L. et al., 1979. Blood flow to fetal organs as a function of arterial oxygen content. *American journal of obstetrics and gynecology*, 135(5), pp.637-46.
- Perimenis, P. et al., 2014. Placental antiangiogenic prolactin fragments are increased in human and rat maternal diabetes. *Biochimica et Biophysica Acta (BBA) - Molecular Basis of Disease*, 1842(9), pp.1783-1793.
- Persson, M. et al., 2009. Obstetric and perinatal outcomes in type 1 diabetic pregnancies: A large, population-based study. *Diabetes care*, 32(11), pp.2005-9.
- Philipps, A.F. et al., 1984. Effects of chronic fetal hyperglycemia upon oxygen consumption in the ovine uterus and conceptus. *The Journal of clinical investigation*, 74(1), pp.279-86.
- Philipps, A.F. et al., 1982. Erythropoietin elevation in the chronically hyperglycemic fetal lamb. *Proceedings of the Society for Experimental Biology and Medicine. Society for Experimental Biology and Medicine (New York, N.Y.)*, 170(1), pp.42-7.
- Pietryga, M. et al., 2005. Abnormal uterine Doppler is related to vasculopathy in pregestational diabetes mellitus. *Circulation*, 112(16), pp.2496-500.
- Pinter, E. et al., 2001. Hyperglycemia-induced vasculopathy in the murine conceptus is mediated via reductions of VEGF-A expression and VEGF receptor activation. *The American journal of pathology*, 158(4), pp.1199-206.
- Pinter, E. et al., 1986. Yolk sac failure in embryopathy due to hyperglycemia: ultrastructural analysis of yolk sac differentiation associated with embryopathy in rat conceptuses under hyperglycemic conditions. *Teratology*, 33(1), pp.73-84.
- Plagemann, A. et al., 1997. Glucose tolerance and insulin secretion in children of mothers with pregestational IDDM or gestational diabetes. *Diabetologia*, 40(9), pp.1094-100.
- Radaelli, T. et al., 2009. Differential regulation of genes for fetoplacental lipid pathways in pregnancy with gestational and type 1 diabetes mellitus. *American Journal of Obstetrics and Gynecology*, 201(2), p.209.e1-209.e10.
- Rajabi, M. et al., 2007. Return to the fetal gene program protects the stressed heart: a strong hypothesis. *Heart failure reviews*, 12(3-4), pp.331-343.
- Reece, E.A. et al., 1996. Is there a correlation between aortic Doppler velocimetric findings in diabetic pregnant women and fetal outcome? *Journal of ultrasound in medicine: official journal of the American Institute of Ultrasound in Medicine*, 15(6), pp.437-40.
- Reece, E.A., et al., 1994. Doppler velocimetry and the assessment of fetal well-being in normal and diabetic pregnancies. *Ultrasound in obstetrics & gynecology: the official journal of the International Society of Ultrasound in Obstetrics and Gynecology*, 4(6), pp.508-14.
- Reed, K.L. et al., 1990. Doppler studies of vena cava flows in human fetuses. Insights into normal and abnormal cardiac physiology. *Circulation*, 81(2), pp.498-505.
- Rees, D.A. & Alcolado, J.C., 2005. Animal models of diabetes mellitus. *Diabetic medicine: a journal of the British Diabetic Association*, 22(4), pp.359-370.
- Reis, L.O. et al., 2010. Evolution on experimental animal model for upper urothelium carcinogenesis. *World journal of urology*, 28(4), pp.499-505.
- Ren, Y. et al., 2011. Characterization of fetal cardiac structure and function detected by echocardiography in women with normal pregnancy and gestational diabetes mellitus. *Prenatal Diagnosis*, 31(5), pp.459-465.
- Respondek, M. et al., 1992. 2D echocardiographic assessment of the fetal heart size in the 2nd and 3rd trimester of uncomplicated pregnancy. *European journal of obstetrics, gynecology, and reproductive biology*, 44(3), pp.185-8.
- Respondek, M.L. et al., 1994. The prevalence and clinical significance of fetal tricuspid valve

- regurgitation with normal heart anatomy. *American journal of obstetrics and gynecology*, 171(5), pp.1265–70.
- Ribeiro, S. et al., 2016. Liver iron is a major regulator of hepcidin gene expression via BMP/SMAD pathway in a rat model of chronic renal failure under treatment with high rHuEPO doses. *BioFactors (Oxford, England)*.
- de Rijk, E.P.C.T. et al., 2002. Pregnancy dating in the rat: placental morphology and maternal blood parameters. *Toxicologic pathology*, 30(2), pp.271–82.
- Del Río, M. et al., 2008. Doppler assessment of the aortic isthmus and perinatal outcome in preterm fetuses with severe intrauterine growth restriction. *Ultrasound in obstetrics & gynecology: the official journal of the International Society of Ultrasound in Obstetrics and Gynecology*, 31(1), pp.41–7.
- Rizzo, G. et al., 1994. Analysis of factors influencing ventricular filling patterns in fetuses of type I diabetic mothers. *Journal of perinatal medicine*, 22(2), pp.149–57.
- Rizzo, G. et al., 1995. Cardiac and venous blood flow in fetuses of insulin-dependent diabetic mothers: evidence of abnormal hemodynamics in early gestation. *American journal of obstetrics and gynecology*, 173(6), pp.1775–81.
- Rizzo, G. & Arduini, D., 1991. Fetal cardiac function in intrauterine growth retardation. *American journal of obstetrics and gynecology*, 165(4 Pt 1), pp.876–82.
- Rizzo, G. et al., 1992a. Accelerated cardiac growth and abnormal cardiac flow in fetuses of type I diabetic mothers. *Obstetrics and gynecology*, 80(3 Pt 1), pp.369–376.
- Rizzo, G. et al., 1991. Cardiac function in fetuses of type I diabetic mothers. *American journal of obstetrics and gynecology*, 164(3), pp.837–43.
- Rizzo, G. et al., 1992b. Umbilical vein pulsations: a physiologic finding in early gestation. *American journal of obstetrics and gynecology*, 167(3), pp.675–7.
- Rizzo, T.A. et al., 1997. Early malnutrition and child neurobehavioral development: insights from the study of children of diabetic mothers. *Child development*, 68(1), pp.26–38.
- Rodriguez, P. & Kranias, E.G., 2005. Phospholamban: a key determinant of cardiac function and dysfunction. *Archives des maladies du coeur et des vaisseaux*, 98(12), pp.1239–43.
- Roest, P.A.M. et al., 2009. Specific local cardiovascular changes of Nepsilon-(carboxymethyl)lysine, vascular endothelial growth factor, and Smad2 in the developing embryos coincide with maternal diabetes-induced congenital heart defects. *Diabetes*, 58(5), pp.1222–8.
- Rollins, M.D. et al., 1993. Cord blood erythropoietin, pH, PaO₂ and haematocrit following caesarean section before labour. *Biology of the neonate*, 63(3), pp.147–52.
- Rosenzweig, A. et al., 1991. Proximal regulatory domains of rat atrial natriuretic factor gene. *Circulation*, 84(3), pp.1256–65.
- Rosner, J. et al., 2014. Intermittent absent end diastolic velocity of the umbilical artery: antenatal and neonatal characteristics and indications for delivery. *The journal of maternal-fetal & neonatal medicine: the official journal of the European Association of Perinatal Medicine, the Federation of Asia and Oceania Perinatal Societies, the International Society of Perinatal Obstetricians*, 27(1), pp.94–7.
- Rounioja, S. et al., 2003. Intra-amniotic lipopolysaccharide leads to fetal cardiac dysfunction. A mouse model for fetal inflammatory response. *Cardiovascular research*, 60(1), pp.156–164.
- Rudolph, A.M., 1985. Distribution and regulation of blood flow in the fetal and neonatal lamb. *Circulation research*, 57(6), pp.811–21.
- Russell, N.E. et al., 2008. Effect of pregestational diabetes mellitus on fetal cardiac function and structure. *American journal of obstetrics and gynecology*, 199(3), p.312.e1-7.
- Russell, N.E. et al., 2016. Heart rate variability in neonates of type 1 diabetic pregnancy. *Early Human Development*, 92, pp.51–55.
- Russell, N.E. et al., 2009. Troponin T and pro-B-type natriuretic Peptide in fetuses of type 1 diabetic mothers. *Diabetes care*, 32(11), pp.2050–2055.
- Rutland, C.S. et al., 2011. Knockdown of embryonic myosin heavy chain reveals an essential role in the morphology and function of the developing heart. *Development*, 138(18), pp.3955–3966.
- Räsänen, J. & Kirkinen, P., 1987. Growth and function of human fetal heart in normal, hypertensive and diabetic pregnancy. *Acta obstetrica et gynecologica Scandinavica*, 66(4), pp.349–53.
- Räsänen, J. et al., 1989. Right ventricular dysfunction in human fetal compromise. *American journal of obstetrics and gynecology*, 161(1), pp.136–40.
- Räsänen, J. et al., 1997. Human fetal right ventricular ejection force under abnormal loading conditions during the second half of pregnancy. *Ultrasound in obstetrics & gynecology: the official journal of the International Society of Ultrasound in Obstetrics and Gynecology*, 10(5), pp.325–32.
- Räsänen, J. et al., 1998. Reactivity of the human fetal pulmonary circulation to maternal hyperoxygenation increases during the second

- half of pregnancy: a randomized study. *Circulation*, 97(3), pp.257–62.
- Räsänen, J. et al., 1996. Role of the pulmonary circulation in the distribution of human fetal cardiac output during the second half of pregnancy. *Circulation*, 94(5), pp.1068–73.
- Räsänen, J. et al., 1988. Fetal aortic blood flow and echocardiographic findings in human pregnancy. *European journal of obstetrics, gynecology, and reproductive biology*, 27(2), pp.115–124.
- Sah, R. et al., 2003. Regulation of cardiac excitation-contraction coupling by action potential repolarization: role of the transient outward potassium current (I_{to}). *The Journal of physiology*, 546(Pt 1), pp.5–18.
- Sakanaka, M. et al., 1998. In vivo evidence that erythropoietin protects neurons from ischemic damage. *Proceedings of the National Academy of Sciences of the United States of America*, 95(8), pp.4635–40.
- Salas, A. et al., 2017. Expression Is Regulated by Activin A Proinflammatory Macrophages and Its The Prolyl Hydroxylase PHD3 Identifies The Prolyl Hydroxylase PHD3 Identifies Proinflammatory Macrophages and Its Expression Is Regulated by Activin A. *The Journal of Immunology*.
- Salbaum, J.M. et al., 2011. Altered gene expression and spongiotrophoblast differentiation in placenta from a mouse model of diabetes in pregnancy. *Diabetologia*, 54(7), pp.1909–1920.
- Salvesen, K.Å., 2011. Ultrasound in pregnancy and non-right handedness: meta-analysis of randomized trials. *Ultrasound in Obstetrics & Gynecology*, 38(3), pp.267–271.
- Schmidt, N.M. et al., 2004. Endogenous and recombinant erythropoietin levels decline in human amniotic fluid and fetal plasma in vitro at 37 degrees C. *Journal of perinatology: official journal of the California Perinatal Association*, 24(4), pp.218–22.
- Schnedl, W.J. et al., 1994. STZ transport and cytotoxicity. Specific enhancement in GLUT2-expressing cells. *Diabetes*, 43(11), pp.1326–1333.
- Schneider, H., 2011. Oxygenation of the placental-fetal unit in humans. *Respiratory physiology & neurobiology*, 178(1), pp.51–8.
- Schulman, H. et al., 1971. Development of uterine artery compliance in pregnancy as detected by Doppler ultrasound. *American Journal of Obstetrics & Gynecology*, 155(5), pp.1031–1036.
- Schwartz, R. et al., 1994. Hyperinsulinemia and macrosomia in the fetus of the diabetic mother. *Diabetes care*, 17(7), pp.640–648.
- Schwartz, R. & Teramo, K.A., 2000. Effects of diabetic pregnancy on the fetus and newborn. *Seminars in perinatology*, 24(2), pp.120–135.
- Sciullo, E. et al., 1997. Glucose transporter (Glut1, Glut3) mRNA in human placenta of diabetic and non-diabetic pregnancies. *Early pregnancy: biology and medicine: the official journal of the Society for the Investigation of Early Pregnancy*, 3(3), pp.172–82.
- Scott-Drechsel, D.E. et al., 2013. Hyperglycemia Slows Embryonic Growth and Suppresses Cell Cycle via Cyclin D1 and p21. *Diabetes*, 62(1), pp.234–242.
- Semenza, G.L., 2007. Oxygen-dependent regulation of mitochondrial respiration by hypoxia-inducible factor 1. *The Biochemical journal*, 405(1), pp.1–9.
- Severi, F.M. et al., 2000. Intrauterine growth retardation and fetal cardiac function. *Fetal diagnosis and therapy*, 15(1), pp.8–19.
- Sheldon, R.E. et al., 1979. Redistribution of cardiac output and oxygen delivery in the hypoxemic fetal lamb. *American journal of obstetrics and gynecology*, 135(8), pp.1071–8.
- Sisino, G. et al., 2013. Diabetes during pregnancy influences Hofbauer cells, a subtype of placental macrophages, to acquire a pro-inflammatory phenotype. *Biochimica et biophysica acta*, 1832(12), pp.1959–68.
- Stanek, J. et al., 2001. Nitrotyrosine immunostaining correlates with increased extracellular matrix: evidence of postplacental hypoxia. *Placenta*, 22 Suppl A, pp.S56-62.
- Stanirowski, P.J. et al., 2016. Impact of pre-gestational and gestational diabetes mellitus on the expression of glucose transporters GLUT-1, GLUT-4 and GLUT-9 in human term placenta. *Endocrine*.
- Stewart, P.A. et al., 1990. Blood flow velocity waveforms from the fetal external iliac artery as a measure of lower extremity vascular resistance. *British journal of obstetrics and gynaecology*, 97(5), pp.425–30.
- Stonestreet, B.S. et al., 1989. Effects of prolonged hyperinsulinemia on erythropoiesis in fetal sheep. *The American journal of physiology*, 257(5 Pt 2), pp.R1199-204.
- Stuart, A. et al., 2010. Ductus venosus blood flow velocity waveform in diabetic pregnancies. *Ultrasound in obstetrics & gynecology: the official journal of the International Society of Ultrasound in Obstetrics and Gynecology*, 36(3), pp.344–349.
- Su, J.Y. & Friedman, W.F., 1973. Comparison of the responses of fetal and adult cardiac muscle to hypoxia. *The American journal of physiology*, 224(6), pp.1249–53.
- Sudoh, T. et al., 1988. Brain natriuretic peptide-32: N-terminal six amino acid extended form of

- brain natriuretic peptide identified in porcine brain. *Biochemical and biophysical research communications*, 155(2), pp.726–32.
- Sutton, M.S. et al., 1991. Assessment of right and left ventricular function in terms of force development with gestational age in the normal human fetus. *British heart journal*, 66(4), pp.285–9.
- Sutton, M.S. et al., 1990. Changes in placental blood flow in the normal human fetus with gestational age. *Pediatric research*, 28(4), pp.383–7.
- Szukiewicz, D. et al., 2013. Fractalkine (CX3CL1) and Its Receptor CX3CR1 May Contribute to Increased Angiogenesis in Diabetic Placenta. *Mediators of Inflammation*, 2013, pp.1–8.
- Takada, S. et al., 2013. Angiotensin II receptor blocker improves the lowered exercise capacity and impaired mitochondrial function of the skeletal muscle in type 2 diabetic mice. *Journal of applied physiology (Bethesda, Md. : 1985)*, 114(7), pp.844–57.
- Takahashi, T. et al., 1992. Expression of A-, B-, and C-type natriuretic peptide genes in failing and developing human ventricles. Correlation with expression of the Ca(2+)-ATPase gene. *Circulation research*, 71(1), pp.9–17.
- Tang, X. et al., 2015. Protective Effect of sRAGE on Fetal Development in Pregnant Rats with Gestational Diabetes Mellitus. *Cell Biochemistry and Biophysics*, 71(2), pp.549–556.
- Tarantal, A.F. & Hendrickx, A.G., 1989a. Evaluation of the bioeffects of prenatal ultrasound exposure in the cynomolgus macaque (*Macaca fascicularis*): I. Neonatal/infant observations. *Teratology*, 39(2), pp.137–47.
- Tarantal, A.F. & Hendrickx, A.G., 1989b. Evaluation of the bioeffects of prenatal ultrasound exposure in the cynomolgus macaque (*Macaca fascicularis*): II. Growth and behavior during the first year. *Teratology*, 39(2), pp.149–62.
- Tarantal, A.F. et al., 1993. Evaluation of the bioeffects of prenatal ultrasound exposure in the cynomolgus macaque (*Macaca fascicularis*): III. Developmental and hematologic studies. *Teratology*, 47(2), pp.159–70.
- Tchirikov, M. et al., 1998. Blood flow through the ductus venosus in singleton and multifetal pregnancies and in fetuses with intrauterine growth retardation. *American journal of obstetrics and gynecology*, 178(5), pp.943–9.
- Tchirikov, M. et al., 2010. Cardiac output and blood flow volume redistribution during acute maternal hypoxia in fetal sheep. *Journal of perinatal medicine*, 38(4), pp.387–92.
- Tekay, A. & Jouppila, P., 2000. Fetal adrenal artery velocimetry measurements in appropriate-for-gestational age and intrauterine growth-restricted fetuses. *Ultrasound in obstetrics & gynecology: the official journal of the International Society of Ultrasound in Obstetrics and Gynecology*, 16(5), pp.419–24.
- Tennant, P.W.G. et al., 2014. Pre-existing diabetes, maternal glycated haemoglobin, and the risks of fetal and infant death: a population-based study. *Diabetologia*, 57(2), pp.285–94.
- Teramo, K. et al., 2004b. High amniotic fluid erythropoietin levels are associated with an increased frequency of fetal and neonatal morbidity in type 1 diabetic pregnancies. *Diabetologia*, 47(10), pp.1695–703.
- Teramo, K.A. et al., 2004a. Amniotic fluid and cord plasma erythropoietin levels in pregnancies complicated by preeclampsia, pregnancy-induced hypertension and chronic hypertension. *Journal of perinatal medicine*, 32(3), pp.240–7.
- Teramo, K.A. & Widness, J.A., 2009. Increased fetal plasma and amniotic fluid erythropoietin concentrations: markers of intrauterine hypoxia. *Neonatology*, 95(2), pp.105–116.
- Tessler, F.N. et al., 1990. Inter- and intra-observer variability of Doppler peak velocity measurements: an in-vitro study. *Ultrasound in medicine & biology*, 16(7), pp.653–7.
- Thaler, I. et al., 1992. Systolic or diastolic notch in uterine artery blood flow velocity waveforms in hypertensive pregnant patients: relationship to outcome. *Obstetrics and gynecology*, 80(2), pp.277–82.
- Thomas, C.R. et al., 1990. Effects of maternal diabetes on placental transfer of glucose in rats. *Diabetes*, 39(3), pp.276–282.
- Thompson, R.S. & Trudinger, B.J., 1990. Doppler waveform pulsatility index and resistance, pressure and flow in the umbilical placental circulation: an investigation using a mathematical model. *Ultrasound in medicine & biology*, 16(5), pp.449–58.
- Thornburg, K. et al., 2011. Regulation of the cardiomyocyte population in the developing heart. *Progress in biophysics and molecular biology*, 106(1), pp.289–299.
- Thornburg, K.L. & Morton, M.J., 1986. Filling and arterial pressures as determinants of left ventricular stroke volume in fetal lambs. *The American journal of physiology*, 251(5 Pt 2), pp.H961-8.
- Thuring, A. et al., 2012. Placental ischemia and changes in umbilical and uteroplacental arterial and venous hemodynamics. *The journal of maternal-fetal & neonatal medicine: the official journal of the European Association of Perinatal Medicine, the Federation of Asia and Oceania Perinatal Societies, the International Society of Perinatal Obstetricians*, 25(6), pp.750–5.
- Todorov, V. et al., 2000. Endogenous nitric oxide attenuates erythropoietin gene expression in

- vivo. *Pflügers Archiv: European journal of physiology*, 439(4), pp.445–8.
- Trudinger, B.J. et al., 1985. Fetal umbilical artery flow velocity waveforms and placental resistance: clinical significance. *British journal of obstetrics and gynaecology*, 92(1), pp.23–30.
- Tsang, R.C. et al., 1976. Hypomagnesemia in infants of diabetic mothers: perinatal studies. *The Journal of pediatrics*, 89(1), pp.115–9.
- Tsutsumi, T. et al., 1999. Serial evaluation for myocardial performance in fetuses and neonates using a new Doppler index. *Pediatrics international: official journal of the Japan Pediatric Society*, 41(6), pp.722–727.
- Tsyvian, P. et al., 1998. Assessment of left ventricular filling in normally grown fetuses, growth-restricted fetuses and fetuses of diabetic mothers. *Ultrasound in obstetrics & gynecology: the official journal of the International Society of Ultrasound in Obstetrics and Gynecology*, 12(1), pp.33–8.
- Tulzer, G. et al., 1994. Diastolic function of the fetal heart during second and third trimester: a prospective longitudinal Doppler-echocardiographic study. *European journal of pediatrics*, 153(3), pp.151–4.
- Turan, S. et al., 2011. Decreased fetal cardiac performance in the first trimester correlates with hyperglycemia in pregestational maternal diabetes. *Ultrasound in obstetrics & gynecology: the official journal of the International Society of Ultrasound in Obstetrics and Gynecology*, 38(3), pp.325–31.
- Turner, G. et al., 2016. The time course of endogenous erythropoietin, IL-6, and TNF α in response to acute hypoxic exposures. *Scandinavian Journal of Medicine & Science in Sports*.
- Ursem, N.T. et al., 1999. Fetal heart rate and umbilical artery velocity variability in pregnancies complicated by insulin-dependent diabetes mellitus. *Ultrasound in obstetrics & gynecology: the official journal of the International Society of Ultrasound in Obstetrics and Gynecology*, 13(5), pp.312–6.
- Uusimaa, P.A. et al., 1992. Endothelin-induced atrial natriuretic peptide release from cultured neonatal cardiac myocytes: the role of extracellular calcium and protein kinase-C. *Endocrinology*, 130(5), pp.2455–64.
- Veille, J.C. et al., 1993. Fetal cardiac size in normal, intrauterine growth retarded, and diabetic pregnancies. *American journal of perinatology*, 10(4), pp.275–9.
- Veille, J.C. et al., 1992. Interventricular septal thickness in fetuses of diabetic mothers. *Obstetrics and gynecology*, 79(1), pp.51–4.
- Vessières, E. et al., 2016. Long Lasting Microvascular Tone Alteration in Rat Offspring Exposed In Utero to Maternal Hyperglycaemia. *PloS one*, 11(1), p.e0146830.
- Vlachová, Z. et al., 2015. Increased metabolic risk in adolescent offspring of mothers with type 1 diabetes: the EPICOM study. *Diabetologia*, 58(7), pp.1454–63.
- de Vlaming, A. et al., 2012. Atrioventricular valve development: New perspectives on an old theme. *Differentiation*, 84(1), pp.103–116.
- Walker, A.M. et al., 1990. Autonomic control of heart rate differs with electrocortical activity and chronic hypoxaemia in fetal lambs. *Journal of developmental physiology*, 14(1), pp.43–8.
- Watanabe, S. et al., 2009. Characterization of ventricular myocardial performance in the fetus by tissue Doppler imaging. *Circulation journal: official journal of the Japanese Circulation Society*, 73(5), pp.943–7.
- Weber, H.S. et al., 1994. Sequential longitudinal evaluation of cardiac growth and ventricular diastolic filling in fetuses of well controlled diabetic mothers. *Pediatric cardiology*, 15(4), pp.184–9.
- Weiner, Z. et al., 1999. Cardiac compliance in fetuses of diabetic women. *Obstetrics and gynecology*, 93(6), pp.948–951.
- Weiner, Z. et al., 1994. Central and peripheral hemodynamic changes in fetuses with absent end-diastolic velocity in umbilical artery: correlation with computerized fetal heart rate pattern. *American journal of obstetrics and gynecology*, 170(2), pp.509–15.
- White, P., 1949. Pregnancy complicating diabetes. *The American journal of medicine*, 7(5), pp.609–16.
- White, V. et al., 2015. Diabetes-associated changes in the fetal insulin/insulin-like growth factor system are organ specific in rats. *Pediatric research*, 77(1–1), pp.48–55.
- Wichi, R.B. et al., 2005. Increased blood pressure in the offspring of diabetic mothers. *American journal of physiology. Regulatory, integrative and comparative physiology*, 288(5), pp.R1129–33.
- Widness, J.A. et al., 1990. Direct relationship of antepartum glucose control and fetal erythropoietin in human type 1 (insulin-dependent) diabetic pregnancy. *Diabetologia*, 33(6), pp.378–83.
- Widness, J.A. et al., 1981. Increased erythropoiesis and elevated erythropoietin in infants born to diabetic mothers and in hyperinsulinemic rhesus fetuses. *The Journal of clinical investigation*, 67(3), pp.637–42.
- Willruth, A.M. et al., 2011. Comparison of global and regional right and left ventricular longitudinal peak systolic strain, strain rate and velocity in healthy fetuses using a novel feature

- tracking technique. *Journal of perinatal medicine*, 39(5), pp.549–56.
- Witte, D.P. et al., 1994. Temporally and spatially restricted expression of apolipoprotein J in the developing heart defines discrete stages of valve morphogenesis. *Developmental Dynamics*, 201(3), pp.290–296.
- Wladimiroff, J.W. et al., 1987. Cerebral and umbilical arterial blood flow velocity waveforms in normal and growth-retarded pregnancies. *Obstetrics and gynecology*, 69(5), pp.705–9.
- Wladimiroff, J.W. et al., 1991. Fetal and umbilical flow velocity waveforms between 10-16 weeks' gestation: a preliminary study. *Obstetrics and gynecology*, 78(5 Pt 1), pp.812–4.
- Wong, S.F. et al., 2003. Cardiac function in fetuses of poorly-controlled pre-gestational diabetic pregnancies--a pilot study. *Gynecologic and obstetric investigation*, 56(2), pp.113–6.
- Wong, S.F. et al., 2010. Ductus venosus velocimetry in monitoring pregnancy in women with pregestational diabetes mellitus. *Ultrasound in obstetrics & gynecology: the official journal of the International Society of Ultrasound in Obstetrics and Gynecology*, 36(3), pp.350–4.
- Xia, Y. et al., 2015. Inhibition of prolyl hydroxylase 3 ameliorates cardiac dysfunction in diabetic cardiomyopathy. *Molecular and cellular endocrinology*, 403, pp.21–9.
- Yan, J. et al., 2014. Long-term effects of maternal diabetes on blood pressure and renal function in rat male offspring. *PLoS one*, 9(2), p.e88269.
- Yang, P. et al., 2015. Decoding the oxidative stress hypothesis in diabetic embryopathy through proapoptotic kinase signaling. *American Journal of Obstetrics and Gynecology*, 212(5), pp.569–579.
- Yasuda, Y. et al., 2002. Erythropoietin and erythropoietin-receptor producing cells demonstrated by in situ hybridization in mouse visceral yolk sacs. *Anatomical science international*, 77(1), pp.58–63.
- Yasuda, Y. et al., 1996. Erythropoietin in mouse avascular yolk sacs is increased by retinoic acid. *Developmental dynamics: an official publication of the American Association of Anatomists*, 207(2), pp.184–94.
- Yoshioka, K. & Fisher, J.W., 1995. Nitric oxide enhancement of erythropoietin production in the isolated perfused rat kidney. *The American journal of physiology*, 269(4 Pt 1), pp.C917-22.
- Yue, P. et al., 2007. Magnetic resonance imaging of progressive cardiomyopathic changes in the db/db mouse. *American journal of physiology. Heart and circulatory physiology*, 292(5), pp.H2106-18.
- Zabihi, S. et al., 2008. Altered Uterine Perfusion is Involved in Fetal Outcome of Diabetic Rats. *Placenta*, 29(5), pp.413–421.
- Zhang, Q. et al., 2007. Role of phospholamban in cyclic GMP mediated signaling in cardiac myocytes. *Cellular physiology and biochemistry: international journal of experimental cellular physiology, biochemistry, and pharmacology*, 20(1–4), pp.157–66.
- Zhou, J. et al., 2015. microRNA-340-5p Functions Downstream of Cardiotrophin-1 to Regulate Cardiac Eccentric Hypertrophy and Heart Failure via Target Gene Dystrophin. *International heart journal*, 56(4), pp.454–8.
- Zielinsky, P. et al., 2011. Aortic isthmus blood flow in fetuses of diabetic mothers. *Prenatal diagnosis*, 31(12), pp.1176–80.
- Zimmermann, P. et al., 1994. Doppler flow velocimetry of the uterine and uteroplacental circulation in pregnancies complicated by insulin-dependent diabetes mellitus. *Journal of perinatal medicine*, 22(2), pp.137–47.
- Zimmermann, P. et al., 1992. Doppler velocimetry of the umbilical artery in pregnancies complicated by insulin-dependent diabetes mellitus. *European journal of obstetrics, gynecology, and reproductive biology*, 47(2), pp.85–93.
- Zisman, A. et al., 2000. Targeted disruption of the glucose transporter 4 selectively in muscle causes insulin resistance and glucose intolerance. *Nature medicine*, 6(8), pp.924–8.